Life Attached: Examining the Implications of Epibiosis on a North Pacific Cirripede and a Gulf of Mexico Seep Sabellid

by

Lauren N. Rice

A dissertation accepted and approved in partial fulfillment of the

requirements for the degree of

Doctor of Philosophy

in Biology

Dissertation Committee:

Michelle Wood, Chair

Craig M. Young, Advisor

Aaron W.E. Galloway, Core Member

Erik E. Cordes, Core Member

Edward B. Davis, Institutional Representative

University of Oregon

Summer 2024

© 2024 Lauren N. Rice
This work is licensed under a Creative Commons BY Attribution License.

DISSERTATION ABSTRACT

Lauren N. Rice

Doctor of Philosophy in Biology

Title: Life Attached: Examining the Implications of Epibiosis on a North Pacific Cirripede and a Gulf of Mexico Seep Sabellid

Epibiotic species, which can either facultatively or obligatorily settle on living hosts, are commonly found in marine habitats. Despite this commonality, the biology and ecology for many epizoic organisms remain unknown and understudied. In this dissertation, I investigated how two marine invertebrate species accommodate life on living hosts.

In Chapter II, I discuss the reproductive and settlement patterns for the barnacle *Solidobalanus hesperius* and how they correlate to the molting patterns for host crab species in the Oregon subtidal. I found that *S. hesperius* reproduces year-round and that brooded embryos hatch in approximately a week. Furthermore, I utilized a new method to examine the spatial distributions of barnacle individuals on their crab hosts and they were tightly correlated to the microtopography of the host carapace.

The remaining chapters of the dissertation focus on a facultative epibiotic relationship found at methane seeps in the Gulf of Mexico, involving a sabellid polychaete species. In Chapter III, we found that the species are gregarious settlers and are abundant within the methane seep habitats investigated. Furthermore, we present morphological and phylogenetic evidence and identify the sabellid as belonging to a new genus and species: *Seepicola viridiplumi* sp. nov.

As the newly described sabellid is facultatively epibiotic, Chapter IV examined the trophic ecology of the species using stable isotopes. Additional tables showing the statistical pairwise comparisons highlighting the effects of season, sample site, and microhabitat on carbon, nitrogen, and sulfur isotopic ratios are provided as supplemental materials. We found that *S. viridiplumi* are generalist suspension feeders within the methane seeps and, using microbial evidence, show that the species does not rely on chemosynthetic symbionts. The rarefaction curves for the sequencing depth is also provided in the supplemental material section. However, individuals can occupy differing trophic niches depending on whether they are epibiotic or free-living.

The different trophic niches occupied by epibiotic and free-living *S. viridiplumi* individuals may impact other aspects of the biology for this species. To test this, we examined and compared the reproductive output for individuals from each microhabitat using paraffin histology. In doing so, we found that epibiotic individuals consistently had slightly larger oocytes and higher levels of fecundity. The individual oocyte size distributions for all female sabellids examined in this study are shown as a supplemental figure. We also observed an apparent lack of gametogenic seasonality in this sabellid species.

Taken together, the work presented in this dissertation provides unique insights into how epibiotic associations can develop and persist within an ecosystem. The results also provide additional insight into the adaptations and biology for epizoic species, which can aid in attempts for modeling community functioning.

This dissertation includes unpublished co-authored material.

CURRICULUM VITAE

NAME OF AUTHOR: Lauren N. Rice

GRADUATE AND UNDERGRADUATE SCHOOLS ATTENDED:

University of Oregon, Eugene, Oregon, USA
University of Maine, Orono, Maine, USA

DEGREES AWARDED:

Doctor of Philosophy, Biology, 2024, University of Oregon
Bachelor of Science, *summa cum laude*, Marine Science, 2017, University of Maine

AREAS OF SPECIAL INTEREST:

Deep-sea biology

Reproductive ecology

Marine Ecology

PROFESSIONAL EXPERIENCE:

Graduate Employee, Department of Biology, University of Oregon, Eugene
September 2018 – June 2024

Research Technician, Waller laboratory, School of Marine Sciences, University of Maine, Orono

Research Technician, Resource Access International, LLC Labs, Brunswick, Maine
Summer 2014 – Summer 2017

GRANTS, AWARDS, AND HONORS:

Donald E. Wimber Fund Award, University of Oregon, 2023

Oregon Society of Conchologists Scholarship, Oregon Society of Conchologists, 2022

William R. Sistrom Memorial Scholarship, University of Oregon, 2020

University of Oregon First Year Merit Award, University of Oregon, 2018

PUBLICATIONS:

R.A. Beinart, S.M. Arellano, M. Chaknova, J. Meagher, A.J. Davies, J. Lopresti, E.J. Cowell, M. Betters, T.A. Ladd, C.Q. Plowman, L.N. Rice, D. Davis, M. Heffernan, V. Jimenez, T. Beaver, J. Becker, S. Bergen, L. Brunner, A. Calhoun, M. Hauer, A. Taradash, T. Giachetti, C.M. Young (2024) Deep seafloor hydrothermal vent communities buried by volcanic ash from the 2022 Hunga eruption. *Communications Earth and Environment* 5: 254.

S. Rist, L.N. Rice, C.Q. Plowman, C.T. Fountain, A.E. Calhoun, C. Ellison, C.M. Young (2022) Reproductive biology of the bathyal asteroid *Ctenodiscus crispatus* in the NE Pacific. *Invertebrate Biology*. doi: 10.1111/ivb.12384

R.G. Waller, R.P. Stone, L.N. Rice, J. Johnstone, A.M. Rossin, E. Hartill, K. Feehan, C.L. Morrison (2019) Phenotypic plasticity or a reproductive dead end? *Primnoa pacifica* (Cnidaria: Alcyonacea) in the Southeastern Alaska Region. *Frontiers in Marine Science* 6 (709). doi: 10.3389/fmars.2019.00709.

L.N. Rice, P.D. Rawson, S.M. Lindsay (2018) Genetic homogeneity among geographically distant populations of the blister worm *Polydora websteri*. *Aquaculture Environment Interactions* 10: 437-446. doi:10.3354/aei00281.

ACKNOWLEDGMENTS

This work is thanks in large part to the continued support and assistance of family, friends, collaborators, and mentors. You all have my deepest gratitude.

First, my most sincere thank you to my advisor, Dr. Craig Young. You have given me so many amazing opportunities over the years, starting with the chance to work in your lab as a PhD student. You have taught me so much, from how to build experimental equipment for deployment at sea, how to prep for a research cruise, the best ways to use a microscope, and how to pivot when things aren't going according to plan. There have been so many moments working with you that I will cherish.

I am ever thankful to my advisory committee members. Michelle Wood, you have provided so much advice and guidance over the past several years, and I have always been appreciative of all the discussions over coffee. Edward Davis, thank you for always keeping me on track with statistics and for your advice. Aaron Galloway, thank you for pushing me to look at the bigger picture and for your advocacy. Erik Cordes, thank you for all the advice, wisdom, and help over the years Erik Cordes. I could not have asked for a better committee. Thank you all for the encouragement and kind words along the way.

My biggest and most sincere gratitude is extended to my lab mates: Caitlin Plowman and Avery Calhoun. Caitlin, you welcomed me wholeheartedly from the onset and provided friendship, mentorship, and guidance countless times over the years. Words cannot express the depth of my gratitude and appreciation. Avery, you always brought such a unique perspective and found a way to keep everyone in the lab smiling. Thank you for all your help and friendship and commiseration.

A huge thank you to the whole of the Oregon Institute of Marine Biology (OIMB) community. This campus has been my home for the past 6 years, and my work would not have been possible without all of you. Trish Mace, Laura Screen, Jeremy Worthington, Ian Washington, Bradd Beckett, James Johnson, Trystan Berry: thank you all for your friendship over the years, and for all that you do to keep this campus running.

To the OIMB grad student community (and extended partners), thank you for all your advice, guidance, support, commiseration, and friendship. Erin Jezuit, Christina Ellison, Nicole Nakata, Jesse Borland, you have all done so much to make this tiny campus feel like home and have brought so much to this community.

This work would not have been possible without the support of the William R. Sistrom Memorial Fellowship of the University of Oregon, and the Oregon Society of Conchology Scholarship. This work and my degree was also supported by the NSF grants 1851383 and 1737382.

Lastly, I must thank my parents, Mike and Lori Rice, as well as my brothers, Garrett, and Ryan. You have all supported this crazy dream of mine since I first set my heart towards this path so many years ago. Your encouragement never wavered, despite all the late-night calls, years spent apart due to distance and COVID, and even when you had no idea what I was talking about. Words cannot capture my gratitude and love.

DEDICATION

And to my grandmothers and my parents. You gave me all that I have, believed in me from the start, and reminded me how deep resilience can be in the face of hardship.

TABLE OF CONTENTS

LIST OF FIGURES

LIST OF TABLES

CHAPTER I

INTRODUCTION

Habitats along continental shelves and slopes are dominated by soft bottom habitats composed of sand and mud, and rocky substrata are often patchy and scarce. The marine communities that occur on hard surfaces are frequently dominated by sessile invertebrate fauna, leading to competition for space and access to settlement locations (Jackson 1977, Osman 1977, Harder 2009, Wahl 2009). This intense competitive pressure is thought to have given rise to a commensal, spatial association known as epibiosis (Wahl 1989). In this association, a sessile organism called an epibiont, settles on and attaches to the surface of a living host, called a basibiont (Wahl 1989, 1997, 2009). Epibiotic organisms are represented by a diverse array of taxa, including polychaetes, bryozoans, tunicates, mollusks, diatoms, rotifers, barnacles, and sponges (Wahl 2009). Epibiotic species can be further categorized as epizoans (animals) or epiphytes (algae) and can either facultatively or obligatorily settle on living substrates (Wahl & Mark 1999).

Epibiotic associations have been regarded as non-symbiotic due to their predominantly facultative nature and lack of obligate trophic exchange (Wahl 1989, 2009, Wahl & Mark 1999, Romero et al. 2022). However, epibiosis is still frequently categorized as an interspecies relationship (McLeod et al. 2020) where differing species “live together” in physical contact (Martin & Schwab 2012, Esteban & Fenchel 2020). In this dissertation, we identify epibiosis as a symbiotic, commensal association in recognition of the broad definition of symbiosis (Martin & Schwab 2012), the previous studies categorizing the outcomes of these associations (e.g. Uriz et al. 1992, Silina & Zhukova 2014, Puccinelli & McQuaid 2021), and the examples of obligate epibiotic species (e.g. Thamrin et al. 2001, Nájera-Hillman et al. 2012, Robinson et al. 2019).

Although there are some notable exceptions (McLeod et al. 2020), epibiotic species are usually smaller than their hosts and frequently act as abundant, primary consumers (Chen et al. 2021). Epibiotic associations can be observed at most latitudes, depths, and marine habitats (Wahl 2009). Despite this ubiquitous presence, many epizoan species are understudied compared to the host taxa. This is primarily due to the smaller size of epizoic species, greater difficulty in sampling and processing, epizoans compared to hosts, and that epizoans often belong to taxa with poor phylogenetic resolution and are difficult to identify (Chen et al. 2021). The advantages and disadvantages of epibiotic settlement has been well studied (Wahl 1989, 1997, 2009, Harder 2009). More frequently, however, studies attempt to identify and categorize the nature of epibiotic relationships from the perspective of the basibiont (e.g. Xu & Burns 1991, Wargo & Ford 1993b, Manning & Lindquist 2003, Eschweiler & Buschbaum 2011, Burris et al. 2014, Silina & Zhukova 2014). This focus often fails to capture the dynamic nature of the relationships (Zapalski 2011) and overlooks the biology and ecology of the epizoan.

In this dissertation, I sought to investigate how epizoan species adapt to life on living hosts. Some generalizations have been proposed for how epibiotic species have adapted, including abbreviated life spans compared to free-living relatives, the ability to facultatively or obligately undergo asexual reproduction, and general trophic independence from their host (Wahl & Mark 1999, Fernandez-Leborans 2010). However, quantitative evidence supporting these claims remains scant, especially given the commonality of epibiotic associations. The following chapters focus on two different epizoic species and examine how epibiotic life impacts settlement timing, patterns of reproduction, and trophic ecology.

In Chapter II, I discuss a species of balanid barnacle local to the Oregon subtidal that is primarily attached to crab hosts. While the barnacle is known to be a short-lived species, I

hypothesized that it has adapted its reproductive cycle to coordinate with the regular molting of the host exoskeleton. Additionally, I developed a novel way to investigate the spatial distributions of barnacle individuals on the host exoskeleton. Chapter II is unpublished but will include Dr. Craig M. Young as a co-author, as he provided editorial assistance.

Chapters III, IV, and V focus on a facultative hyper-epibiotic species of sabellid feather duster polychaete from shallow methane seep habitats within the Gulf of Mexico. While the species is highly abundant, the sabellid has remained unidentified. In Chapter III, I present the morphological and phylogenetic description of the sabellid and simultaneously erect a new genus. This chapter is unpublished and will include co-authors Dr. Mariana Tovar-Hernandez for assistance with the morphological description; Christina Ellison, who contributed to the genetic identification; and Dr. Craig M. Young who provided funding. All coauthors contributed to manuscript preparation.

While individuals of the newly described sabellid are commonly found in authigenic carbonate along the seafloor, they can also be found atop a file clam that is an obligate epizoan on tubeworms within methane seeps. This means that epibiotic sabellids may be a meter or more above their free-living conspecifics and provides an ideal system to examine the impacts of epibiosis on a species from a chemosynthetic habitat, which had not previously been examined. In Chapter IV, I hypothesized that the difference in height above the seafloor could impact the diet of the sabellid individuals. As a sabellid species at methane seeps off Costa Rica was recently found to harbor chemosynthetic bacterial symbionts (Goffredi et al. 2020), I also investigated the microbial communities associated with the newly described sabellid between each microhabitat. Chapter IV is unpublished but will include Dr. Stilianos Louca for assistance with microbiome analysis and manuscript preparation, Dr. Erik Cordes for project guidance and assistance with data

interpretation, and Dr. Craig M. Young for funding and manuscript preparation assistance.

In Chapter V, I hypothesized that any potential differences in diet and trophic ecology may influence the overall fitness of sabellids from each microhabitat. Thus, I examined the reproductive patterns of the newly described sabellid in order to: 1) obtain the first reproductive data for any deep-water sabellid species, and 2) determine if there was a difference in reproductive output (i.e. fecundity and oocyte size) between epibiotic and free-living sabellids. Chapter V is unpublished but will include Dr. Craig M. Young as a coauthor for providing funding and assistance with manuscript preparation.

Despite the commonality of epibiotic species in marine ecosystems, many epizoans remain unidentified (Chen et al. 2021), and the biology and ecology of these organisms largely remain unknown. As these associations have the potential to drive environmental change (McLeod et al. 2020), there is a need to better understand the species diversity that exists for epizoans and their ecological roles both from a trophic perspective and due to the influences they can exert on host taxa (Wahl 1989, 2009, Chen et al. 2021). The work presented here directly addresses some of these key knowledge gaps.

CHAPTER II

PATTERNS OF DISTRIBUTION AND REPRODUCTION IN THE EPIZOOIC BARNACLE *SOLIDOBALANUS HESPERIUS* AND THEIR CORRELATION WITH THE LIFE HISTORIES OF THEIR HOSTS

This work includes coauthor Dr. Craig Young as contributor to manuscript preparation.

1. INTRODUCTION

Continental shelves are generally dominated by soft-bottom habitats made of sand and mud, and rocky substrata can be scarce and patchy. Sessile invertebrates living on marine hard bottoms often experience intense competition for settlement sites and space to grow (Osman 1977, Harder 2009, Wahl 2009). Epibiosis is a common strategy among sessile suspension- and filter-feeding species (Wahl 1989), and biological substrata increase the available surfaces that can be used for settlement (Gili et al. 1993). For example, crabs and other decapods found in areas with sandy bottoms often support epibiotic communities (Heath 1976, Gili et al. 1993, Negreiros-Fransozo et al. 1995, Key et al. 1997, Pasternak et al. 2002, McGaw 2006, Campos et al. 2022, Dvoretsky & Dvoretsky 2023). Potential advantages of epibiotic settlement on a crab include increased access to food particles due to the activities of the host (Heath 1976) and protection from predators (Key et al. 1997, Harder 2009, Wahl 2009). At the same time, epibionts must contend with host behaviors such as hiding in crevices, burial (Negreiros-Fransozo et al. 1995, Becker & Wahl 1996), and the periodic molting of the exoskeleton (Gili et al. 1993). Many epibiotic species have high rates of growth and reproduction as well as abbreviated life cycles (Jackson 1977, Seed 1985), which may allow epibionts to accommodate to the ephemeral availability of a crab exoskeleton. In this study, we sought to examine a short-lived acorn barnacle to determine if the reproductive patterns might be related to the molting of their host crabs.

Acorn barnacles are frequently found as epibionts and have been well-documented on sea turtles (Farrapeira 2010, Razaghian et al. 2019, Robinson et al. 2019), shellfish (Gabaev 2013, Silina & Zhukova 2014, Puccinelli & McQuaid 2021), corals (Newman et al. 1976, Lewis 1992, Thamrin et al. 2001, Frick & Ross 2002), crabs (Heath 1976, Key et al. 1997, McGaw 2006, Campos et al. 2022), and horse shoe crabs (Key et al. 1996, Lim et al. 2021). On crabs, epibiotic barnacles have been shown to concentrate in grooved regions of the carapace (Heath 1976, Key et al. 1997, McGaw 2006).

The barnacle *Solidobalanus hesperius* (formerly *Hesperibalanus*) is broadly distributed across the North Pacific, with most observations and studies from the Sea of Japan (Zhukova 2000, Silina 2002, Korn & Scherbakova 2012). Fewer observations come from Washington (Barnes & Barnes 1959) and Oregon (Shanks 2001, Carlton 2007, Meyer et al. 2018) despite a long-term history of presence in the area (Zullo & Marincovich 1990). *Solidobalanus hesperius* frequently settle as epibionts on crabs and cultured shellfish (Zhukova 2000, Korn & Scherbakova 2012, Gabaev 2013) and are readily outcompeted for space by other organisms such as algae (Ovsyannikova 2010). The species is reported to have a short life span of six to seven months, with few individuals surviving longer than a year (Ovsyannikova & Levin 1982), and has been described as a pioneer species (Meyer et al. 2018). However, little is known about the ecology and settlement patterns of *S. hesperius* outside the Sea of Japan, and no study has examined adult populations in the Eastern Pacific.

This study investigated aspects of distribution and life-history biology in *S. hesperius* barnacles attached to Dungeness (*Metacarcinus magister*) and red rock crabs (*Cancer productus*). Both crab species are abundant off Oregon, important to local fisheries, and can be found overlapping in several habitats (Orensanz & Gallucci 1988). While epibiotic communities for *M.*

magister and *C. productus* have been examined in British Columbia (McGaw 2006), the relationship between *S. hesperius* and the crab hosts remains unstudied. Here, we sought to investigate the reproductive and settlement patterns for *S. hesperius* in relation to the known molting patterns of the host crab species. Furthermore, recent work examining the distribution patterns of epibiotic barnacles on crabs have relied on methods that divide the host exoskeleton into broad regions (Heath 1976, Key et al. 1997, McGaw 2006). Such methods do not capture fine-scale patterns and are often difficult to replicate on new host species. We developed and utilized a novel method to examine the density and spatial distributions of *S. hesperius* on the dorsal surfaces of *M. magister*. This method can easily be applied to other species.

2. MATERIALS AND METHODS

2.1 Reproduction in *Solidobalanus hesperius*

To determine the reproductive seasonality of *Solidobalanus hesperius*, we collected live specimens monthly from host crabs between June 2022 and May 2023, except for October and November 2022. *Metacarcinus magister* and *Cancer productus* crabs with epibiotic barnacles were collected using baited crab pots deployed from either the pier at the Oregon Institute of Marine Biology campus (43°20'59"N 124°19'49"W), or the nearby docks at the Charleston Marine Life Center (43°20'43"N 124°19'41"W) during times of significant swell. Monthly collections were at least three weeks apart. Crab pots were deployed for 8-hour intervals and were checked hourly. Any crabs with attached barnacles were kept for further processing.

The carapace length and width of each crab were measured, with carapace width being defined as the distance between the bases of the tenth pair of anterolateral spines. We measured from the base of the anterolateral spines to avoid inconsistencies caused by broken or eroded spines. Carapace length was measured as the distance between the tip of the rostrum and the

posterior edge of the carapace. Epibiotic barnacles were identified using Light and Smith's manual (Carlton 2007), counted, and approximate locations on the crab host were recorded (i.e. dorsal, ventral, appendages). Crabs were then imaged using a Canon PowerShot G12 digital camera (Figure 2.1). Only barnacles identified as *Solidobalanus hesperius* were removed using a scraper and forceps and isolated into individual bowls of seawater filtered through a 0.45 μm membrane filter. This was done to ensure that hatching nauplii (if present) could be counted and tracked to an individual barnacle. For each collection, barnacles were randomly chosen across the full available size range. We measured both carnia-rostrum and lateral diameters for each barnacle before removing the visceral mass to expose the ovary and coelomic cavity. Using a Zeiss Stemi 508 microscope fitted with a Zeiss Axiocam 208 camera, micrographs were taken of the ovary (Figure 2.2), which was then ranked for gametogenic stage using the protocols of Hines (1976) and Yan et al. (2006).

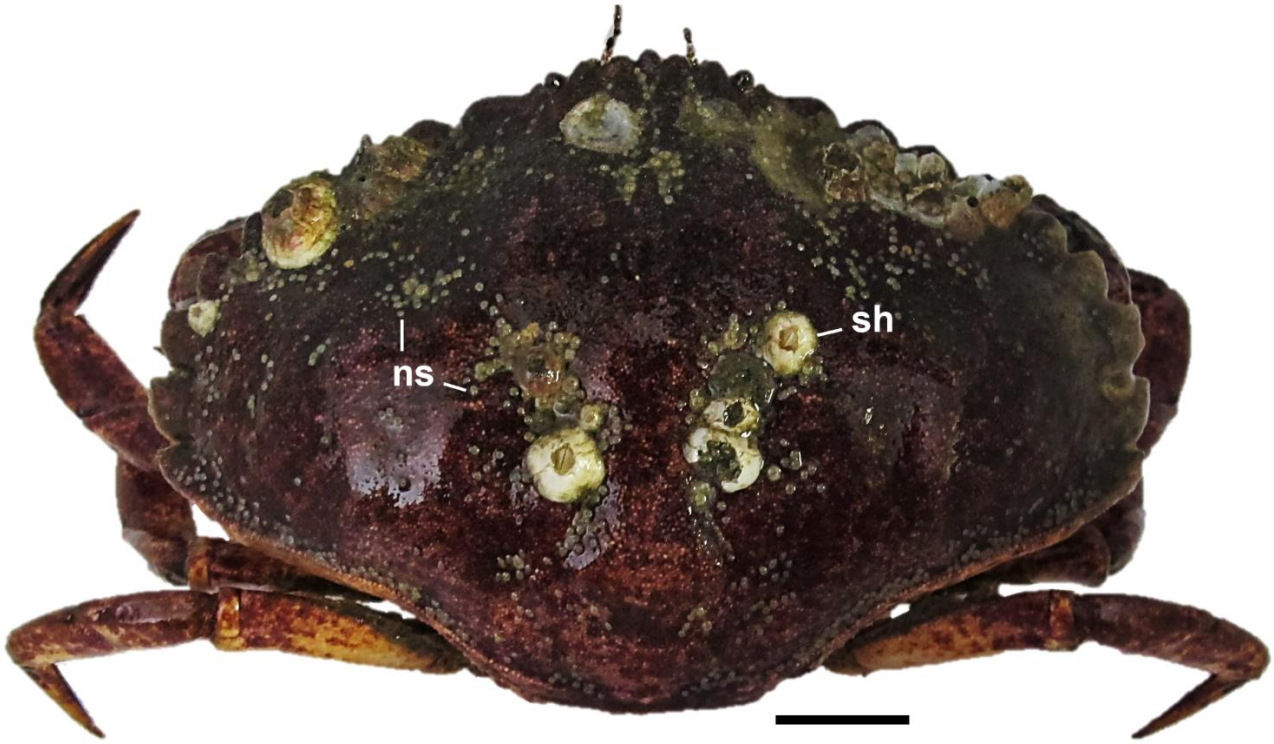

Figure 2.1. Live *Cancer productus* crab bearing adult *Solidobalanus hesperius* (sh) and newly settled individuals (ns). Scale bar represents 2 cm.

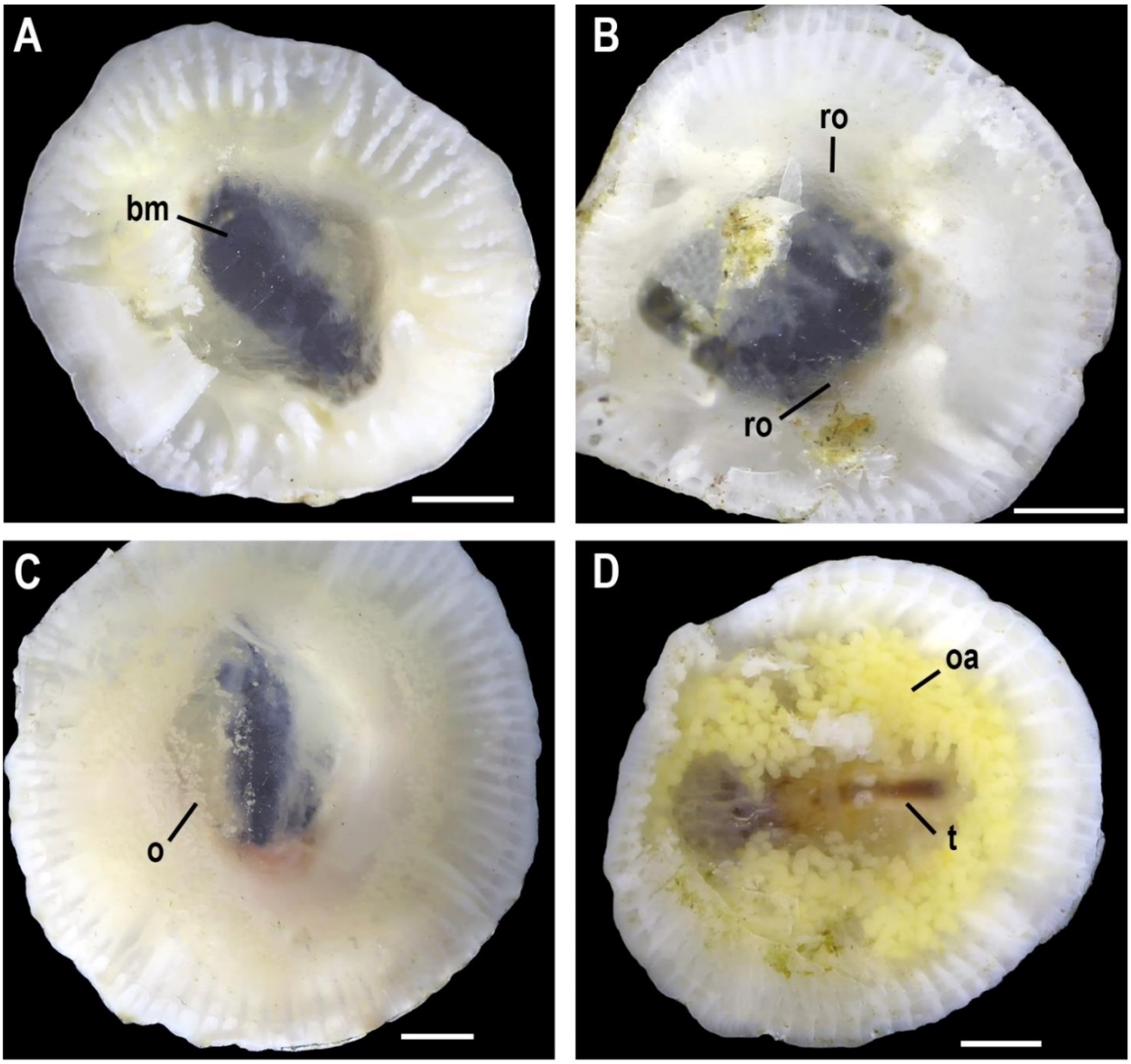

Figure 2.2. Gametogenic ranking of *Solidobalanus hesperius* ovaries: (A) Stage 1– no ovary is visible in the basal membrane (bm); (B) Stage 2 – rudimentary ovarian structures (ro) are faintly discernible as a grainy texture; (C) Stage 3 – a moderately developed ovary (o), which has a yellow coloration and slight grainy appearance; (D) Stage 4 – a fully developed, opaque yellow ovary filled with observable ova (oa) with visible testes. All scale bars represent 1 mm.

If present, brooded embryos from each barnacle were transferred into separate bowls of 0.45 μm filtered seawater and kept partially submerged in a flow-through seawater table. Water temperature was recorded daily. Water was changed daily, and developmental stage was checked every 24 hours to determine an estimated time to hatching. As the time of fertilization was

unknown, the appearance of certain features (individual cells, appendages, eyespots, first movement, appearance of pigment) was used to track progression until hatching. To ensure accuracy, only broods judged to be in "early" developmental stages (individual cells visible, but no naupliar structures) were included in the final estimates of hatching time. Hatched nauplii from all brooding *S. hesperius* individuals were counted to obtain measurements of fecundity.

2.2 Distribution of Barnacle Settlers on *Metacarcinus magister*

To examine patterns of settlement and spatial distribution of *S. hesperius* on *M. magister* hosts, molted carapaces were collected daily from a one kilometer transect spanning the sandy intertidal area in Devil's Kitchen State Park, Oregon (43°04'57"N 124°26'10"W), from April 30th, 2020 to April 30th, 2021. Each day, the total number of observed *M. magsiter* carapaces and the number with epibiotic barnacles were recorded. We carefully brushed all carapaces bearing epibiotic barnacles to remove sand. A total of 1481 carapaces were collected over the study period, and a random subsample of 610, ranging from 2-260 each month depending on availability, was selected for image analysis. Carapaces were imaged using a Canon G12 Powershot camera mounted on a tripod, and only intact carapaces were included. Images were analyzed in Adobe Photoshop (versions 23 and 24.6). Width and length of the crab carapace, as well as carnia-rostrum and lateral diameters of barnacles were measured using the Ruler Tool. Only barnacles attached to the host carapace were examined; individuals affixed on top of other barnacles were excluded. As multiple barnacle species can settle on crab hosts, such as *Balanus crenatus* and *B. glandula*, all attached barnacles were identified using the Light and Smith Manual (Carlton 2007). As individuals could lack the tergum and scutum, the shape of the shell plates were used for species identification. Newly settled barnacles were identified as individuals with carnia-rostrum diameters

less than 1.5 mm. This diameter was selected based on the growth rates described by Ovsyannikova & Levin (1982), who reported that metamorphosing *S. hesperius* cyprids were approximately 0.8 mm in diameter and individuals 2.0 mm in diameter were about a month old. There was a heightened degree of uncertainty for the species identification of smaller, newly settled individuals (<2 mm), and data may include low numbers of other species such as *B. crenatus* and *B. glandula*.

Using a novel method with Adobe Photoshop, we analyzed a subset of 483 carapaces, including representatives from every size class, to examine spatial patterns of *S. hesperius* on the dorsal surface of *M. magister*. First, images were straightened so the tenth pair of anterolateral spines were horizontal at 180º. Images were then proportionally transformed so the carapace width was scaled to 350 mm (arbitrary cutoff). Next, a digital axis origin was manually set in the middle of each carapace using the intersection of lines representing carapace length and width as guides. The center of each barnacle was then recorded and marked using the coordinate-system built into the Photoshop software. The location and number of barnacle clusters, defined as when two or more barnacles were in contact, were also recorded. The transformation of carapace length created a unified observation area and consistent coordinate plane among crabs of various body sizes. This enabled the spatial distributions to be aggregated and viewed against a hypothetical, standardized dorsal carapace.

To investigate the effects of carapace microtopography on barnacle settlement, a random, intact *M. magister* carapace lacking epibiotic barnacles was imaged using an iPhone 13 (iOSv 17.2.1). A three-dimensional point cloud and mesh were then generated using Agisoft Metashape software version 1.22.6 (2016). The resulting mesh was cleaned and aligned before a 25-step interval was applied to generate a scalar height map in CloudCompare version 2.12.4 (2022).

2.3 Statistical Analysis

All statistical analyses were conducted in RStudio version 4.2.3 (R Core Team 2023). The commonality of *C. productus* and *M. magister* bearing *S. hesperius* varied each month. Thus, we pooled measurements of oogenic frequency, fecundity, and barnacle diameter collected from both host species into a single dataset prior to statistical analysis. Linear regression analysis was used to determine the effect of barnacle size (carnia-rostrum diameter) on fecundity for the live-caught barnacles. Chi-square contingency table analyses were used to compare the frequency of oogenic stages between collection months.

Pearson correlation tests were used to examine the linear dependence of the two size metrics recorded for each species. After finding strong correlations between the barnacle diameters ($t = 162.5$, $p = 2.2e\text{-}12$) and the carapace measurements ($t = 152.99$, $p = 2.2e\text{-}12$), we used carnia-rostrum diameters and carapace width measurements in all subsequent statistical tests as proxies for barnacle and crab size. Linear regression was used to examine the relationship between the size of molted *M. magister* carapaces and the number and size of attached *S. hesperius* individuals. We also examined the relationship between carapace size and the number of barnacle clusters. The statistical distributions and variances of barnacle size on molted carapaces were examined using the Shapiro-Wilk test (Shapiro & Wilk 1965) and Levene's Test (Levene 1960), respectively. Measurements of barnacle size for each month were compared using the Kruskal-Wallis Test (Kruskal & Wallis 1952) and Dunn's *post hoc* test (Dunn 1964) with p-value adjustments made using the Holm Method (Holm 1979). To examine the spatial point patterns for individual *S. hesperius* barnacles and barnacle clusters, point distributions were compared to a Complete Spatial Randomness (CSR) model using the quadrat method with a 15 x15 division across a standardized representation of an *M. magister* carapace. Spatial distributions were then tested for both

randomness and levels of spatial clustering, with significance being determined using a chi-squared distribution.

3. RESULTS

Of the 1232 live barnacles observed on 37 captured crab hosts, the majority were on the dorsal carapace (n = 652) and relatively few were found on the ventral side (n = 210). Collected crabs had a wide range of epibiotic loads, with several individuals having only a single barnacle and one *Cancer productus* having 150 barnacles. Instances of high epibiotic load were only observed in July and August, 2022 and most of the observed barnacles during these months were identified as new settlers.

A total of 162 *Solidobalanus hesperius* barnacles were dissected to check oogenic stage and look for brooded embryos. Brooded embryos were observed at most times of the year, with peaks of higher occurrence in June and August 2022, as well as March 2023 (Table 2.1). Broods did not appear to correspond to a specific oogenic stage but were slightly more common in individuals with ovaries at stages 2 and 4 (Table 2.2). Oogenic stage frequencies varied throughout the study period ($\chi^2 = 109.2$, $p < 0.0001$; Figure 2.3). The frequency of individuals with stage 1 ovaries was significantly higher in January and April, and significantly lower in July. Individuals with stage 2 ovaries were observed in every month except March and May and had statistically significant increases in abundance in December, January, and February (Figure 2.3). Individuals with stage 3 ovaries were not observed in December, January, and April. However, stage 3 individuals were significantly more common in July, August, and May. Mature stage 4 ovaries were observed in every month except January and were significantly more common in November and March (Figure 2.3).

Table 2.1. Proportions of observed *Solidobalanus hesperius* barnacles with brooded embryos by month, starting in June 2022 and concluding in May 2023.

Month	Total Number of Barnacles Observed	Number with Broods	Proportion with Broods (%)
June	16	8	50
July	19	4	21.1
August	19	12	63.2
November	16	2	12.5
December	10	0	0
January	11	0	0
February	9	2	22.2
March	21	8	38.1
April	21	3	14.3
May	20	2	10

Table 2.2. Proportions of brooded embryos corresponding to each ovarian gametogenic stage for *Solidobalanus hesperius* collected between June 2022 and May 2023.

	Total Observed	Number with Broods	Proportion (%)
Stage 1	43	7	16.3
Stage 2	19	6	31.6
Stage 3	43	9	20.9
Stage 4	54	18	33.3

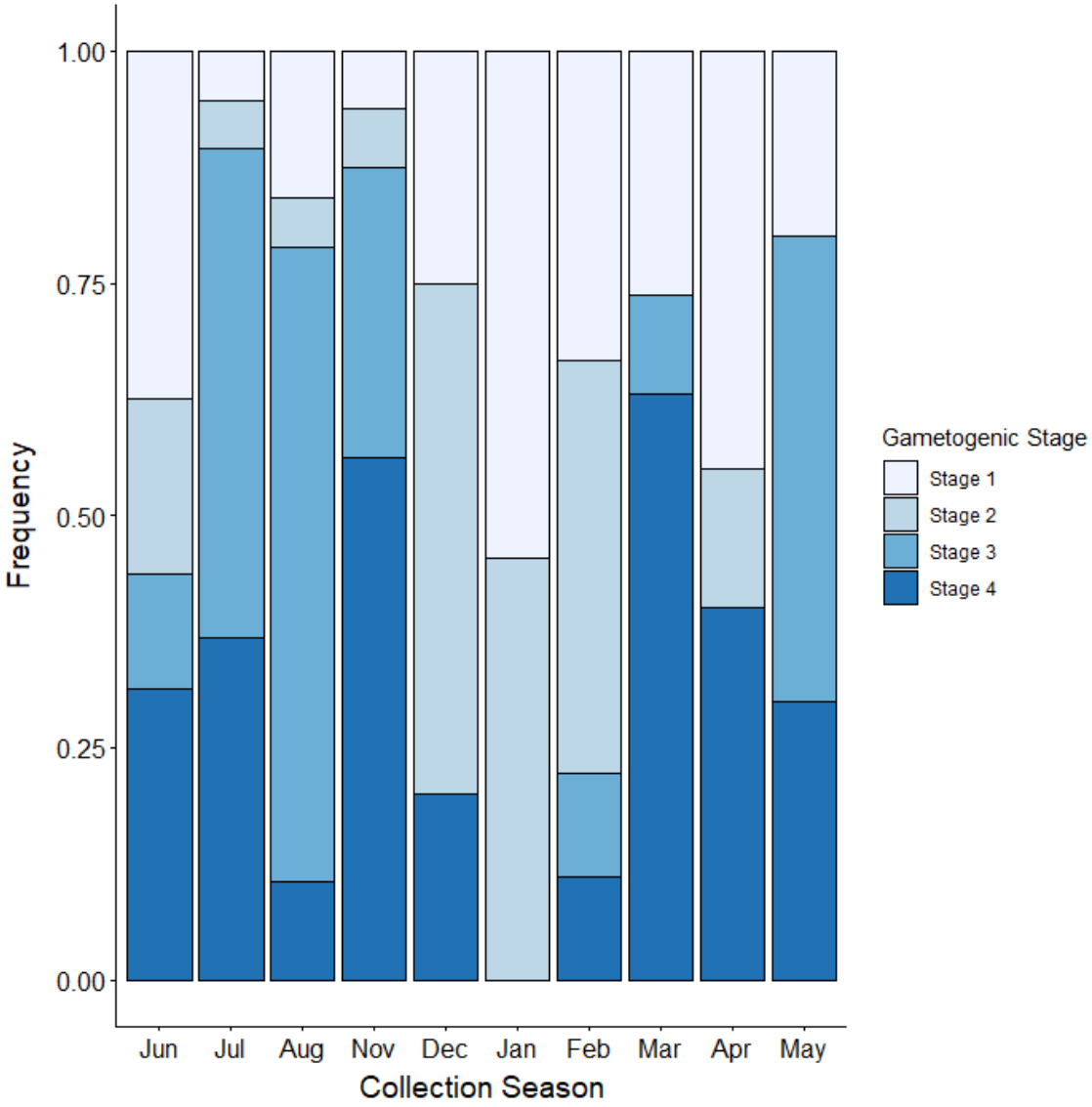

Figure 2.3. Percent frequency distribution of each oogenic stage for each collection month, starting in June 2022 and concluding in May 2023. The number of *Solidobalanus hesperius* individuals examined is shown in Table 2.1. *Solidobalanus hesperius* individuals collected from both *Metacarcinus magister* and *Cancer productus* hosts were pooled to compensate for erratic collections from each host.

A total of 41 live *S. hesperius* barnacles were observed with brooded embryos. Of these, 30 could be used for fecundity counts and 19 were identified as "early" in development. Barnacles collected from the same host crab often had brooded embryos at varying stages of development, with some broods hatching upon dissection and others being recently deposited. Barnacle fecundity increased with body size in a roughly linear relationship ($R^2 = 0.45$, $p < 0.0001$), with larger

individuals often having larger broods (Figure 2.4A). The sizes of reproductive *S. hesperius* individuals varied; the smallest individual with a stage 4 ovary had a diameter of 3.8 mm and the largest had a diameter of 14 mm. The smallest individual with mature testes was 3.0 mm in diameter, and the smallest with an observed brood was 4.5 mm.

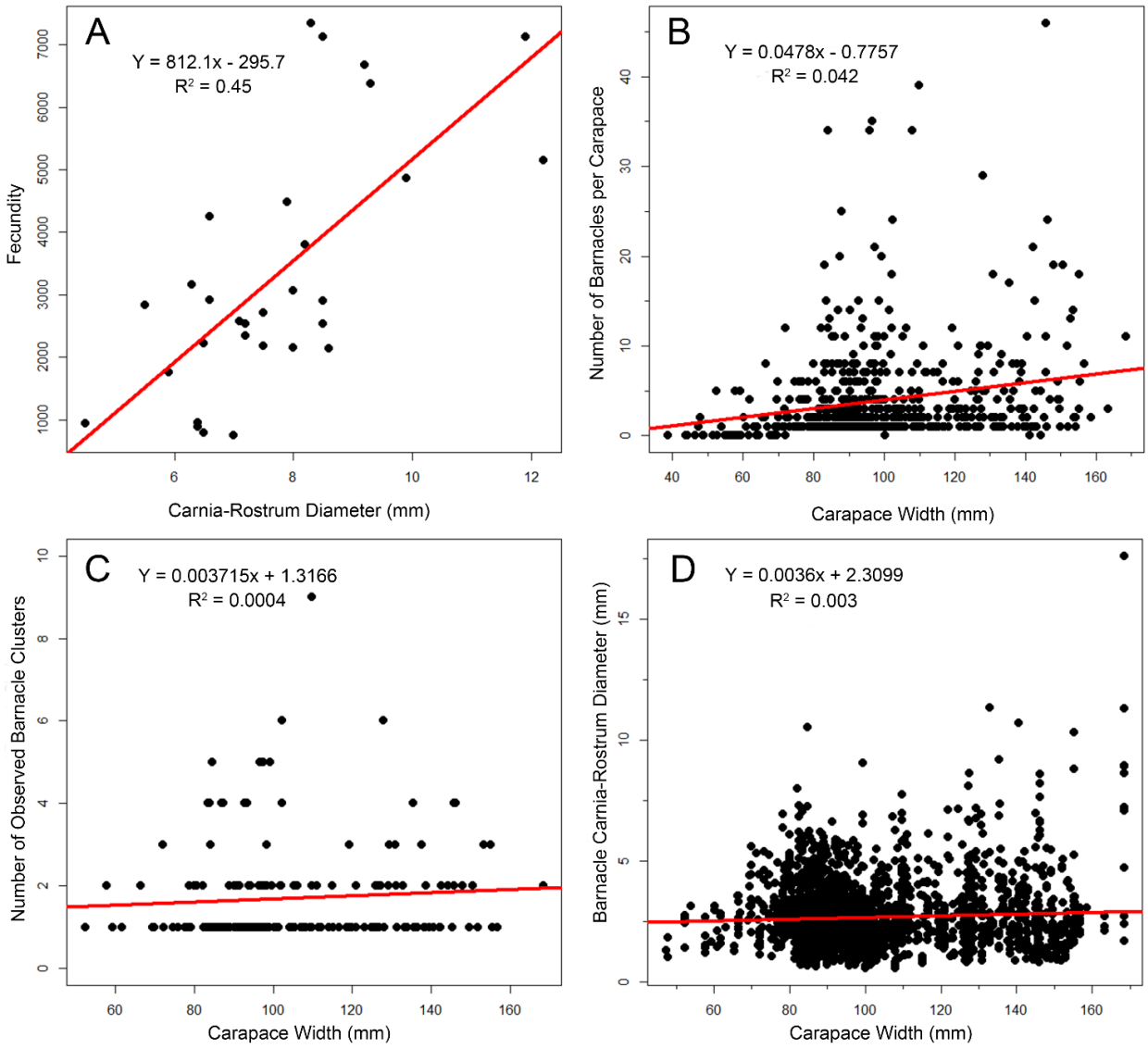

Figure 2.4. Linear relationships between: (A) barnacle fecundity and carnia-rostrum diameter for all brooding females observed in this study (n = 30); (B) the number of barnacles by molted carapace width; (C) the number of observed barnacle clusters by molted carapace width; (D) the carnia-rostrum diameters for barnacles by molted carapace width. The equations and R^2 values for each regression are indicated. Barnacles are *S. hesperius* and molted carapaces are from *M. magister*.

Embryos developed rapidly, with all 19 broods beginning to hatch as nauplii five to seven days after first observation. Isolated broods were exposed to natural fluctuations in seawater temperature, which ranged from 10ºC to 15ºC depending on the season. Broods collected in February and March 2023 experienced colder temperatures (10 – 12ºC) compared to those collected in July and August 2022 (14-15ºC). Broods exposed to temperatures around 12ºC hatched in an average of 6.7 days after first observation (SD ± 0.6), while those reared in temperatures around 14.5ºC hatched in an average of 5.7 days after first observation (SD ± 0.9).

From the molted *Metacarcinus magister* carapaces, the morphometrics of 2158 *S. hesperius* individuals were recorded. Mean *S. hesperius* sizes fluctuated each month during the study period (Figure 2.5A; Table 2.3). The largest body sizes were seen in winter (Nov-Jan) and the next highest in late spring (May-Jun). Both peaks were followed by small average body sizes in February and August, respectively (Figure 2.5A). The lowest mean body sizes, seen in august, correspond to the largest settlement pulse observed during the study (Figure 2.5B). Although this trend could include data from *Balanus crenatus* and *B. glandula*. A similar peak was also seen to a lesser degree in July and September, but the proportions of new settlers remained at approximately 20% of the population for the rest of the year (Figure 2.5B). Of the 2158 *S. hesperius* examined for morphometrics, 926 were observed in clusters and a total of 325 clusters were identified. Clusters consisted of an average of 2.5 (SD ± 1.8) individuals, although clusters with 19 *S. hesperius* were also observed.

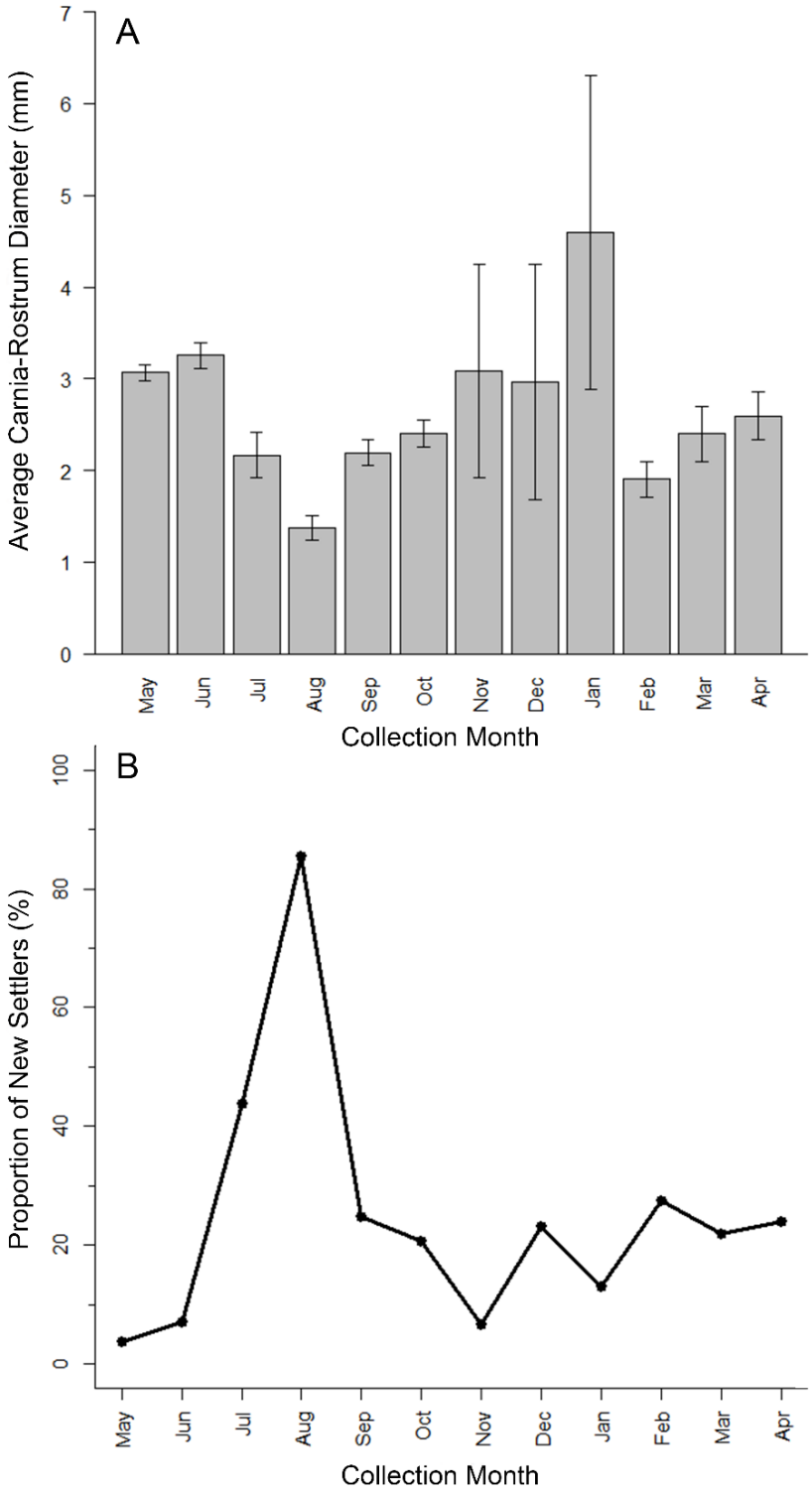

Figure 2.5. (A) The average carnia-rostrum diameter for observed *Solidobalanus hesperius* barnacles attached to molted *Metacarcinus magister* carapaces each month during the collection period, beginning in May 2020 and ending in April 2021. Error bars represent 95% confidence intervals. (B) The proportion of new settlers, defined as individuals smaller than 1.5 mm in carnia-rostrum diameter, observed each month starting in May 2020 and concluding in April 2021.

The number of *S. hesperius* barnacles did not increase in relation to *M. magister* carapace width ($R^2 = 0.042$, $p < 0.0001$; Figure 2.4B). Crabs 75 mm and larger often had more than 10 barnacles, but many had only a single *S. hesperius*. Similarly, the number of barnacle clusters was not dependent on the size of the crab host ($R^2 = 0.0004$, $p > 0.1$), with crabs frequently having only one to two clusters regardless of size (Figure 2.4C). Carnia-rostrum diameters of barnacles also varied greatly on *M. magister* carapaces regardless of host size ($R^2 = 0.003$, $p < 0.001$; Figure 2.4D).

The coordinate locations of 1738 individual barnacles and 237 *S. hesprius* clusters were identified in relation to 483 host crab carapaces. The spatial distributions were pooled and viewed against a hypothetical, standardized dorsal carapace (Figure 2.6A). Spatial distributions for both individual barnacles and *S. hesperius* clusters were non-random (clusters: $X^2 = 216.9$, $p < 0.0001$; individuals: $X^2 = 3323.6$, $p < 0.0001$) and strongly aggregated in space (clusters: $X^2 = 216.9$, $p < 0.0001$; individuals: $X^2 = 3323.6$, $p < 0.0001$). *Solidobalanus hesperius* individuals and clusters were commonly found within areas marked by depressions in the host *M. magister* dorsal carapace (Figure 2.6B), notably in the frontal area behind the rostrum, the depressions in the central region of the carapace above the brachial lobes, and along the outer-most edge of the carapace. The epi- and mesobrachial regions, characterized by higher ridges on the carapace had a lower barnacle presence (Figure 2.6).

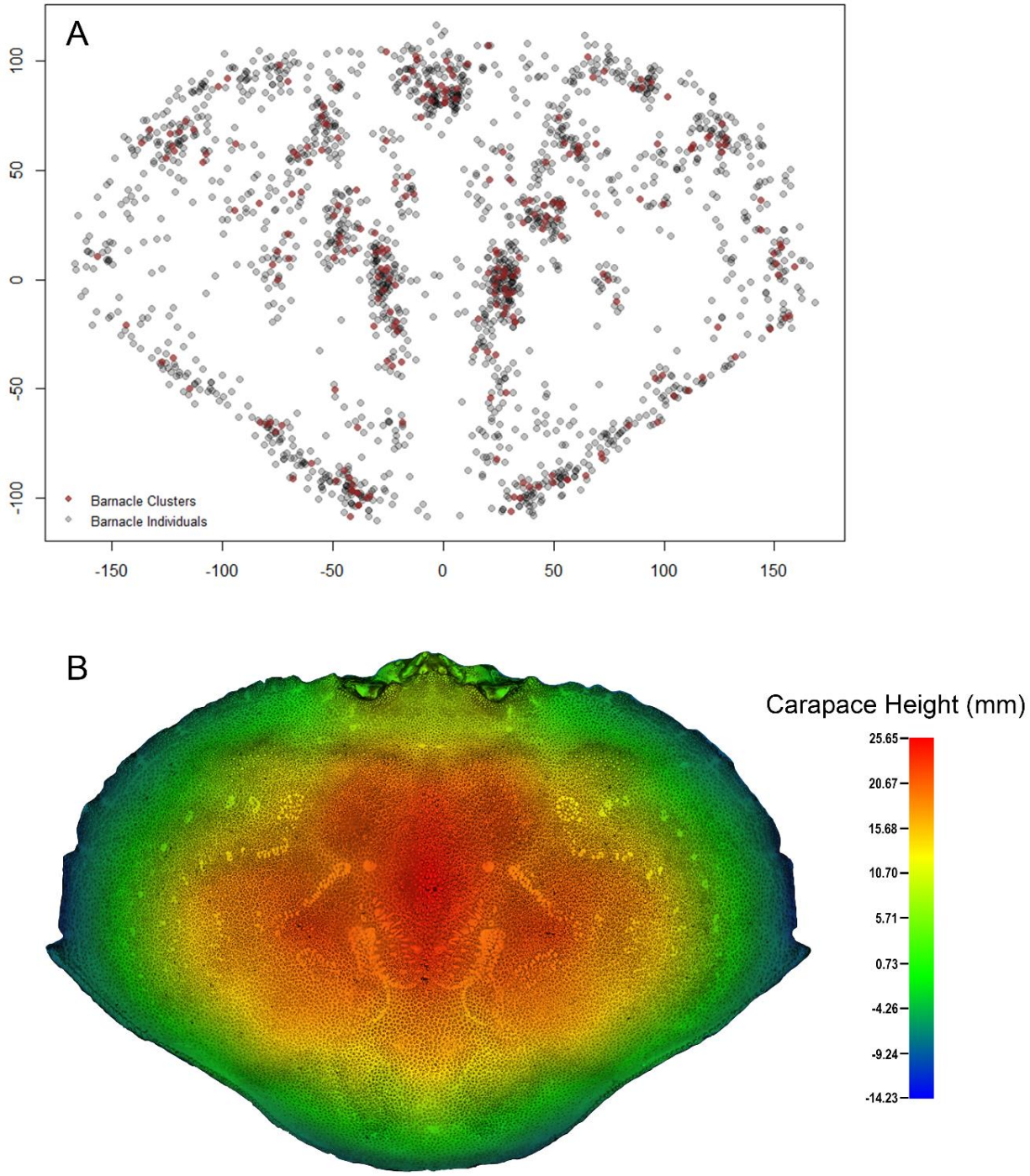

Figure 2.6. (A) Aggregated distribution of all individual *Solidobalanus hesperius* barnacles (grey) and barnacle clusters (red) across a standardized representation of the dorsal surface of a *Metacarcinus magister* carapace. (B) Color coded visualization of the dorsal microtopography present on the dorsal carapace of a *M. magister*. The bar indicates carapace height scaling (cooler colors indicate lower areas, warm colors indicate higher regions). The scan was made of an individual 145 mm in width that had no epibiotic barnacles.

4. DISCUSSION

The majority of epibiotic barnacles were found on the dorsal carapaces for both *Metacarcinus magister* and *Cancer productus* hosts, as opposed to the ventral carapace and appendages for each species. Similar trends have been reported for other epibiotic taxa on crab hosts (Gili et al. 1993, Negreiros-Fransozo et al. 1995, Key et al. 1997, Dvoretsky & Dvoretsky 2023), and several key factors likely influence this pattern. The dorsal carapace is likely the most exposed portion for both *M. magister* and *C. productus* hosts. Both species are known to bury themselves in sand with only portions of their dorsal carapace remaining visible (Bellwood 2002) and can remain covered for prolonged periods of time (McGaw 2005). The ventral carapace likely experiences higher rates of abrasion, either from the action of burial in sand or by movement of the host over the seafloor (Negreiros-Fransozo et al. 1995), which may result in a lower abundance of *S. hesperius* barnacles. Furthermore, the dorsal surfaces of *C. productus* and *M. magister* are more exposed to light and cyprid larvae of other species have been shown to use light fields to aid in orientation before settlement (Visscher 1928, Crisp 1974).

Larval settlement for *Solidobalanus hesperius* appears to consistently occur in late summer for populations in Oregon. In addition to the patterns seen here, the only other reported recruitment event we have found for this species was also documented by Meyer et al. (2018) between August and October 2014. These results reflect similar findings in the Sea of Japan, where *S. hesperius* larval recruitment peaks from August into the fall (Ovsyannikova & Levin 1982, Korn 1999, Gabaev 2013). It has been hypothesized that *S. hesperius* settlement is influenced by changes in the velocity of benthic currents (Ovsyannikova & Levin 1982), and indeed observations off Oregon seem to corroborate this (Meyer et al. 2018).

Mature ovaries with discernible ova were observed every month between June 2022 and

May 2023, with January being the sole exception. The consistency in oogenic stages, and number of broods, observed throughout the sampling period indicate that *S. hesperius* reproduction may be continuous at the population level and that larvae could be produced throughout the year. Continuous reproduction has also been reported for populations in the Sea of Japan (Ovsyannikova & Levin 1982), where spawning was observed throughout the year. The lack of advanced oogenic stages and broods seen in winter (Dec-Jan) months in this study could reflect a reduced sample size in those months. Broods were particularly abundant in the June and August collections. This species is known to feed on detritus, with an increasing dependence on diatoms as individuals grow in size (Zhukova 2000). Diatoms often become increasingly abundant off Oregon throughout the summer season due to upwelling (Du & Peterson 2014) and could provide *S. hesperius* the nutrition needed to increase reproductive output.

Brooded embryos were observed in individuals of various oogenic stages. This could indicate the potential for a rapid turnaround between brood cohorts, which was supported by the rapid developmental times for broods. Brooding times are known to vary widely among barnacle species and across temperature ranges within species, with hatching for *Balanus crenatus* occurring between 15 and 37 days (Hoeg et al. 1987), and between 22 and 27 days for *B. glandula* (Hines 1976). As one-month-old *S. hesperius* are approximately 2.0 mm in diameter (Ovsyannikova & Levin 1982), the small body sizes for reproductively mature individuals seen here provide evidence for rapid development and early reproduction in this species.

While *S. hesperius* larvae may be present within the plankton throughout the year, peaks in settlement and brooding in *S. hesperius* seemingly correlate with the molting patterns in host crabs. *Cancer productus* are known to molt from June to August (Knudsen 1964), and *M. magister* molt from March through June (Rasmuson 2013). The increased number of competent cyprids in July

and August could allow for a large and effective recruitment on the abundant, newly hardened crab carapaces. As the adults for both host crab species are known to molt annually, this peak in *S. hesperius* settlement ensures that most individuals have the maximal amount of time to grow and reproduce. Like most crab species however, *M. magister* and *C. productus* juveniles can molt several times within a year. The continuous production of larvae and settlement of *S. hesperius* throughout the year could ensure that this species is able to take advantage of any available biological substratum. This could include crabs, but also various mollusk species such as scallops (Silina & Zhukova 2014). Rapid maturation and a short life cycle of this species probably increase the likelihood that individuals on young crabs can reproduce before their host molts.

When settling on a crab host such as *M. magister*, *S. hesperius* individuals appear to favor attachment in low points of the microtopography of the dorsal carapace. This is expected, as barnacles are well known to settle in depressions and areas of increased topography (Crisp & Barnes 1954). Similar patterns have also been documented in other cases of barnacle epibiosis on crabs (Heath 1976, Key et al. 1997, McGaw 2006). Barnacles settled on the higher regions of the carapace are more exposed to abrasion when the host crab buries into sand (Negreiros-Fransozo et al. 1995, Key et al. 1997).

Solidobalanus hesperius is well adapted to make use of ephemeral, biological substrata. While this barnacle species is also reported to settle on bivalves and gastropods, *S. hesperius* appears strongly *r* – selected (Pianka 1970). Decapod crustacean exoskeletons have been described as unsuitable for a variety of epibiotic taxa due to their temporary nature (Gili et al. 1993). However, the quick brooding times, coupled with the correlation of *S. hesperius* reproduction and settlement with the molting patterns of common crab species, allow *S. hesperius* to maximize the potential benefits of epibiotic life. These benefits have been well described (Wahl 1989) and

reviewed (Key et al. 1996). Specifically for *S. hesperius*, which is readily outcompeted for space (Ovsyannikova 2010), settlement on crabs and other organisms likely free individuals from competitive pressure.

The effects of epibiotic organisms on decapod crustacean hosts is an active area of research. The nature and composition of the epibiotic community found on the host carapace is known to provide information about the growth, molting frequency, and behavior of the host (Abelló et al. 1990, Gili et al. 1993). This can be particularly useful when the host species is targeted by fisheries, as is the case for both *M. magister* and *C. productus*. Furthermore, examinations of epibiotic communities from a biodiversity prospective can provide insight for shifts in species abundance patterns (Farrapeira 2010, Lim et al. 2021, Dvoretsky & Dvoretsky 2022, 2023). In general though, many studies on epibiota and epibiotic barnacles seek to understand the nature of the association and its potential influence on the health of the host, especially as a high epibiotic load is known to have negative impacts (Key et al. 1997, Ovsyannikova 2010, Babu et al. 2012, Gabaev 2013, Campos et al. 2022). While knowledge of the biology and ecology of the epibiotic species can be gleaned from these studies (Dvoretsky & Dvoretsky 2022), research directly investigating the epibiotic species remains comparatively rare.

5. CONCLUSIONS

By directly examining the reproductive patterns of *Solidobalanus hesperius*, we revealed that this species has an extremely accelerated life history marked by the early onset of reproductive maturity. Furthermore, by reproducing year-round and having a rapid reproductive cycle, *S. hesperius* can accommodate settlement on an unpredictable and ephemeral substratum. Many barnacle individuals die, as evidenced by the high numbers of barnacles on molted *Metacarcinus magister* crab carapaces. The reproductive strategies described here ensure that enough members

of the population can reproduce successfully. We also found that the spatial distributions of *S. hesperius* closely followed the microtopography of the host carapace, and likely enabling individual barnacles to persist despite detrimental host behaviors such as burial.

BRIDGE

In Chapter II, I focused on examining how a short-lived epibiotic barnacle species has adjusted its reproductive patterns to accommodate life on an ephemeral host crab exoskeleton. Nex, I investigated a similar relationship, but in a facultative epibiotic sabellid polychaete found in the specialized environment of hydrocarbon methane seeps. For Chapter III, I focused on describing the morphology and phylogenetics of the sabellid polychaete.

CHAPTER III

A NEW GENUS AND SPECIES OF FEATHER DUSTER WORM (ANNELIDA, SABELLIDA) FROM SHALLOW HYDROCARBON SEEPS IN THE GULF OF MEXICO

This chapter contains unpublished coauthored material. Dr. Mariana Tovar-Hernandez assisted with the morphological description, Christina Ellison contributed to the genetic analysis and phylogenetic identification, and Dr. Craig Young provided funding. All coauthors contributed to manuscript preparation. This chapter is written in the style of *Biodiversity Data Journal*.

1. INTRODUCTION

Polychaetes in the family Sabellidae are diverse with 512 named species across 42 genera (Capa et al. 2021). Sabellids are also recognized as a ubiquitous group with representatives appearing in a variety of marine habitats, although most species have been described from shallow-water systems (reviewed by Capa et al. 2019). However, sabellids have been reported up to depths of 9735 meters (Levenstein 1961). Sabellid diversity in deep-water habitats is relatively undescribed, with only a few reports identifying sabellids to genus name only and others identifying only to taxonomic family (Capa et al. 2021).

Only two sabellid species have been identified from deep-sea chemosynthetic habitats, both belonging to the genus *Bispira* Krøyer, 1856. *Bispira wireni* (Johansson 1922) was described from hydrothermal vent systems in the Okinawa Trough off southern Japan at a depth of 1335 meters (Capa et al. 2013). The second species was identified to the genus *Bispira*, and was found at methane seeps from Jaco Scar, Costa Rica at depths of 1768 to 1887 meters depth (Goffredi et al. 2020). This latter species is a newly identified example of chemosynthetic bacterial symbiosis, where strains of methanotrophic Methylococcales bacteria were embedded in the cuticle of the

radioles (Goffredi et al. 2020).

In the present study, we report findings of a third sabellid species observed at chemosynthetic systems. This species is found in hydrocarbon seeps on the Upper Louisiana Slope in the northern Gulf of Mexico. Individuals are facultative, hyper-epibionts and can be found burrowed into the valves of *Acesta oophaga* Järengren, Schander and Young, 2007 file clams as well as free-living within authigenic carbonate. These worms have a mix of morphological features like those described in the genera *Perkinsiana* Knight-Jones, 1983 and *Pseudopotamilla* Bush, 1905, but not the genus *Bispira.* The new species described here also has several unique features, allowing for the establishment of a new genus and a new species. These findings were also supported through genetic analysis.

2. MATERIALS AND METHODS

2.1 Sample Collection

Specimens were collected from the hydrocarbon seeps Bush Hill, Green Canyon 234, and Brine Pool NR1 using either ROV *Jason* deployed from the R/V *Thomas G. Thompson* (expedition TN391) or HOV *Alvin* deployed from the R/V *Atlantis* (expedition AT50-04). Collections occurred in June 2021 and October 2022, respectively. On each collection, individuals from both authigenic carbonate and *A. oophaga* valves were gathered using the vehicle manipulator arm and subsequently transported to the surface in insulated collection boxes. After recovery to the ship, carbonate slabs were broken into smaller pieces using a hammer and chisel and sabellids were isolated from both substrate types using dental picks. Samples were then fixed in buffered formalin, washed in water, and stored in 70% ethanol. Tissues used in genetic work were frozen to -80ºC at sea. Tissue samples from two additional sabellid individuals were post-fixed in Osmium

Tetroxide for two hours before being dehydrated in a graded ethanol series ending in two 100% ethanol baths for 20-minutes each. The tissues were then critical point dried with CO_2, mounted on stubs, and coated with 20 nm of gold. The stubs were viewed on a Tescan Vega II SBU and ZEISS Ultra-55 scanning electron microscope.

Complete specimens were measured for their mid-thoracic width, trunk length (from chaetiger 1 to pygidium) and radiolar crown length. Other features such as the number of radiolar pairs, thoracic, and abdominal segments were also counted. Description of the new species is based on the holotype, with paratype variations indicated in parentheses. The thoracic glandular pattern was described by staining specimens with methyl green.

Type specimens were deposited in the following collections: Colección Poliquetológica de la Universidad Autónoma de Nuevo León (UANL) and Colección Nacional de Anélidos Poliquetos de México, Instituto de Ciencias del Mar y Limnología, Universidad Nacional Autónoma de México (CNAP–ICML, UNAM).

2.2 Species Abundance Estimates

Observations of sabellid abundance were quantitatively examined from video footage from either the ROV *Jason* in June 2021, or the HOV *Alvin* October 2022. Representative image frames were randomly selected for analysis from video footage of sabellid collections. As the primary mission for the dives was to conduct sample collections and to place scientific instrumentation, clear and continuous footage of the seafloor was scattered. Additionally, scaling lasers were haphazardly enabled throughout the dives and were often not visible in image frames. Thus, the visible surface area for each frame (the area that is well lit and in focus) was estimated using a scaling approach based on observable equipment present in the image. The equipment used had

known dimensions and helped to ensure consistent and accurate scaling. Visible sabellid tubes within each frame were counted using ImageJ (NIH). Epibiotic sabellid density was measured by counting the number of tubes present on each valve of host *Acesta oophaga*. All collected *A. oophaga* had their shell length and width recorded.

2.3 Molecular Analysis

We extracted DNA from each specimen using DNEasy Blood and Tissue Kit (Qiagen) following the manufacturer's protocol. We attempted to amplify and sequence the Folmer region of the mitochondrial protein-coding gene cytochrome c oxidase I from each individual using universal primers LCO1490 5' GGTCAACAAATCATAAAGATATTGG and HCO2198 5' TAAACTTCAGGGTGACCAAAAAATCA (Folmer et al. 1994). Each PCR was performed in a 20 µL volume using 2 µl of unquantified DNA extract, 200 µM of dNTPs (NE Biolabs), 500 nM of each primer (IDT) and 1 unit of Go Taq polymerase with supplied buffer (Promega). We used the following thermocycling profile: initial denaturation at 95°C for 2 min, followed by 35 cycles of: 1) denaturation, 95°C, 40 s; 2) primer annealing, 45°C, 40 s; 3) primer extension, 72°C, 1 min; followed by final extension at 72°C for 2 min. We verified PCR products with gel electrophoresis and purified products producing single bright bands of expected size using SV Wizard Gel and PCR clean up kit (Promega) according to the manufacturer's protocol. PCR products were sequenced at Sequetech (Mountain View, CA) in both directions using PCR primers.

We used resulting chromatograms (.ab1 files) in Geneious Prime (Biomatters) for all initial sequence processing. Sequences with a low percentage of high-quality bases (< 50%) were excluded from subsequent analysis. For included sequences, we trimmed off PCR primers and low-quality end-regions, aligned opposing strands, and manually resolved disagreements between

them to produce a consensus sequence. Nucleotide bases with combined Phred scores of < 20 were converted into "N"s in the consensus sequence or trimmed off. Subsequently, we translated each consensus sequence into amino acids using the Invertebrate Mitochondrial code and checked for the presence of stop codons.

We used NCBI nucleotide BLAST search (GenBank) to screen for contamination and aid in species identification. The top 20 BLAST matches (based on highest pairwise identity to our specimens) were downloaded and included for subsequent analysis. The dataset was then pared to retain a single sequence per species/location and exclude sequences originating from beyond the Americas. Due to the appearance of morphological features commonly present in both *Perkinsiana* and *Pseudopotamilla* genera, sequences from both these genera were specifically included in phylogenetic analyses: the type species of *Pseudopotamilla* (*P. reniformis* (Bruguière 1789) and *Perkinsiana fonticula* (Hoagland 1919), both from their natural range of distribution. In addition, species of *Eudistylia* Bush, 1905 and *Schizobranchia* Bush, 1905 were also included since they constitute part of the apomorphic clade including *Perkinsiana* and *Pseudopotamilla*.

Resulting sequences were aligned using the MAFFT plug-in in Geneious Prime using default parameters. The alignment was visually inspected for gaps and irregularities. The final COI alignment was trimmed to 594 bp and contained a total of 24 sequences (including seven generated in this study). The resulting alignment was used to construct a neighbor-joining tree (not shown) to evaluate pairwise diistances among sequences in the study. All original sequences produced in this study have been deposited in Barcode of Life Datsystems (BOLD) and GenBank (Table 3.1).

We used MEGA X (ver.10.1.8): Molecular Evolutionary Genetics Analysis across computing platforms (Kumar et al. 2018) on the same alignment to determine the best fitting substitution model for the data (using "Find Best DNA/Protein Models ML") and to estimate the

phylogeny using Maximum Likelihood. The best fitting model for the dataset was HKY+I, but not by a very wide margin, so we used the top six models to assess the resulting phylogeny's sensitivity to the substitution model: HKY+I, HKY+G+I, TN93+I, TN93+G+I, GTR+I, GTR+G+I; (I = has invariant sites G = has a gamma distribution of the data). For each estimation we used 1,000 bootstraps, SPR (subtree pruning regrafting heuristic method) level 5, and a branch swap filter of "very strong." For all other settings, we used the default.

Table 3.1. Table of specimen IDs of *Seepicola viridiplumi* sp, nov. and BOLD accession numbers.

Collection Location	Latitude	Longitude	Depth (m)	Sample ID	BOLD Process ID
Bush Hill	27.78237117	-91.50830855	543	BHSa26	GMSE004-24
				BHSa46	GMSE005-24
				BHSa68	GMSE006-24
				BHSa70	GMSE007-24
Green Canyon 234	27.74614894	-91.22191704	538	GCSa44	GMSE008-24
				GCSa47	GMSE009-24
				GCSa49	GMSE010-24

3. RESULTS

3.1 Systematics

Order SABELLIDA Latreielle, 1825

Family SABELLIDAE Latreille, 1825

Seepicola new genus

Type species. *Seepicola viridiplumi* n. sp., herein designated, by monotypy.

ZOOBANK RECORD: urn:lsid:zoobank.org:act:71A03636-1E5F-4734-85F1-C69906B4D666

DIAGNOSIS

Medium-size species in the subfamily Myxicolinae with a moderate number of radioles arranged in semicircular radiolar lobes. Radiolar crown symmetrical with all radioles nearly same length. Radiolar crown with basal, dorsal and ventral flanges. Palmate membrane, radiolar flanges and radiolar eyes absent. Pinnules paired. Radiolar tips entire (unbranched). Dorsal lips with mid-rib (radiolar appendages) and dorsal pinnular appendages. Ventral lips and parallel lamellae present. Ventral sacs absent. Ventral peristomial chambers present, located between the ventral lappets and parallel lamellae. Peristomial loops absent. Peristomial eyes present. Collar chaetae narrowly hooded. Glandular ridge on chaetiger 2 absent. Ventral shields are well differentiated. Thoracic chaetae with a superior group of narrowly hooded chaetae, inferior group with paleate chaetae. Neurochaetae with tear-drop shaped companion chaetae and avicular uncini (teeth above main fang of equal size, hood absent, breast well developed, expanded, handles of medium length). Interamal eyespots absent. Abdominal chaetae elongate, broadly hooded (a basal broad knee and distal end narrowing abruptly *sensu* Knight-Jones 1983). Abdominal avicular uncini with teeth above the main fang of equal size, breast well developed, short handled. Pygidium without anal cirrus. Pygidial eyes absent.

ETYMOLOGY

The genus name refers to the fact that the type species was found in hydrocarbon seeps (Seeps, combined with the Latin -cola = ‘dweller’). It should be regarded as invariant compound noun in apposition (Read et al. 2017; pg. 19).

Seepicola viridiplumi sp. nov.

Figures 1-10

ZOOBANK RECORD: urn:lsid:zoobank.org:act:78FAA822-18F2-4D0E-A31C-FA223BC469E6

TYPE MATERIAL:

Holotype (CNAP–ICML, UNAM, 0000): BHSa144, Cruise Code TN391, 14 June 2021, 27.78237117, -91.50830855, 562 m, epibiotic on *Acesta oophaga.*

Paratype 1 (CNAP–ICML, UNAM, 0000): BPSa115, Cruise Code AT50-04, 16 October 2022, 27.723677, -91.279372, 651 m, epibiotic on *Acesta oophaga.*

Paratype 2 (CNAP–ICML, UNAM, 0000): BHSa167, Cruise Code TN391, 14 June 2021, 27.78237117, -91.50830855, 562 m, epibiotic on *Acesta oophaga.*

Paratype 3 (UANL-0000): BPSa92, Cruise Code AT50-04, 16 October 2022, 27.723677, -91.279372, 651 m, epibiotic on *Acesta oophaga.*

Paratype 4 (UANL-0000): BHSa127, Cruise Code AT50-04, 15 October 2022, 27.723677, -91.279372, 562 m, free-living in authigenic carbonate.

Paratype 5 mounted in stubs 1 and 2 for SEM (CNAP–ICML, UNAM, 0000): BPSa88, Cruise Code AT50-04, 16 October 2022, 27.723677, -91.279372, 651 m, epibiotic on *Acesta oophaga.*

Paratype 6 mounted in stubs 4 and 5 for SEM (CNAP–ICML, UNAM, 0000): BPSa123, Cruise Code AT50-04, 16 October 2022, 27.723677, -91.279372, 651 m, epibiotic on *Acesta oophaga.*

DIAGNOSIS

Radiolar crown symmetrical with all radioles nearly same length, except 2-3 ventral-most developing radioles that are shorter than the dorsal radioles. Radiolar tips variable: long-filiform or short button-like. Those radioles with short tips have a massive, unknown brown tissue along their internal margins. Peristomial chambers ventrally located between the ventral lappets and parallel lamellae. Anterior peristomial ring is slightly exposed dorso-laterally between dorsal pockets and the lateral collar margin. Mid-dorsal collar margins fused to fecal groove.

DESCRIPTION

Gregarious, facultative hyper-epibiotic sabellid with individuals found free-living in authigenic carbonate cements and on the file clam *Acesta oophaga* Järnegren, Schander, and Young, 2007 (Figure 3.1). Commonly found at depths between 562 and 651 meters. Radiolar crowns a soft green and body a cream to red-brown color in live worms. Preserved worms have a dark to pale cream colored body with radiolar crowns appearing whitish. Radiolar crown length is 7.2 mm (4 – 7.5 mm) with 12 pairs of radioles (all paratypes with 12 pairs). Trunk length is 39 mm (28 – 32 mm) with a body width of 2.5 mm (1.4 – 2 mm). Thoracic segments number 15 (13 – 18) with 121 abdominal chaetigers (97 – 143).

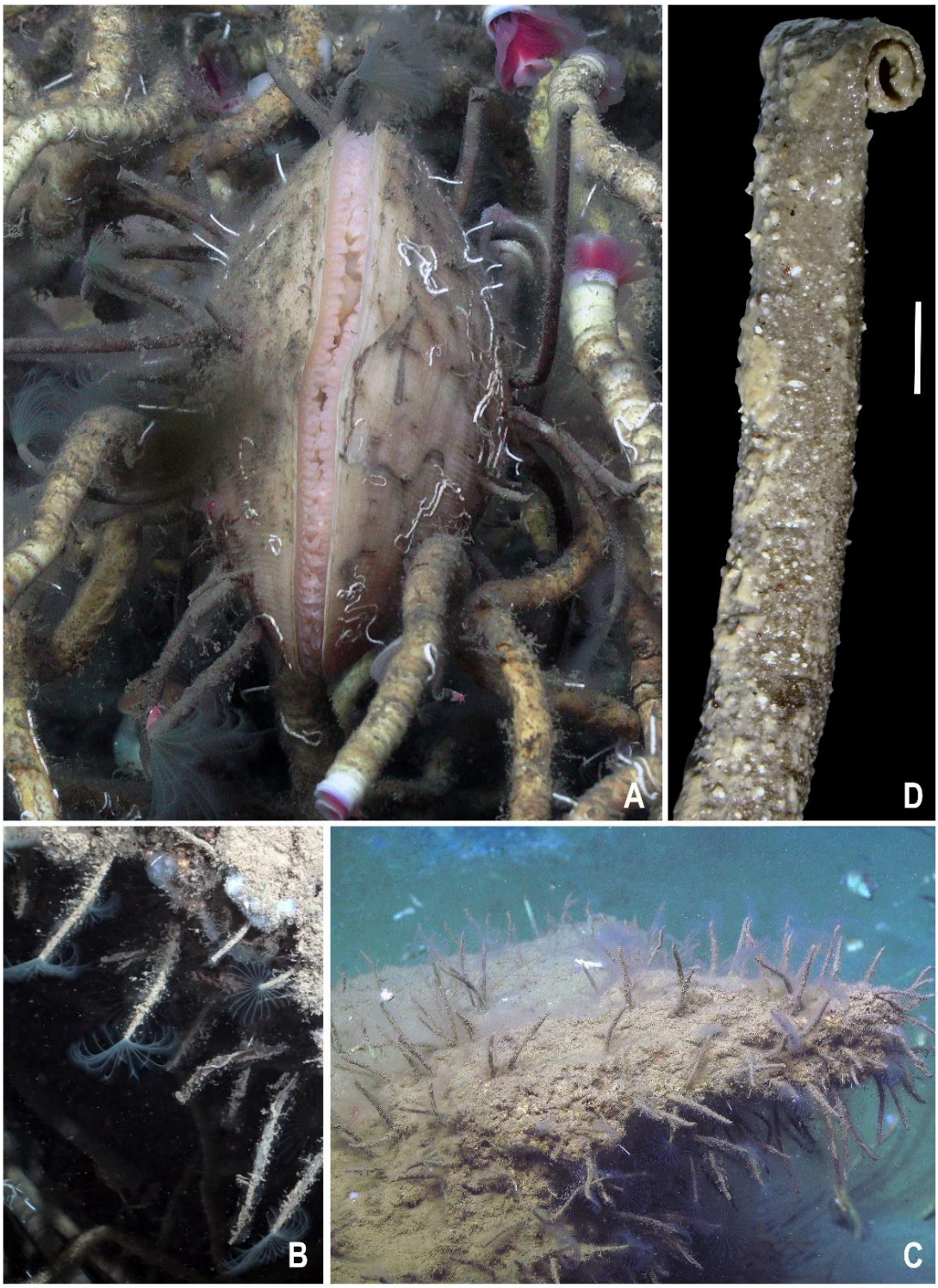

Figure 3.1**.** *In situ* images of *Seepicola viridiplumi* sp. nov. A) Epibiotic individuals on a host *Acesta oophaga* file clam. Red-pink plumes belong to the siboglinid tube worm *Lamellibrachia luymesi*. B) Close up of free-living individuals and plumes on authigenic carbonate. C) Aggregation of individuals on authigenic carbonate. D) Tube of *Seepicola viridiplumi* sp. nov. with a muddy outer lining and a curled end. Scale bar represents 2 mm.

Radiolar crown is mostly symmetrical (Figure 3.3B) with the 2 – 3 ventral-most developing radioles with long, filiform radiolar tips as long as the space of 12 pinnules (Figure 3.4A). These are 1/8 the length of the dorsal radioles. Radiolar lobes are short, as long as the collar segment (Figure 3.2A – C), with dorsal flanges. The dorsal pair of basal flanges is long, narrow, erect, and translucid (Figure 3.2C, E, 4A) and the ventral pair is short, broad, has a rounded margin, and is translucid (Figures 3.2D, 3D, 4A). Radiolar flanges and palmate membrane is absent (Figure 3.2D). Pinnules are very long, of a similar length along the radioles. Radiolar eyes are absent. Except for the ventral-most radioles, the radioles of the holotype have button-like tips and are as short as the space of one pinnule (Figure 3.4B). The radioles with short tips have a massive brown tissue along their internal margins (Figures 3.4C – H). Near the radiolar tip this tissue is broader than that basally, forming a rounded tip that seems like a distal radiolar eye, but this structure lacks ommatidia (Figure 3.4D – G). Some paratypes have mixed radiolar tips (long-filiform, short button-like). Radiolar skeleton is composed of 4 cells in side view (Figure 3.4E, H). Apparently, the crown of paratype 1 (BPSa115) is undergoing regeneration: it is shorter in comparison to the holotype and other paratypes, and the pinnules are incipient.

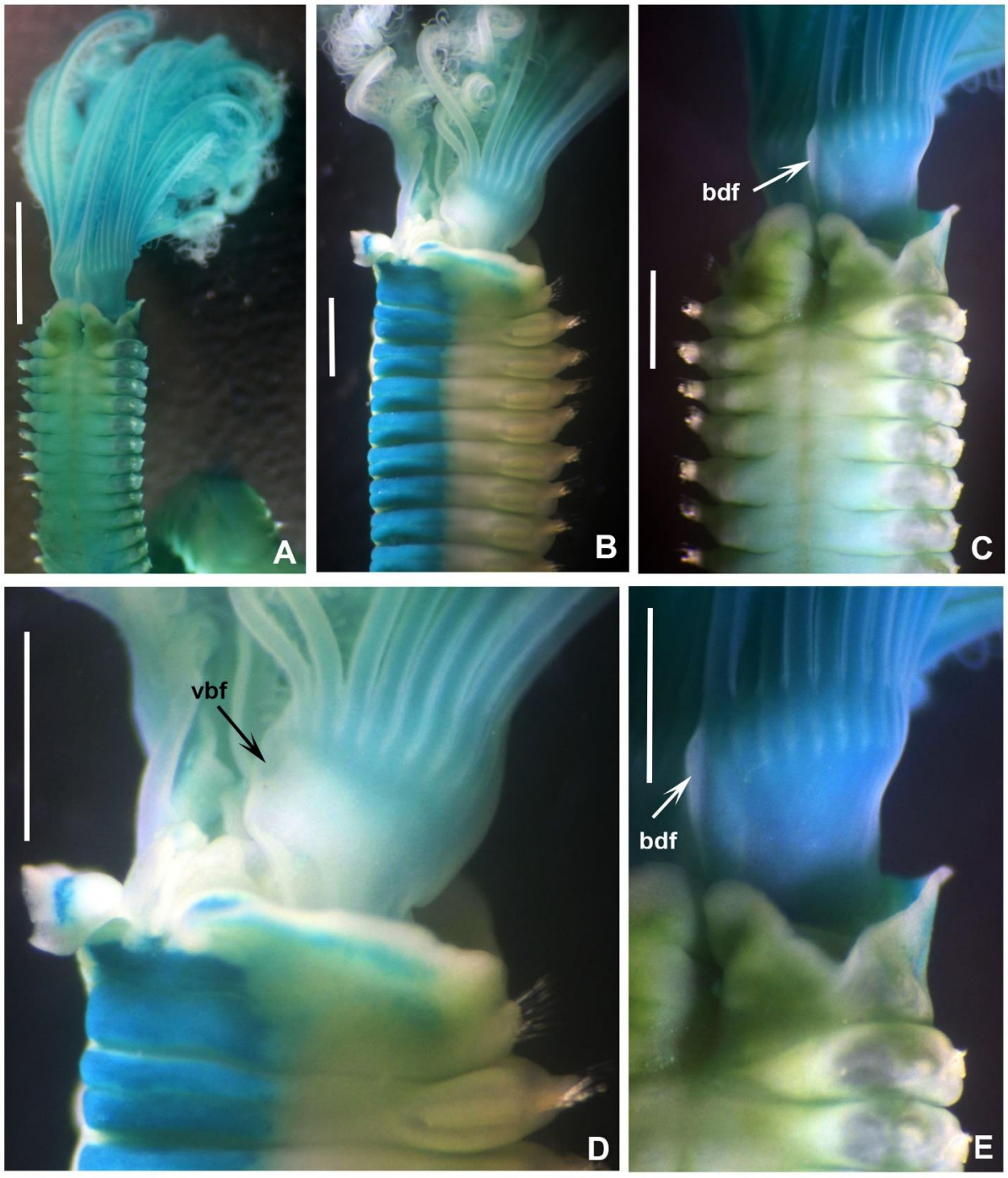

Figure 3.2. *Seepicola viridiplumi* sp. nov. A) Radiolar crown and thorax, dorsal view. B) Thorax and base of radiolar crown, ventrolateral view. C) Thorax and base of radiolar crown, dorsal view. D) Detail of the dorsal basal flange of the radiolar crown. E) Detail of the dorsal basal flange of the radiolar crown. A-E) Holotype (CNAP–ICML, UNAM, 0000). Abbreviations: bdf = basal dorsal flange, vbf = ventral basal flange. Scale bars: A) 1 mm, B-E) 0.8 mm.

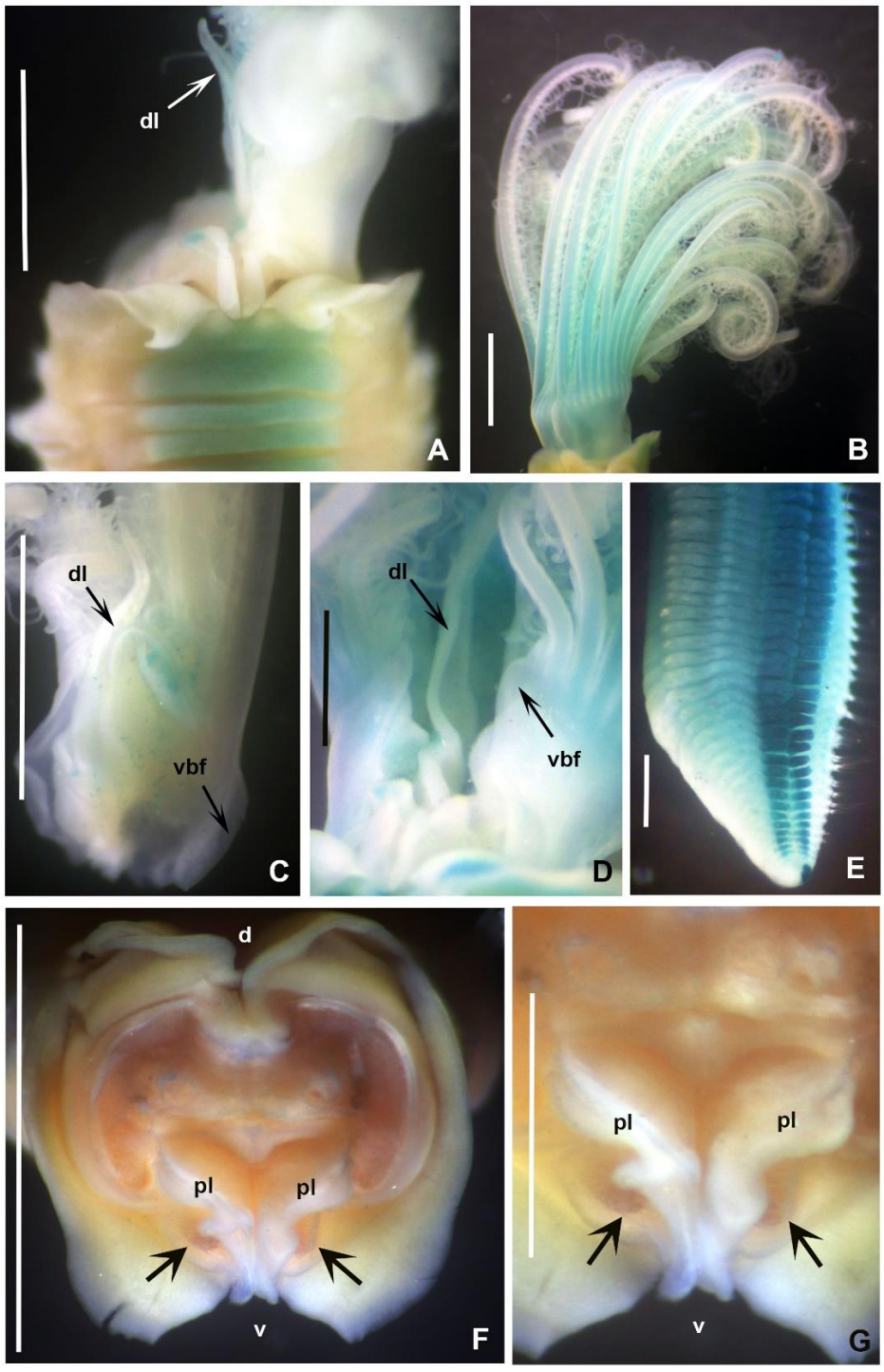

Figure 3.3. *Seepicola viridiplumi* sp. nov. A) Collar, ventral view with the right radiolar lobe removed. B) Radiolar crown, lateral view. C) Base of the right radiolar lobe. D) Detail of the dorsal lip and ventral basal flange of the radiolar crown. E) Posterior end and pygidium. F) Peristomium, frontal view with the radiolar crown removed, peristomial chambers indicated with arrows. G) Detail of the mouth and peristomial chambers pointed with arrows. A, C, F-G) Paratype 3, B, D-E) Holotype (CNAP–ICML, UNAM, 0000). Abbreviations: d = dorsal, dl = dorsal lip, pl = parallel lamella, v = ventral, vbf = ventral basal flange. Scale bars: A-C) 1 mm, D-E, G) 0.5 mm, F) 1.5 mm.

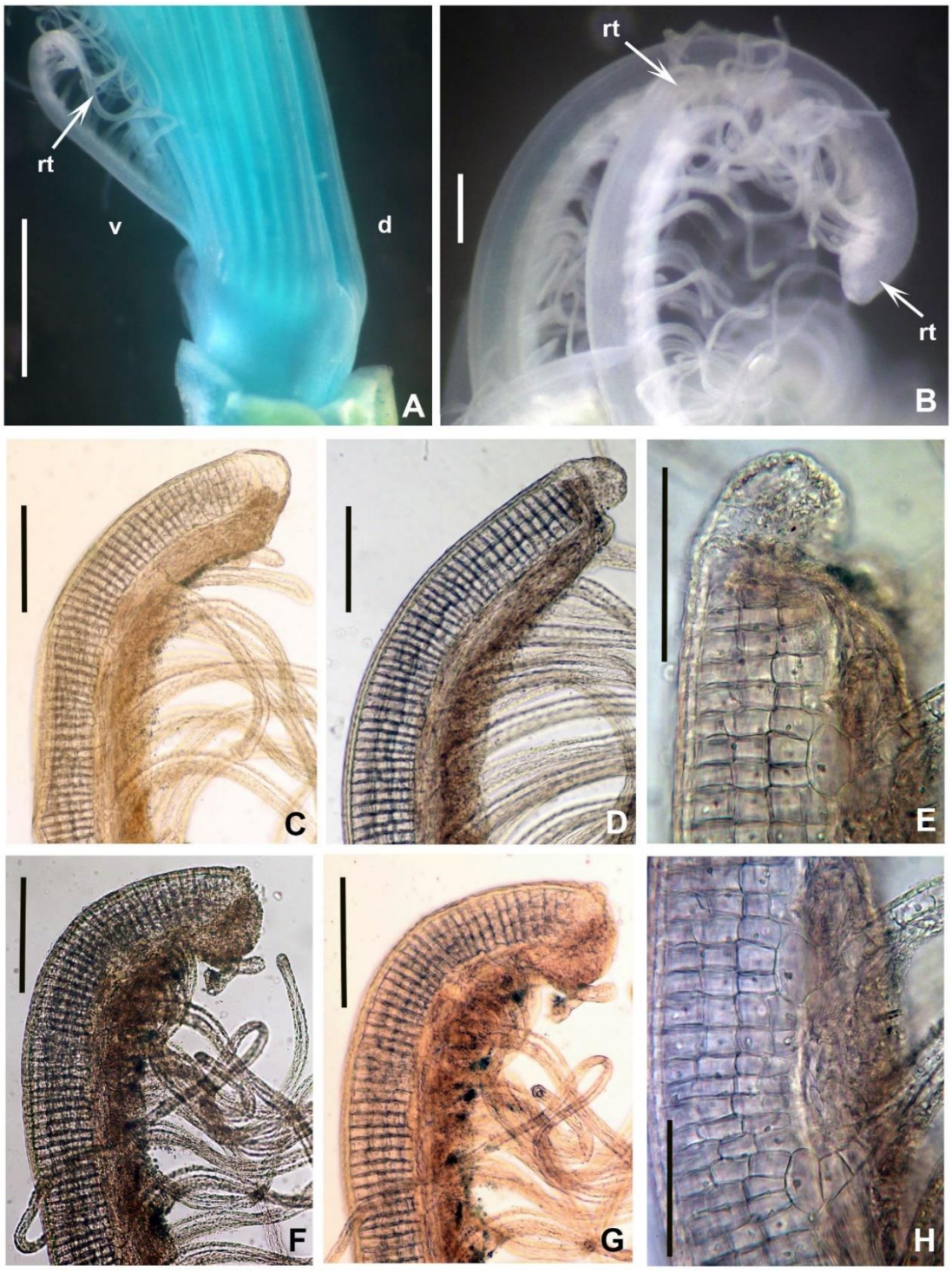

Figure 3.4. *Seepicola viridiplumi* sp. nov. A) Base of the radiolar crown, lateral view (Paratype 2). B) Radiolar tips. C – G) Details of the radiolar tips showing cartilaginous skeletal cells and massive tissue on the inner margin of the radioles, attached to the base of the pinnules. H) Detail of radiolar and pinnular skeletal cells. A) Holotype (CNAP–ICML, UNAM, 0000), B-H) Paratype 1 (CNAP–ICML, UNAM, 0000). Abbreviations: d = dorsal, v = ventral, rt = radiolar tips. Scale bars: A) 1 mm, B-G) 150 µm, H) 75 µm.

The anterior peristomial ring is slightly exposed dorso-laterally between dorsal pockets and the lateral collar margin (Figures 3.2E, 7A). The posterior peristomial ring collar has mid-dorsal margins fused to fecal groove (Figures 3.2E, 7A) and the dorsal collar margins form two low, rounded lappets (Figure 3.2A, C). The dorso-lateral collar margins are entire, forming a "V" (Figure 3.2A, C, E). Ventral lappets are triangular with rounded distal margins that are divided mid-ventrally by an incision (Figures 3.2D, 3A, 7A). Parallel lamellae are present, forming a triangular structure surrounding the mouth ventrally (Figures 3.3A, F – G, 3.7A). A pair of translucent chambers lies between the ventral lappets and parallel lamellae, with brown spots inside (Figures 3.3A, F – G, 3.7A-B). Peristomial eyes are seen in paratypes 1 (BPSa115) and 2 (BHSa167) when radiolar crowns were removed (Figure 3.3F). The dorsal lips are triangular, erect, and have a mid-rib (radiolar appendages) (Figure 3.3A, C – D) and dorsal pinnular appendages; ventral lips are short and rounded, ventral sacs are absent.

Chaetiger 1 (collar chaetiger): two groups of hooded chaetae (Figures 3.6A-C, 3.7A, C), the anterior one with long, narrowly hooded notochaetae (Figures 3.6A-B, 3.7C), and the inferior one half as short than the superior one with hoods slightly broader than the superior group (Figures 3.6C, 3.7C). The ventral shield is rectangular, slightly divided transversally, and higher than the following thoracic shields (Figure 3.3A). Chaetigers 2 – 16 (2 – 13, 2 – 15, 2 – 16, or 2- 18) have rectangular ventral shields divided transversally in two equal parts; the tori do not contact the ventral shields (separated by a reduced space) (Figures 3.2B, 3.3A). Chaetigers have noto- and neurochaetae (Figure 3.5A). Notochaetae have two groups (Figure 3.5C, 3.8A): superior group are elongate and narrowly hooded; inferior ones paleate and arranged in two rows with pointed mucro (Figure 3.5D, 3.8A-C). Neurochaetae with companion chaetae and avicular uncini (Figure 3.5A – B, 3.8E-F). Avicular uncini have several rows of small, similar sized teeth above the main fang

(covering half of the main fang) (Figure 3.8D), the breast is well developed with a high crest above the main fang and handles as long as 2.5 times the length of the main fang (or half of handles of companion chaetae) (Figure 3.5E – F). The companion chaetae have symmetrical membranes and are teardrop-shaped (Figures 3.5B, E, 3.8E-F) with long handles (Figure 3.5A, E).

Abdominal segments with elongate neurochaetae and broadly hooded (Figures 3.6A-D, 3.9A), with a basal, broad knee and the distal end narrowing abruptly in all chaetigers (Figures 3.6E, 3.9F). Those from the last quarter of the body are very long (twice as long as those in the anterior abdominal segments) (Figure 3.9B). Notopodial uncini are avicular with several rows of teeth above the main fang and extending over ¾ of the main fang (Figure 3.9C, E-G). The breast is well defined, and the handles are very short, shorter than the length of the main fang (Figure 3.6F – H). The pygidium is rounded and without eyes (Figure 3.3E). The tubes are composed of fine sand and curl tightly at the end (Figure 3.1D). Gametes were not observed in either the holotype or the paratypes.

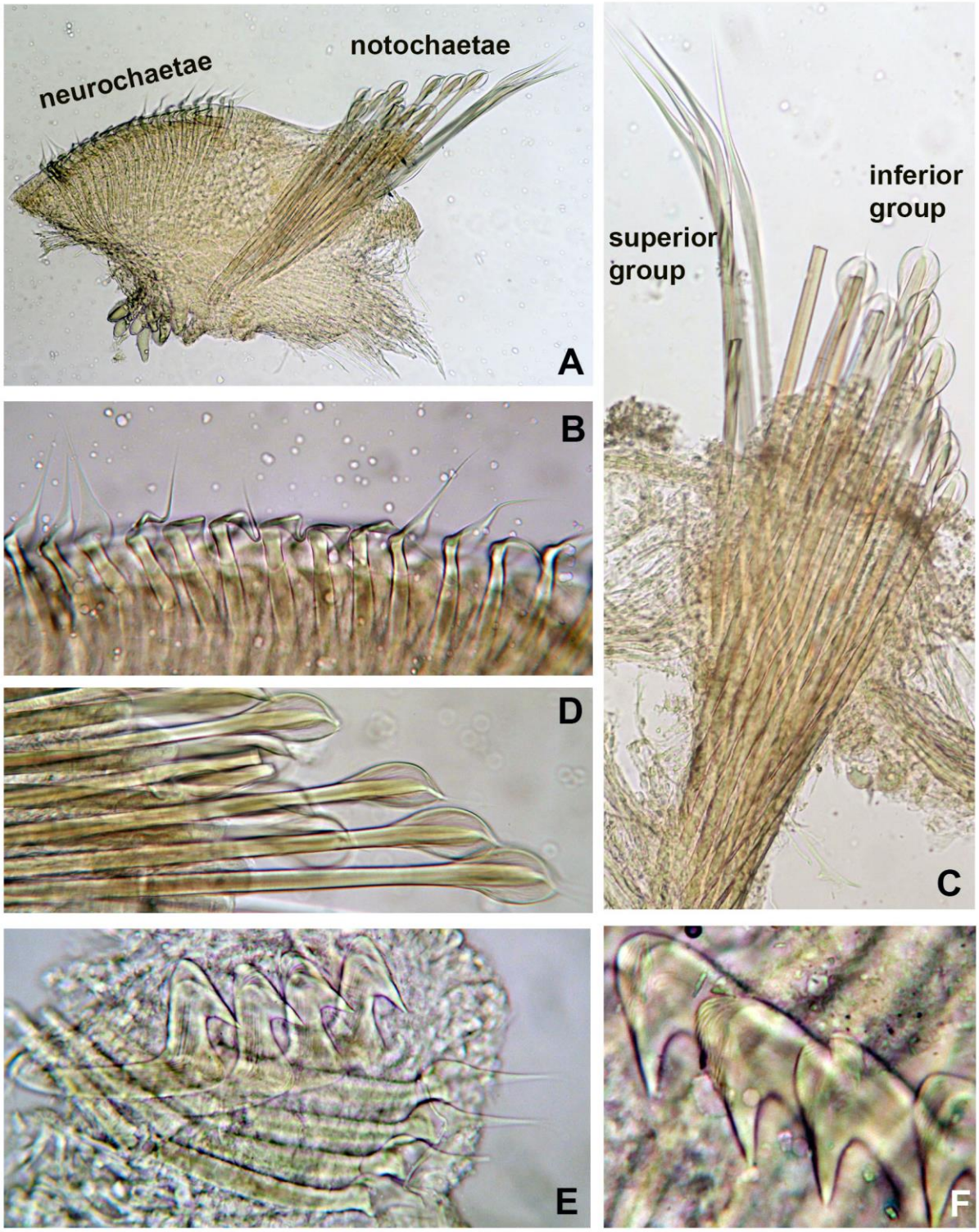

Figure 3.5. *Seepicola viridiplumi* sp. nov., thoracic chaetae. A) Thoracic noto- and neurochaetae. B) Companion chaetae. C) Notochaetae. D) Inferior rows of paleate chaetae. E). Avicular uncini and companion chaetae. F) Detail of heads (main fangs) of uncini. A-F) Holotype (CNAP–ICML, UNAM, 0000). Magnification: A) 4 x, B, D-E) 40 x, C) 10 x, F) 100 x.

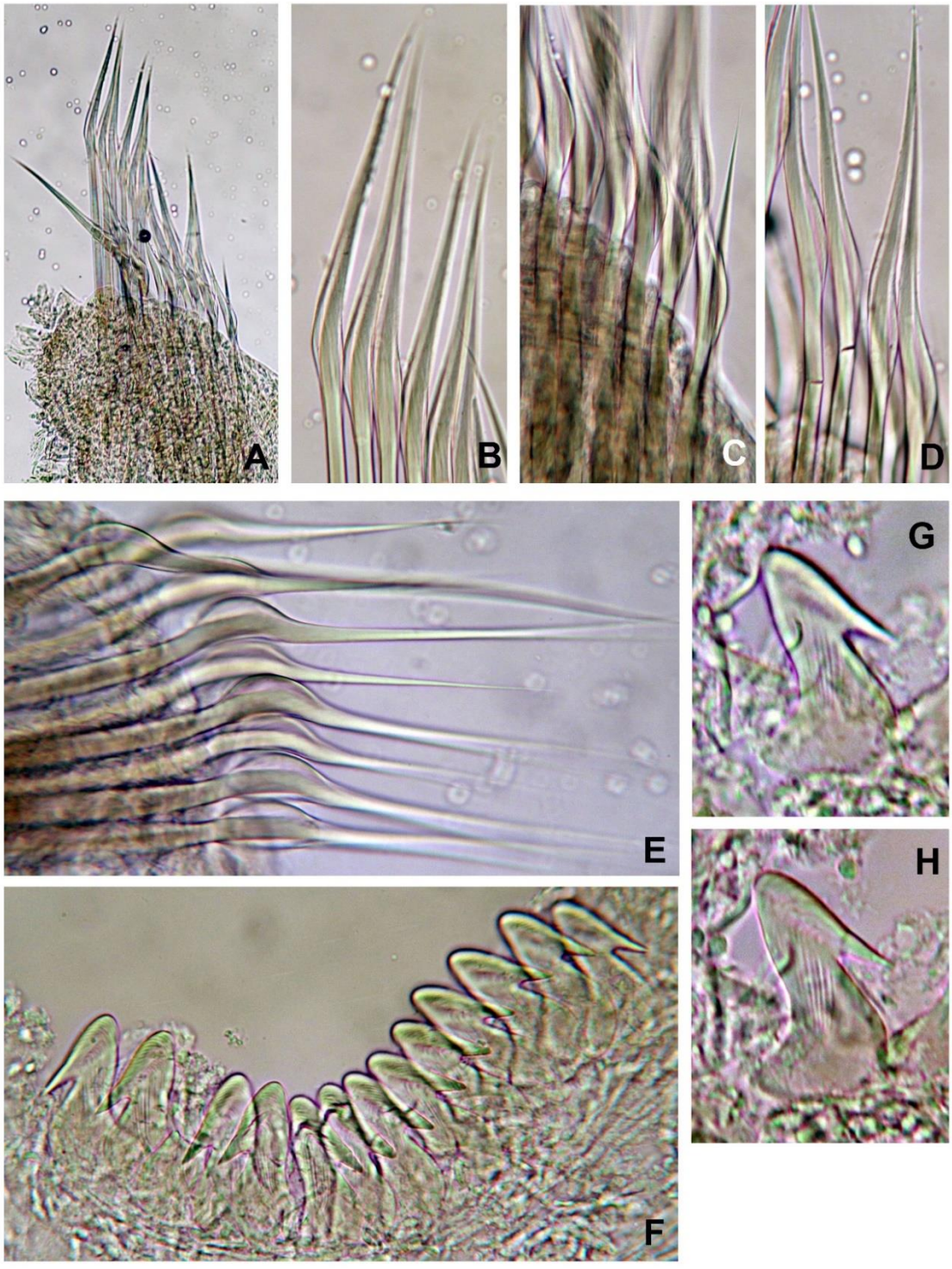

Figure 3.6**.** *Seepicola viridiplumi* sp. nov., collar and abdominal chaetae. A) Collar chaetigers (chaetigers 1). B) Superior group of collar chaetigers composed of elongate, narrowly hooded and slightly curved chaetae. C) Inferior group of collar chaetigers composed of elongate, hooded chaete broader than the superior group. D) Abdominal chaetae. F) Abdominal torus of avicular uncini. G) Details of uncini in side view. A-H) Holotype (CNAP–ICML, UNAM, 0000). Magnification: A) 10 x, B-H) 40 x.

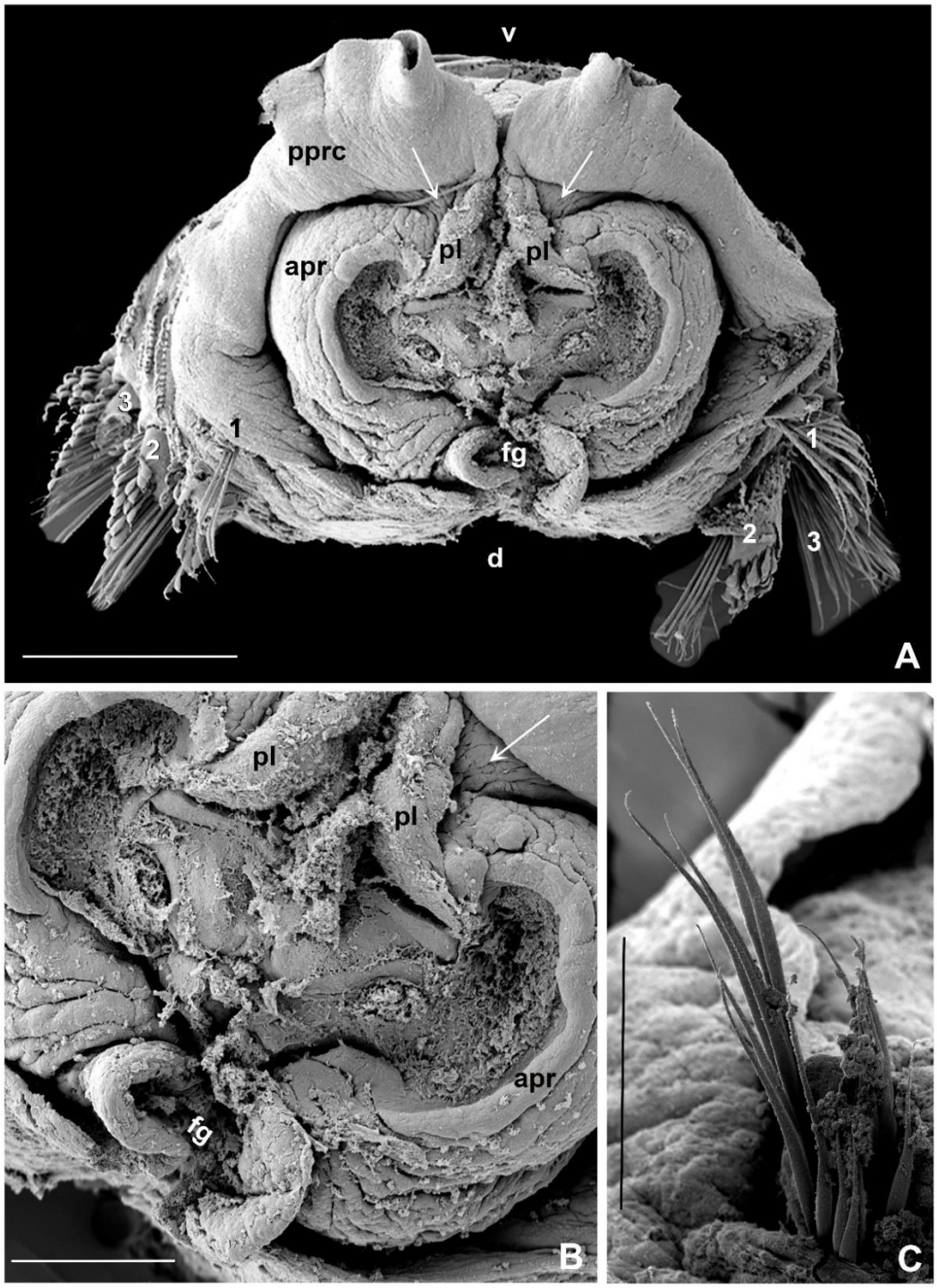

Figure 3.7. *Seepicola viridiplumi* sp. nov. Scanning electron microscopy of peristomium. A) Apical view of peristomium (crown removed) and vascular chambers pointed with white arrows, B) detail of vascular chambers between right ventral lappet of collar and parallel lamella, C) collar chaetiger with two groups of elongate narrowly hooded chaetae. A-B) Stub 1, C) Stub 2 (BPSa88, CNAP–ICML, UNAM, 0000). Abbreviations: apr: anterior peristomial ring, d: dorsal, fg: faecal groove, pl: parallel lamellae, pprc: posterior peristomial ring collar, v: ventral, 1, 2 and 3 in A indicates number of chaetigers. Scale bars: A) 500 µm, B) 200 µm, C) 100 µm.

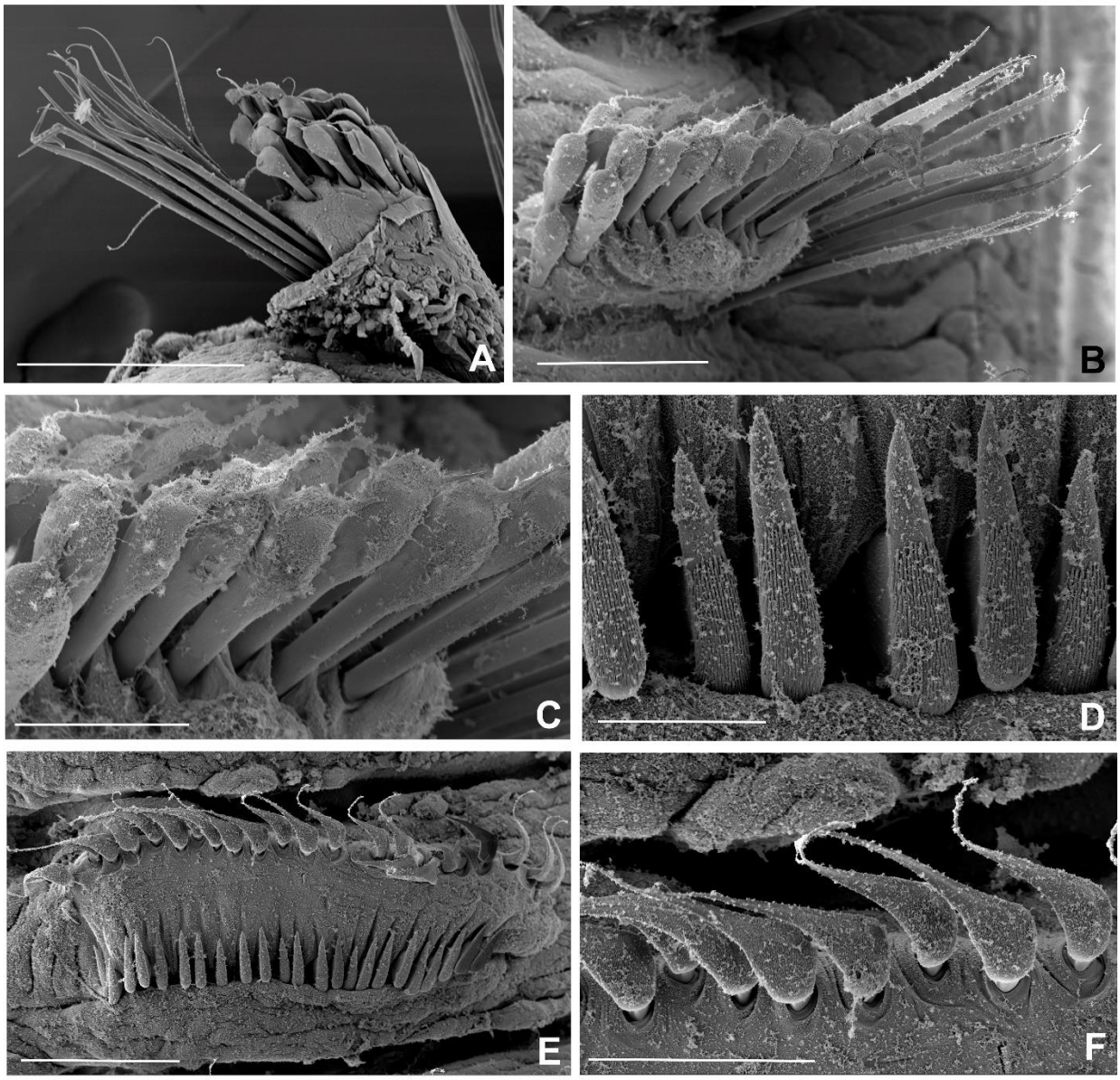

Figure 3.8. *Seepicola viridiplumi* sp. nov., thoracic chaetae and uncini under SEM. A) Chaetiger #2, B) chaetiger #5, C) detail of paleate chaetae from chaetiger #5, D) dentition of uncini from chaetiger #5, E) torus 5, F) detail of companion chaetae from chaetiger # 5. A) Stub 1 (BPSa88, CNAP–ICML, UNAM, 0000), B-C) Stub 5 and D-F) Stub 4 (BPSa123, CNAP–ICML, UNAM, 0000). Scale bars: A) 200 µm, B) 100 µm, C) 50 µm, D) 20 µm, E) 100 µm, F) 50 µm.

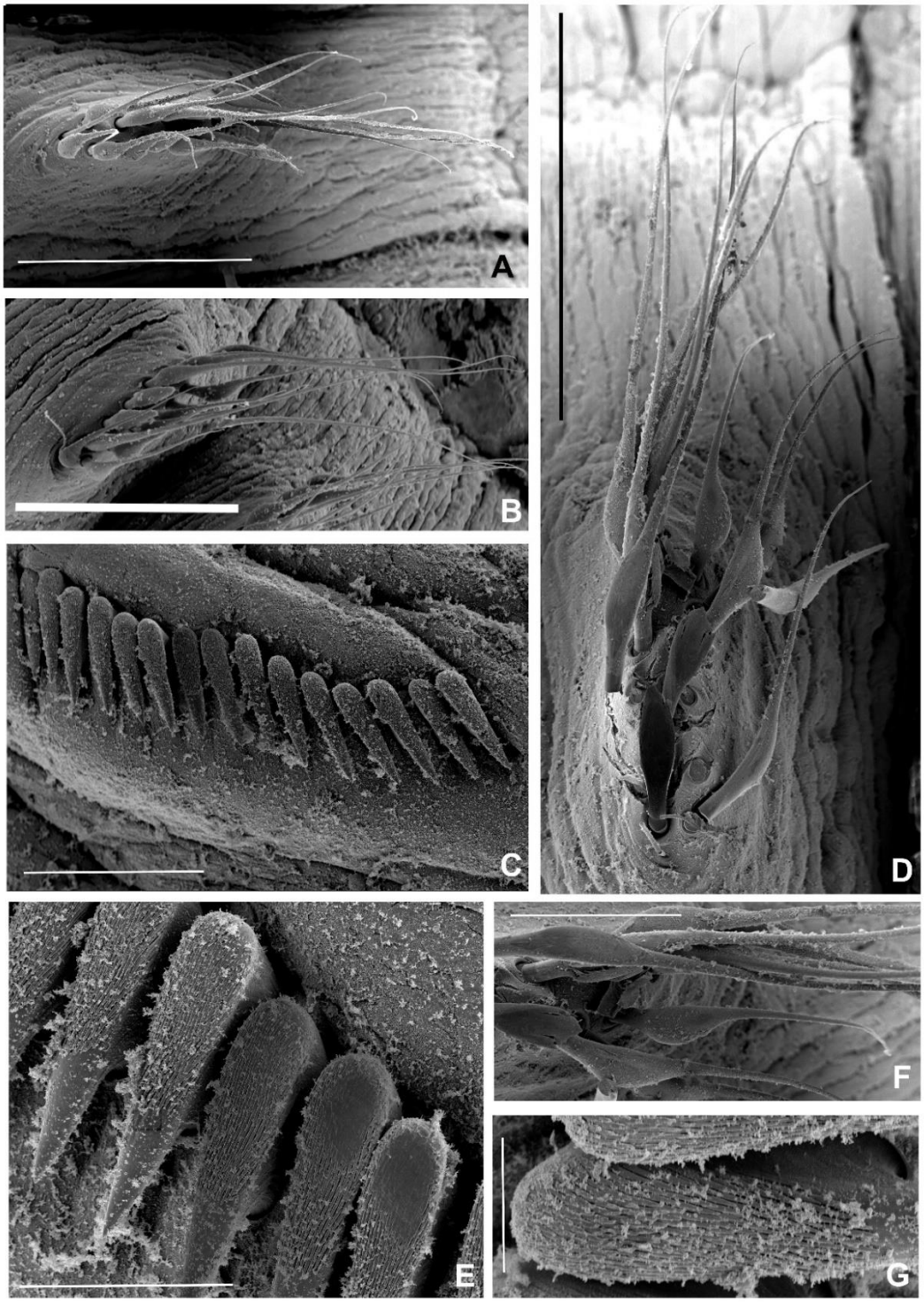

Figure 3.9. *Seepicola viridiplumi* sp. nov., abdominal chaetae and uncini under SEM. A) Anterior abdominal chaetiger, B) posterior abdominal chaetiger, C) anterior abdominal torus, D) detail of chaetae from anterior abdomen, E, G) uncini dentition, F) detail of broadly hooded chaetae. A-B, D, F) Stub 4 (BPSa123, CNAP–ICML, UNAM, 0000), C, E, G) Stub 2 (BPSa88, CNAP–ICML, UNAM, 0000). Scale bars: A-B, D) 200µm, C) 50 µm, E) 20 µm, F) 100 µm, G) 8 µm.

GLANDULAR PATTERN

The ventral shield of the collar, thoracic and abdominal shields stained a deep, uniform blue (Figures 3.2B, 3.3A, E).

ETYMOLOGY

The species epithet refers to the color of the radiolar crown in living specimens, from the Latin *viridi*, meaning green and *-plumi*, meaning many plumes.

REMARKS

Placing the taxon described here in either *Pseudopotamilla* Bush, 1905 or *Perkinsiana* Knight-Jones, 1983 is a difficult task when morphology is first examined. The specimens described here from hydrocarbon seep habitats in the Gulf of Mexico have dorsal and ventral basal flanges at the base of the radiolar crown, such as is described in *Pseudopotamilla*. However, it lacks the remarked compound radiolar eyes and the asymmetrical radiolar crown common in *Pseudopotamilla* species (Table 2). On the other hand, the genus *Potamilla* Malmgren, 1866 also lacks radiolar eyes (Knight-Jones 1983, Fitzhugh 1989). Our specimens cannot be attributable to *Potamilla* because these have dorsal lips elongate, triangular, with mid-rib (radiolar appendages) and lacks a palmate membrane, whereas *Potamilla* have dorsal lips without radiolar appendages, but a palmate membrane is present, among other differences (Table 3.2).

Regarding the genus *Perkinsiana*, some authors already commented on the existing problems. Fitzhugh (1989) emphasized that *Perkinsiana* Knight-Jones, 1983 is not a definable group as there is no evidence to support monophyly. Capa (2007) and Tovar-hernández et al. (2012) both described new species of *Perkinsiana* and remarked on the existing problem of properly assigning species to this genus. In the same context, *Pseudopotamilla* is not defined by any synapomorphies (Fitzhugh 1989, Capa 2007). In both genera, species are known to burrow in

hard limestone, dead coral, barnacles, and mollusk shells (Chughtai & Knight-Jones 1988, Knight-Jones et al. 2017, Capa et al. 2019, Tovar-Hernández et al. 2020). There are 18 valid described species in *Perkinsiana* and 23 in *Pseudopotamilla* after Tovar-Hernández et al. (2020), but the status of some nominal species in the latter genus are still questionable.

Our specimens lack the palmate membrane and radiolar flanges present in some *Perkinsiana* species. Additionally, our specimens had abdominal uncini with reduced handles whereas these structures are short to medium length in *Perkinsiana*. Three types of abdominal chaetae can be present in species of *Perkinsiana* whereas these are elongate, broadly hooded chaetae in all chaetigers of the new taxon here described.

Furthermore, the new species described here have unique, distinctive features not previously described: the peculiar shape of the radiolar tips, the presence of the brown tissue on the radioles, and the presence of a pair of peristomial chambers between the internal wall of ventral lappets and parallel lamellae. Other features of chaetae and uncini are typical of *Pseudopotamilla*. As the new species here described, some species of *Pseudopotamilla* also have tubes curl tightly at the end (Knight-Jones et al. 2017), but branched or bifurcated tubes were not seen in the specimens here examined, which is indication of asexual reproduction.

Table 3.2. Distinctive features of the genera *Perkinsiana* Knight-Jones, 1983, *Potamilla* Malmgren, 1866, *Pseudopotamilla* Bush, 1905 and *Seepicola* new genus.

Feature	***Perkinsiana* Knight-Jones, 1983 *sensu* a variety of author as specified in each feature**	***Potamilla* Malmgren, 1866 *sensu* Fitzhugh, 1989**	***Pseudopotamilla* Bush, 1905 *sensu* Knight-Jones et al. 2017**	***Seepicola* new genus**
Radiolar crown	Symmetrical with most radioles same length (except 2-3 ventral-most developing radioles)(Tovar-Hernández, obs. pers.)	?	Asymmetrical with longest radioles dorsally	Symmetrical with all radioles same length (except 2-3 ventral-most developing radioles)
Dorsal and ventral basal flanges of crown	Absent (Tovar-Hernández et al. 2012, Capa et al. 2019)	Absent	Present	Present
Palmate membrane	Absent (Fitzhugh, 1989, Capa, 2007); present or absent (Tovar-Hernández et al. 2012, Capa et al. 2019)	Present	Absent	Absent

Radiolar flanges	Absent (Fitzhugh, 1989, Capa, 2007); absent or present (Tovar-Hernández et al. 2012)	Absent	Absent	Absent
Radiolar eyes	Absent	Absent	Present, unpaired, compound in all radioles except dorsal most pair and some ventral most radioles, usually limited to proximal half of radioles	Absent
Peristomial eyes	Present in juveniles (Capa et al. 2019	?	May be present	Present
Mid-rib of dorsal lips (radiolar appendages)	Present (Fitzhugh, 1989, Capa 2007, Tovar-Hernández et al. 2012, Capa et al. 2019)	Absent	Present	Present
Dorsal pinnular appendages	Present (Fitzhugh, 1989); present or absent (Capa 2007, Tovar-Hernández et al. 2012, Capa et al. 2019)	Present	Present	Present

Ventral lips	Present (Fitzhugh, 1989, Capa 2007, Tovar-Hernández et al. 2012, Capa et al. 2019)	Present	Present	Present
Parallel lamellae	Present (Fitzhugh, 1989, Capa 2007, Tovar-Hernández et al. 2012, Capa et al. 2019)	Present	Present	Present
Ventral sacs	Absent (Capa 2007, Tovar-Hernández et al. 2012, Capa et al. 2019)	?	Present	Absent
Peristomial chambers	Never reported	Never reported	Never reported	Oval, translucent with a brown spot inside
Anterior margin of anterior peristomial ring	Low, of even height all around (Fitzhugh, 1989, Capa 2007, Tovar-Hernández et al. 2012)	Low, of even height all around	Low, of even height all around	Low, of even height all around

Collar chaetae	Arranged in oblique rows, similar to superior notochaetae of following chaetigers (elongate, narrowly hooded) (Capa 2007, Tovar-Hernández et al. 2012, Capa et al. 2019)	?	Similar to superior notochaetae of following chaetigers (elongate, narrowly hooded)	Two groups of hooded chaetae, the anterior one with long, narrowly-hooded chaetae, and the inferior one half as short than the superior one with hoods slightly broader than the superior group
Inferior thoracic notochaetae	Paleate, arranged in two or more transverse rows (Fitzhugh, 1989, Capa 2007, Tovar-Hernández et al. 2012)	Paleate, arranged in two or more transverse rows	Paleate, arranged in two or more transverse rows	Paleate, arranged in 2-3 transverse rows
Thoracic uncini (avicular)	Teeth above main fang of equal size, hood absent, breast well developed, expanded; handles of medium length (Fz, 1989); handles of variable length (Capa 2007, Tovar-Hernández et al. 2012, Capa et al. 2019)	Teeth above main fang of equal size, hood absent, breast well developed, expanded; handles of medium length	Teeth above main fang of equal size, hood absent, breast well developed, expanded; handles of medium length	Teeth above main fang of equal size, hood absent, breast well developed, expanded; handles of medium length

Companion chaetae	Distal ends as roughly symmetrical, tear-drop shaped membranes (Fitzhugh 1989, Capa 2007, Tovar-Hernández et al. 2012, Capa et al. 2019)	Distal ends as roughly symmetrical, tear-drop shaped membranes	Distal ends as roughly asymmetrical, tear-drop shaped membranes	Distal ends as roughly asymmetrical, tear-drop shaped membranes
Abdominal uncini (avicular)	Teeth above the main fang of equal size; breast well developed, expanded; long handled (Fitzhugh, 1989); short to medium length handle (Capa 2007, Tovar-Hernández et al. 2012)	Teeth above the main fang of equal size; breast well developed, expanded; long handled	Teeth above the main fang of equal size; breast well developed, expanded; medium handled	Teeth above the main fang of equal size; breast well developed; short handled

Abdominal chaetae	Elongate, broadly hooded chaetae in all chaetigers (Fitzhugh, 1989, Capa, 2007). Broadly-hooded and progressively tapering to distal tip (type A), or elongate broadly-hooded chaetae (type B), or elongate, narrowly-hooded chaetae (type C) (Tovar-Hernández et al. 2012). Anterior abdominal segments with broadly hooded chaetae and posterior segments with elongate, narrowly hooded chaetae (Capa et al. 2019)	Elongate, broadly hooded chaetae in all chaetigers	Elongate, broadly hooded chaetae in all chaetigers	Elongate, broadly hooded chaetae in all chaetigers, but those from the last abdominal quarter being longer than anterior abdominal segments

3.2 Phylogenetic Analysis

All phylogenetic estimations recovered the same topology with very minor variations in boostrap support for some clades. All of them recover a clade comprised of only specimens in this study with a high degree of confidence (100% bootstrap support, and less than 1% divergence among all sequences). We present the tree produced using the HKY+I model of sequence evolution as it was the best fitting model for the data (Figure 3.10).

The phylogeny suggests that *Seepicola viridiplumi* sp. nov. is distantly related to the closest sequences in reference databases (Genbank, BOLD; with only 70-75% similarity), which is perhaps not surprising given the paucity of data from sabellids collected in similar habitats and depths. A clade comprised of *Seepicola* new genus, *Eudistylia* and *Schizobranchia* is recovered with low bootstrap support (65%) so is not informative about how the genus is related to other sabellid genera, except that it is distantly related to those in this study. These results provide strong evidence that the specimens collected in this study are unique (at least among the barcoded sabellids) and thus constitute a new genus. The phylogeny and distance calculations also show that the species here is not closely related to either *Pseudopotamilla reniformis* (27% sequence divergence) or *Perkinsiana fonticula* (30% divergence), despite the morphological similarities outlined above.

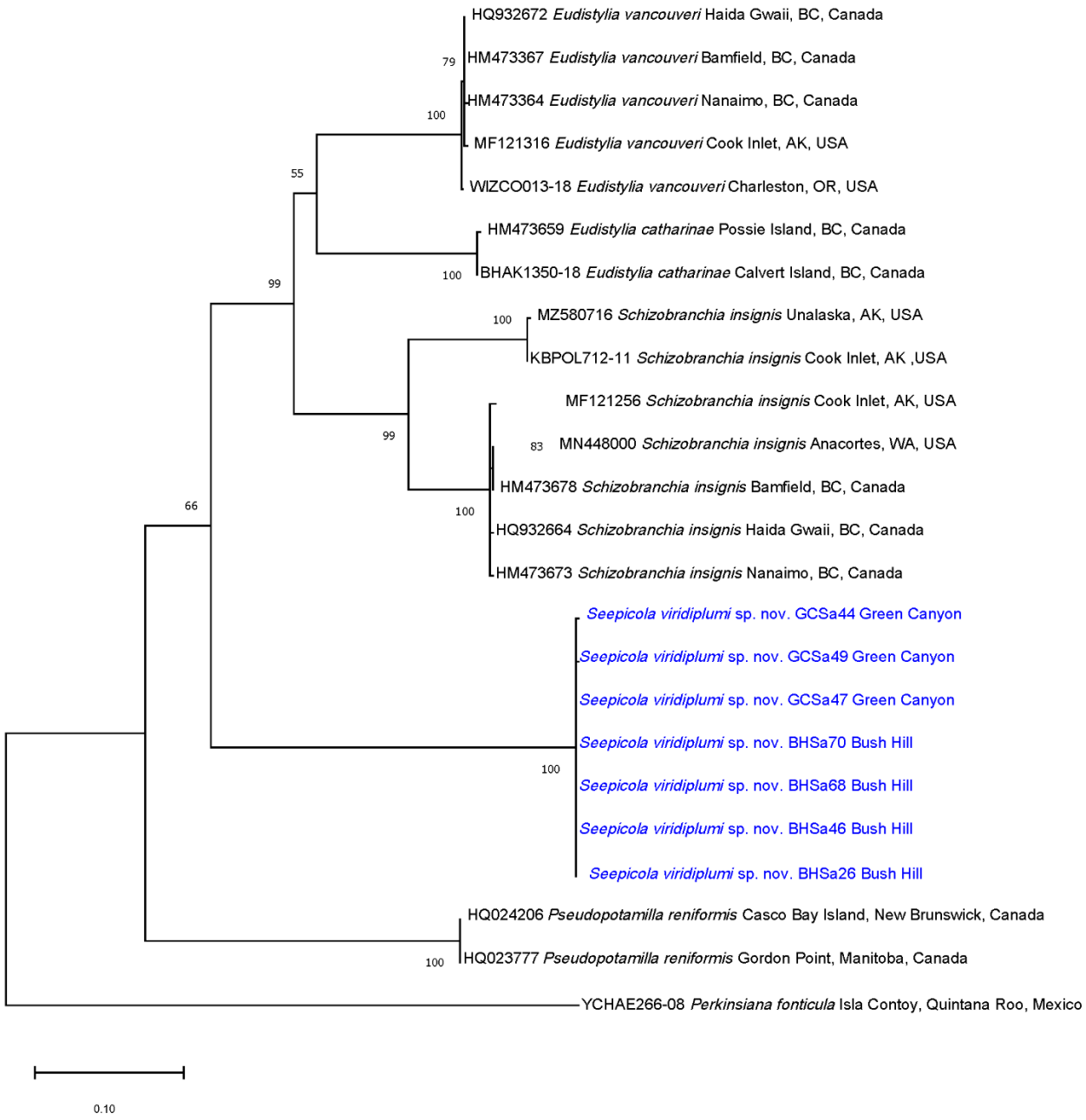

Figure 3.10**.** Maximum Likelihood (ML) tree showing the phylogenetic relationships between *Seepicola viridiplumi* sp. nov. and four other Sabellidae genera. Numbers refer to bootstrap support (%).

The first phylogenetic approach of Sabellidae nested the genera *Potamilla*, *Perkinsiana*, *Potaspina*, *Pseudopotamilla*, *Eudistylia*, and *Schizobranchia* within the "Clade VII" based on morphology (Fitzhugh, 1989). This "Clade VII" resulted monophyletic based on the occurrence of

dorsal pinnular appendages and elongate, broadly hooded chaetae in all abdominal fascicles. *Potamilla, Potaspina* and *Perkinsiana* formed a polygamy with the Clade *Pseudopotamilla-Eudistylia-Schizobranchia,* which was defined by the presence of unpaired compound radiolar eyes and dorsal basal flanges of crown (Fitzhugh, 1989).

Posteriorly, that group ("Clade VII" *sensu* Fitzhugh, 1989) was recovered in a combined analysis using morphological and molecular data, called "clade IB" that includes many other genera, supported by the presence of companion chaetae in thorax and broadly hooded abdominal chaetae (Capa et al. 2011).

More recently, using transcriptomes, *Eudistylia* and *Pseudopotamilla* were nested within the Tribe Amphiglenini, Subfamily Myxicolinae according to Tilic et al. (2020), which is equivalent to the "clades V, VI and VII" by Fitzhugh (1989) and "Clade IB" by Capa et al. (2011). Under this scenario, *Seepicola* new genus would belong to the Amphiglenini Tribe, Myxicolinae subfamily.

3.3 Species Abundance Measures

The density of the sabellids was variable within the seep systems. From the analysis of ROV images, sabellid density within the seep systems averaged 330 ± 233.3 (stdev) m^{-2} but ranged from 98 to 655 individuals m^{-2} within the authigenic carbonate. Sabellid density was most concentrated at vertical facies on authigenic carbonate outcrops and more dispersed on horizontal surfaces (Figure 3.1C). Occasionally, individuals were observed on deposits of shell hash. *In situ* observations and video footage showed that the sabellid aggregations at each of the collection sites were composed of specimens of varying sizes and likely belonged to younger (shorter sabellid tubes) and older (taller) individuals. Observed sabellid tubes ranged from approximately 4 mm to

104 mm and were intermingled within the aggregations. The aggregations at Bush Hill appeared to be more extensive than at Brine Pool NR1 and Green Canyon 234, although this could not be quantified. This difference likely corresponds to the abundance of exposed authigenic carbonate at Bush Hill. Epibiotic *Seepicola viridiplumi* sp. nov. also had varying densities on host *Acesta oophaga* file clams. While several *A. oophaga* bore only a single sabellid, one file clam 10 cm long and 8 cm across, collected from Bush Hill, had a total of 58 individual sabellids.

4. **DISCUSSION**

This study expands the number of sabellid species known from chemosynthetic habitats and identifies a species of high abundance at some of the best described hydrocarbon seeps (Cordes et al. 2009). *Seepicola viridiplumi* sp. nov. is the third to be identified from chemosynthetic habitats and helps to elucidate the diversity of sabellid polychaetes from these environments. Several species of sabellid polychaetes are known to form dense aggregations similar to *Seepicola viridiplumi* sp. nov. (Capa et al. 2019), and this may impact ecological aspects of the hydrocarbon seep habitat. Gregarious sabellid species such as *Bispira riccardi* have been found to significantly increase local meiofaunal diversity and abundance (Enrichetti et al. 2022). Suspension feeding organisms, such as sabellid polychaetes, also aid in coupling the pelagic realm to the benthos by transferring energy and nutrients between various trophic levels (Buhl-Mortensen et al. 2010). Indeed, an unidentified species of sabellid from the Green Canyon 234 seep was identified as a prey source for crustaceans like *Alvinocaris* shrimp (Cordes et al. 2010a). It remains unknown if the unidentified species is the same as the one here described.

The biology and adaptations of sabellids to deep-sea and chemosynthetic habitats is mostly unknown (Capa et al. 2021), although they are hypothesized to act as opportunistic suspension

feeders (Capa et al. 2019). However, with the identification of a chemosynthetic species of *Bispira* at methane seeps in Costa Rica (Goffredi et al. 2020), sabellid taxa have become recognized as having a high potential for chemosymbiosis (Sinner et al. 2023). The presence of massive brown tissue along the radioles of *Seepicola viridiplumi* sp. nov. could indicate a potential for symbiotic bacterial presence, although this warrents further investigation. A chemosymbiotic relationship could help explain the high abundances of *Seepicola viridiplumi* sp. nov. within the three study systems. It is also likely that the species is simply utilizing the abundance of hard substrate within the seeps and the abundances could be supported by the heightened local productivity.

The facultative epibiotic nature of *Seepicola viridiplumi* also warrents further study, as this may reveal other unique adaptations for sabellid taxa (Capa et al. 2021) as well as unquantified trophic pathways within methane seep systems (Levin et al. 2016). The differences in height above the seafloor between epibiotic and free-living *Seepicola viridiplumi* sp. nov. may have ramifications on diet and fitness of individuals. By settling on the epizooitic *Acesta oophaga* file clams, the epibiotic sabellids are potentially exposed to stronger currents unhindered by the benthic boundary layer. At the same time, epibiotic individuals have more limited access to dissolved methane and other chemicals important to potential symbiotic bacteria.

BRIDGE

Chapter III identified and described *Seepicola viridiplumi*, a sabellid commonly observed at shallow methane seep sites within the Gulf of Mexico. In Chapter IV, I focused on determining whether *S. viridiplumi* relies on chemosynthetic bacterial symbionts and, as they are facultative, I compared the trophic niches of epibiotic and free-living individuals using stable isotopes.

CHAPTER IV

TROPHIC NICHES AND THE ASSOCIATED MICROBIAL COMMUNITY FOR A NEWLY DESCRIBED METHANE SEEP SABELLID

This chapter contains unpublished coauthored material. Dr. Stilanos Louca assisted with the 16S microbial sequencing, Dr. Erik Cordes contributed to project conception and stable isotopic analysis, and Dr. Craig Young provided funding. All coauthors contributed to manuscript preparation.

1. INTRODUCTION

Hydrocarbon seeps, also referred to as methane seeps or cold-seeps, are common chemosynthetic systems characterized by the release of compounds such as methane gas from the seafloor (Kiel & Tyler 2010). The input of these compounds supports communities of free-living Bacteria and Archaea in the surrounding water column and in the sediment subsurface (Thurber et al. 2013, Levin et al. 2016). Additionally, macrofaunal communities in these systems are often dominated by siboglinid tubeworms and bathymodiolin mussels (Bergquist et al. 2003, Cordes et al. 2009), which rely on chemosynthetic bacteria housed within their tissues. Both tubeworms and mussels act as foundation species, adding complex texture to the seafloor and providing habitat for other species (Bergquist et al. 2003, Cordes et al. 2007, Govenar 2010, Levin et al. 2016). Food webs at these habitats are underpinned by methanotrophy and thiotrophy, where either methane or sulfide are oxidized (Macavoy et al. 2002, DeChaine & Cavanaugh 2005, Thiel et al. 2012, Toone & Washburn 2020).

Numerous fauna can be found in association with hydrocarbon seeps, attracted by the formation of hard substrate on the seafloor in the form of authigenic carbonate (Levin et al. 2015)

and the increase in local production (Olu et al. 1996). These include primary consumers such as sessile, suspension-feeding invertebrates (Bergquist et al. 2003, Cordes et al. 2005, Govenar 2010). Suspension-feeding taxa are often epibiotic, with sponges, serpulids, and hydroids attaching to the *Lamellibrachia luymesi* tubes (Cordes et al. 2009). Placement and settlement location within a seep habitat can exert a variety of influences on sessile taxa, including access to currents out of the benthic boundary layer (Levin et al. 2016) and resuspended particles from the seabed (Olu et al. 1996), as well as protection from predators (Govenar 2010). In the Gulf of Mexico, epifauna and epibiotic species at methane seeps have often been examined from a biodiversity and food web perspective (Bergquist et al. 2003, Cordes et al. 2007, Becker et al. 2013), however the specific trophic ecology for many of these organisms remains unstudied. Furthermore, while many studies have attempted to broadly examine the trophic and food web structure at methane seep systems (Macavoy et al. 2002, MacAvoy et al. 2008, Becker et al. 2009, Cordes et al. 2010a, Zhao et al. 2020), research examining potential epibiotic linkages in detail (Järnegren et al. 2005, Arellano et al. 2013) remain comparatively scarce and many trophic pathways remain unresolved (Levin et al. 2016).

Isotopic studies have shown that heterotrophic primary consumers within cold-seep systems are often generalists and rely on nutrition from chemosynthetic and photosynthetic sources (Cordes et al. 2010a, Levin et al. 2015, Toone & Washburn 2020). Ratios of Carbon isotopes ($\delta^{13}C$) vary depending on carbon source, with photosynthetically derived carbon ranging from -24 to -18 ‰ (Gearing et al. 1984, Paull et al. 1985, Brooks et al. 1987). In contrast, chemosynthetically derived carbon ratios are more depleted, often exceeding -42 ‰ for methanotrophy on biogenic methane (Paull et al. 1985) and between -38 to -10 ‰ for Calvin-Benson-Bassham Cycle thiotrophy (Hügler & Sievert 2011, Toone & Washburn 2020). Nitrogen

ratios ($\delta^{15}N$) are readily used to examine trophic position (Minagawa & Wada 1984), with photosynthetic material having ratios from 2 to 8 ‰ (Paull et al. 1985). Isotopic ratios of sulfur ($\delta^{34}S$) can also be used to trace nutrition derived from thiotrophy. For example, the sulfur ratios for siboglinid tubeworm tissues (-37 to -24 ‰; Macavoy et al. 2002) are distinct from Gulf of Mexico bottom water sulfate, which averages around 20.3 ‰ (Aharon & Fu 2003).

Fanworm polychaetes in the family Sabellidae are frequently observed as epifaunal representatives at methane seep systems (Cordes et al. 2010a, Vestheim & Kaartvedt 2016, Capa et al. 2021). Despite this commonality and tendency to reach high abundances (Jumars et al. 2015, Enrichetti et al. 2022), few have been identified beyond the family level (Becker et al. 2009, Goffredi et al. 2020). Like their shallow-water counterparts, sabellids at chemosynthetic habitats are thought to be generalist suspension feeders, consuming a variety of particulate organic matter (POM), detritus, phytoplankton, and bacterioplankton (Capa et al. 2019). However, recent work identifying a species of *Bispira* harboring methanotrophic bacterial symbionts brought into question the ecological role these organisms might fill within these habitats (Goffredi et al. 2020).

This study examined a newly described sabellid species, *Seepicola viridiplumi*, common at methane seeps on the Upper Louisiana Slope within the Gulf of Mexico. *Seepicola viridiplumi* is gregarious, and individuals are facultative hyper-epibionts within the seep habitats, found within authigenic carbonate on the seabed and the valves of the epibiotic file-clam *Acesta oophaga* (chapter 3). *Acesta oophaga* themselves are obligate epibionts on *Lamellibrachia luymesi* tubeworms, and affix themselves at the ends of the *L. luymesi* tubes (Järnegren et al. 2007). Epibiotic sabellids can be upwards of 2 meters above the free-living individuals (Figure 4.1). Such a difference in height could have implications on the environmental conditions *S. viridiplumi* individuals are exposed to, including gradients of dissolved methane, exposure to hydrogen sulfide,

and access to particulate matter due to changes in current flow. Few studies have compared diets between epibiotic and free-living conspecifics. However, Puccinelli & McQuaid (2021) found that free-living *Chthamalus dentatus* barnacles consistently had lower $\delta^{13}C$ and higher $\delta^{15}N$ ratios compared to epibiotic individuals, potentially caused by differences in consumption of remineralized resources and small-scale variability in food supply. Additionally, *S. viridiplumi* specimens have been observed with consistent aggregations of brown tissue on the ends of their radioles, which have been hypothesized to be bacterial symbionts (chapter 3). We first investigated the bacterial and archaeal communities associated with the radiolar crowns to determine if *S. viridiplumi* has any potential chemosymbionts. We then utilized tissue stable isotopic ratios to determine the general nutrient resources and trophic niche for this species. Finally, due to the distinct vertical separation between the two microhabitats, we examined the potential impacts of epibiotic settlement on the diet and microbiome of *S. viridiplumi* sabellids.

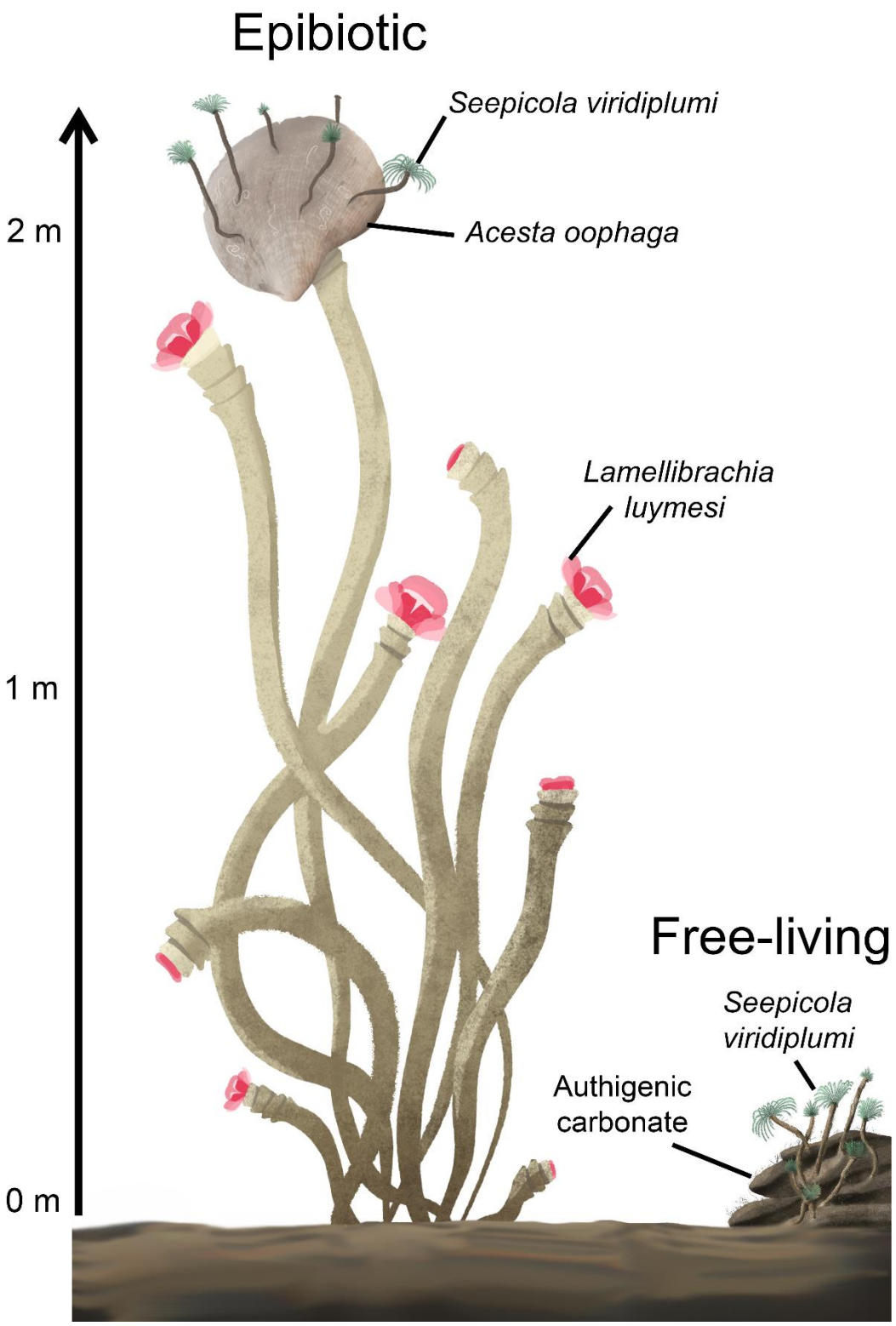

Figure 4.1: Artistic illustration showing the microhabitats of the sabellid *Seepicola viridiplumi* and the upper threshold of vertical height separation between epibiotic and free-living sabellid individuals. Artwork by AEC.

2. MATERIALS AND METHODS

2.1 Sample Collection

Seepicola viridiplumi samples and their associated substrata were collected from three sample sites within the Gulf of Mexico, Brine Pool NR1, Bush Hill, and Green Canyon 234 using either HOV *Alvin* deployed from the R/V *Atlantis* or ROV *Jason* deployed from the R/V *Thomas G. Thompson* (Table 4.1). At each site, collection efforts targeted both microhabitats the sabellids inhabit: *Acesta oophaga* file clam valves and authigenic carbonate outcroppings. File clams bearing multiple *S. viridiplumi* individuals were collected only when 10 or more *A. oophaga* individuals were observed within the seep site. Samples were transported to the surface in insolated boxes.

Once recovered to the ship, collected carbonate rock and *A. oophaga* clams were transferred to buckets of chilled seawater and were kept in cold rooms (7^{o}C) with aeration until processing. Sabellids were processed within 48 hours of collection. Carbonate slabs were carefully broken into smaller fragments using a hammer and chisel, while *A. oophaga* clams were shucked and their valves separated. Individual *S. viridiplumi* were isolated from each substrate type using dental picks with the aid of dental loupes. Once removed, worms were cut from their tubes and measured for total length. The anterior regions (~10 segments) and radiolar crowns of a subset of sabellids from each site were removed, rinsed in MilliQ water, and frozen to -80^{o}C for stable isotope analysis (Table 4.1). Similarly, the anterior region and attached radiolar crown of 20 *S. viridiplumi* from the October collection were rinsed in 0.3 μm filtered seawater and were flash frozen and stored at -80^{o}C for 16S rRNA gene sequencing.

Table 4.1. Collection information for the three study sites and sample sizes (number of individuals) for the stable isotopic and microbial community analyses.

Site	Depth (m)	Latitude (°N)	Longitude (°W)	Collection	Condition	Sample Sizes			
						$^{13}\delta C$	$^{15}\delta N$	$^{34}\delta S$	16S rRNA
Brine Pool NR1	658	27.72347544	-91.27924444	Feb, 2020	Epibiotic	5	5	0	0
					Free-living	6	6	0	0
				Jun, 2021	Epibiotic	0	0	0	0
					Free-living	10	10	4	0
				Oct, 2022	Epibiotic	10	10	8	3
					Free-living	12	12	4	5
Bush Hill	540	27.78237117	-91.50830855	Feb, 2020	Epibiotic	0	0	0	0
					Free-living	13	13	0	0
				Jun, 2021	Epibiotic	10	10	3	0
					Free-living	9	9	3	0
				Oct, 2022	Epibiotic	0	0	0	0
					Free-living	21	21	16	6
Green Canyon 234	528	27.74614894	-91.22191704	Feb, 2020	Epibiotic	2	2	0	0
					Free-living	2	2	0	0
				Jun, 2021	Epibiotic	10	10	0	0
					Free-living	8	8	3	0
				Oct, 2022	Epibiotic	0	0	0	0
					Free-living	18	18	16	6

2.2 16S rRNA Sequencing and Analysis

DNA was extracted from 20 collected tissue samples using a Qiagen Power Biofilm kit (Qiagen, Valencia, CA, USA). Concentrations of extracted DNA were quantified using a Qubit 4 Fluorometer (Invitrogen). Amplification, sequencing, and library preparation of the V6V8 region of the 16S rRNA gene for each of the 20 samples were performed by the Integrated Microbiome Resource laboratory (IMR) at Dalhousie University (https://imr.bio/index.html, Halifax, NS).

The extracted DNA was amplified using both Bacteria-specific (B969F 5'-ACGCGHNRAACCTTACC-3' and BA1406R 5'-ACGGGCRGTGWGTRCAA-3') and Archaea-specific primers (A956F 5'-TYAATYGGANTCAACRCC-3' and A1401R 5'-CRGTGWGTRCAAGGRGCA-3') (Comeau et al. 2011). Amplicon fragments were amplified using a high-fidelity Phusion Plus polymerase, and separate amplification runs were conducted for Bacteria and Archaea. The polymerase chain reaction (PCR) thermocycling conditions were: 98ºC for 30 seconds, 30 cycles of: 98ºC for 10 seconds, 55ºC for 30 seconds, and 72ºC for 30 seconds; followed by a final extension step at 72ºC for 5 minutes (Comeau et al. 2011). PCR products were verified on a high-throughput Hamilton Nimbus Select liquid handling system using Coastal Genomics Analytical gels before being normalized using the Charm Biotech Just-a-Plate Normalization kit. Library sequencing was performed using a NextSeq2000 (2 x 300 bp) at 3-4x depth.

Sequenced reads obtained from IMR were processed using the DADA2 pipeline (Callahan et al. 2016) in RStudio (v. 4.2.3). Sequences were checked for quality following package guidelines before being filtered and trimmed to remove low-quality regions (Bacteria: truncLen = c(270,232), maxEE = c(3,3), truncQ = 2, trimLeft = 17; Archaea: truncLen = c(264, 190), maxEE = c(2,2), trunQ = 2, trimLeft = 18). Paired-end reads were merged and Amplicon Sequence

Variants (ASVs) were generated. Chimeric sequences were removed and taxonomy was assigned using the naïve Bayesian classifier method (Wang et al. 2007) against the Silva Database (r138.1; Quast et al. 2013). High taxonomic-level unknowns as well as sequences identified as Eukaryotic, Mitochondria, and Chloroplast were removed. As 10 samples amplified poorly at the PCR stage (Supplementary Figure S4.1, Table 4.2), resulting differences in sequencing depth were accounted for by normalizing the final phyloseq object using the Trimmed mean of M-values (TMM) method in the microbiomeMarker package (v. 1.3.3; Cao et al. 2022). Differences in sequencing depth were then further accounted for by converting ASV abundance counts to proportions for all community analyses (McKnight et al. 2019). Sequences were then analyzed in RStudio using the phyloseq (McMurdie & Holmes 2013) and vegan (Okansen et al. 2022) packages. Functional metabolic diversity of the observed microbial community was assigned using the microeco package (v.1.6.0; Liu et al. 2021) and FAPROTAX database (Louca et al. 2016).

The effect of sample site on ASV richness and Shannon diversity were examined using an analysis of variance (ANOVA) after testing for normality and homogeneity of variances across groups using the Shapiro-Wilk and Brown-Forsythe tests, respectively. For the samples collected at Brine Pool NR1, the effect of epibiosis on ASV richness and Shannon diversity was further explored using *t*-tests after confirming data were normally distributed with a Shapiro-Wilk test. Changes in microbial community structure and composition between sites and microhabitats were examined using principal coordinate analyses (PCoA) and PERMANOVAs run on Bray-Curtis dissimilarity matrices.

Table 4.2. Sample collection and 16S rRNA bioinformatic information obtained from the use of Bacteria-specific primers. Samples with the highest sequencing depth are bolded.

Site	Condition	Sample ID	DNA concen.	Raw Reads	Final Reads	Reads retained (%)	# ASVs
Brine Pool NR1	Epibiotic	BPSa91	46.2	1416	981	69.3	33
		BPSa93	20.8	1474	967	65.3	32
		BPSa96	**40.8**	**5749**	**4049**	**70.5**	**139**
		BPSa97	69.4	2345	1725	73.6	33
		BPSa109	3.68	4868	3672	75.4	72
	Free-living	**BPSa137**	**90.2**	**13031**	**9264**	**71.1**	**158**
		BPSa152	89.2	435	189	43.4	15
		BPSa154	1.18	2890	1666	57.6	64
Bush Hill	Free-living	BHSa85	39.1	1432	749	52.2	50
		BHSa87	**146.0**	**8676**	**6540**	**75.4**	**69**
		BHSa93	**64.2**	**9932**	**6034**	**60.7**	**160**
		BHSa118	**48.2**	**12275**	**7834**	**64.0**	**120**
		BHSa120	12.9	1853	1065	57.5	66
		BHSa121	**96.6**	**30173**	**21043**	**69.7**	**169**
Green Canyon 234	Free-living	**GCSa59**	**78.4**	**27013**	**18945**	**70.1**	**150**
		GCSa63	71.4	3770	2250	59.8	57
		GCSa64	**60.4**	**50859**	**40468**	**79.6**	**172**
		GCSa67	**34.4**	**38921**	**25524**	**65.6**	**229**
		GCSa71	106	1459	576	39.3	74
		GCSa72	**92.6**	**35847**	**21340**	**59.5**	**247**

2.3 Stable Isotope Analysis

Tissue samples were lyophilized in a Labconco FreeZone lyophilizer for 48 hours prior to being homogenized. The resulting powder was packaged into tin cups and sent to the Core Stable Isotope Laboratory at Washington State University for 13C, 15N, and 34S isotopic measurements. The February collection did not include samples for 34S. Isotopic ratios were measured using a continuous flow-elemental analysis-isotopic ratio mass spectrometry with an ECS 4010 elemental analyzer (Costech Analytical, Valencia, CA) and a Delta PlusXP isotope ratio mass spectrometer (Thermofinnigan, Breman). Isotopic ratios were reported in ‰ following the standard δ notation (Coplen, 2011). All data were calibrated to reference materials from the National Institute of Standards and Technology (NIST), and the standards were interspersed with samples during analysis.

Isotopic data were analyzed in RStudio (v. 4.2.3). All isotopic values were checked for normality and homogeneity of variances using Shapiro-Wilk and Levene's tests, respectively. Two-way analysis of variance tests (ANOVA) followed by Tukey HDS post-hoc tests were used to compare isotopes of either carbon, nitrogen, or sulfur across collection season and study site. Ratios of carbon were non-normally distributed and skewed despite attempts at data transformation. A two-way ANOVA was still utilized to compare carbon ratios as it has been shown that this test is not overly sensitive to normality deviations and the rate of false positives are not impacted by violation of this assumption (Glass et al. 1972, Harwell et al. 1992, Lix et al. 1996).

Similarly, despite deviations from normality in carbon and sulfur ratios, isotopic values were compared using two-way ANOVAs to investigate the potential impacts of epibiosis. Ecological niche overlaps were also calculated using the Stable Isotope Bayesian Ellipses in R

(SIBER) package (v. 2.1.4; Jackson et al. 2011). Only collections with paired microhabitat samples were included in these analyses. Green Canyon 234 samples collected in February 2020 were not included due to low sample sizes. Similarly, sulfur isotopes from the June 2021 collection at Green Canyon 234 were not included. Standard 95% confidence interval ellipses for epibiotic and free-living samples were constructed using δ13C and δ15N data, as well as δ13C and δ34S data. Standard ellipse areas, corrected for small sample sizes, were calculated, and the maximum likelihood overlap between ellipses was estimated. Measurements of ellipse overlap are presented as a proportion of the sum of the non-overlapping ellipse areas, with 0 indicating distinct trophic niches and 100% representing trophic niches with complete overlap.

3. RESULTS

3.1 Bacterial and Archaeal Communities

Bacterial sequencing and filtering efforts resulted in a total of 174,881 reads and 855 unique ASVs that were used for analysis. Rarefaction curves indicated that the sequencing depth was sufficient in most samples to recover the bacterial communities present (Supplementary Figure S4.1). No Archaeal ASVs were successfully amplified or identified from the collected sabellid tissue samples using the Archaeal-specific primers. Instead, the radiolar crowns and anterior regions of *Seepicola viridiplumi* were dominated by bacterial taxa primarily belonging to the phyla Proteobacteria and Bacteroidota, making up approximately 98% of all observed ASVs. The taxonomic families with the highest mean relative abundances across all samples belonged to the phylum Proteobacteria and included Colwelliaceae (40.6%), Endozoicomonadaceae (genus *Endozoicomonas*; 16.5%), Moritellaceae (5.1%), Pseudoalteromonadaceae (4.4%), and Vibrionaceae (3.5%). Bacterial taxa belonging to the order Methylococcales and the families

Arcobacteraceae and Sulfurovaceae, identified from other seep chemosymbiotic macrofaunal associations, had low mean relative abundances (<1%). Although, Acrobacteraceae did have a higher relative abundance at Green Canyon 234 (2.8%). The functional diversity of the observed microbial community was not particularly diverse, with anaerobic and aerobic chemoheterotrophs and fermentation-based metabolisms dominating. Microbes specializing in methyl- and methanotrophy as well as nitrogen and sulfur cycling were much rarer.

Overall, bacterial community composition differed among collection sites (PERMANOVA $p < 0.01$; Figure 4. 2B). While certain bacterial families were common at each of the study sites, mean relative abundances varied substantially (Figure 4.2A**)**. Taxa belonging to the family Colwelliaceae appeared to be most abundant on *S. viridiplumi* radiolar crowns at Green Canyon 234, with a mean relative abundance of 55.8%. Colwelliaceae only represented 15% and 15.5% of the microbial communities at Brine Pool NR1 and Bush Hill, respectively. Bush Hill had the highest mean relative abundance of Endozoicomonadaceae at 30.9%, which was more than double that seen at Brine Pool NR1 (13.7%) and Green Canyon 234 (11.3%). *Seepicola viridiplumi* collected from Brine Pool NR1 had a high mean relative abundance of Vibrionaceae bacteria (15.6%), which was relatively rare at Bush Hill (2.9%) and Green Canyon 234 (1.3%). Each site also contained one or two outlier individuals with notably different microbial communities on their radiolar crowns (Figure 4.2A). For example, Brine Pool NR1 and Green Canyon 234 both had a single individual with higher relative abundances of Flavobacteriaceae than all other individuals collected. A single *S. viridiplumi* at Brine Pool NR1 and Bush Hill had higher relative abundances of Moraxellaceae compared to all other individuals (Figure 4.2A). It should be noted, however, that these specimens also experienced poor amplification and had lower sequencing depth (Table 4.2, Supplementary Figure S4.1).

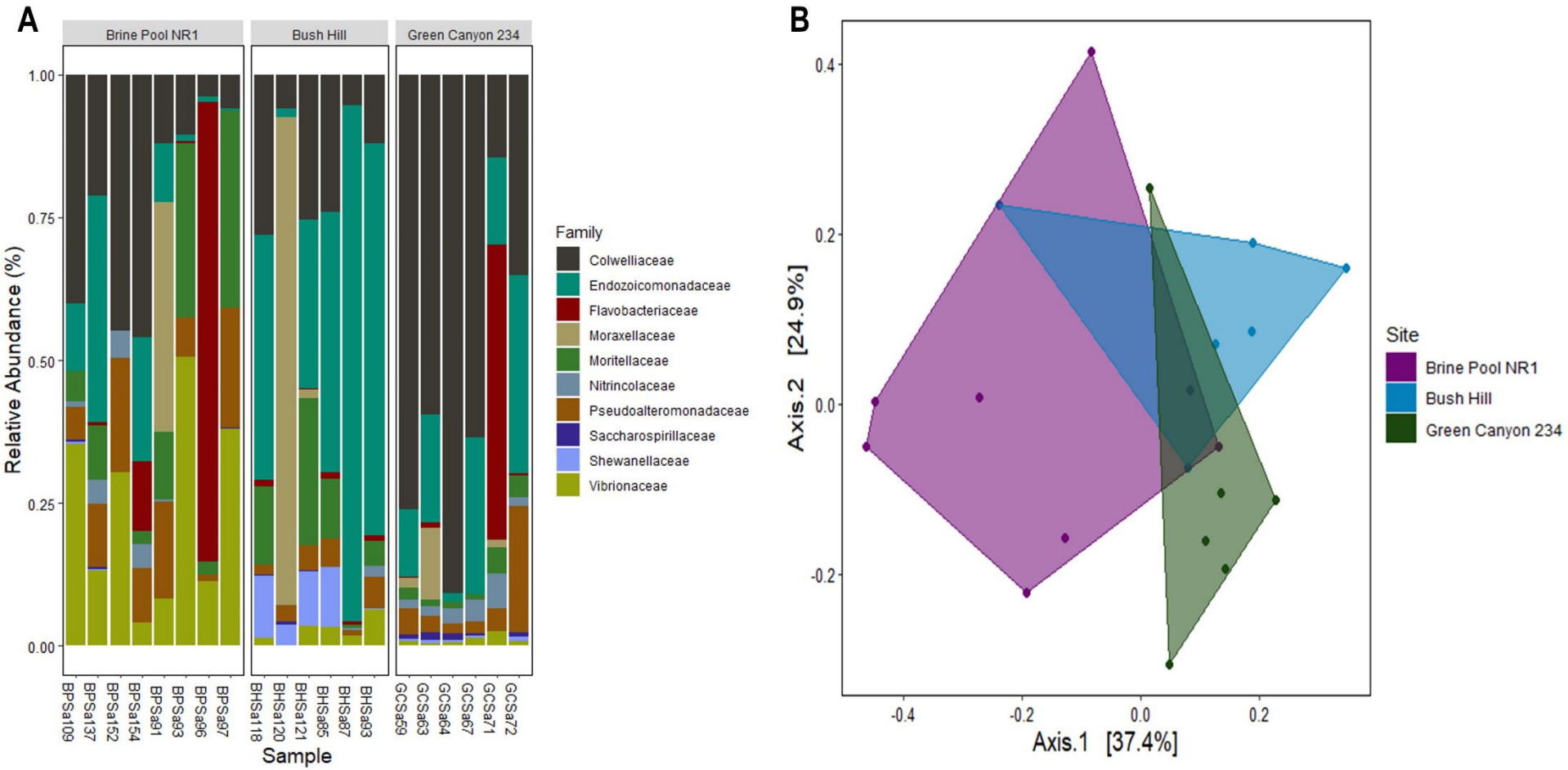

Figure 4.2. Bacterial diversity associated with *Seepicola viridiplumi* radiolar crowns. (A) The relative abundance of the top 20 most numerous bacterial ASVs, colored by taxonomic Family. Samples are organized by study site. (B) Principle Coordinate Analysis (PCoA) of the Bray -Curtis dissimilarity matrix based on ASV relative abundance by collection site.

Despite the differences in overall bacterial community composition observed between sites, sample site did not impact observed ASV richness (ANOVA, $p > 0.05$) or Shannon diversity (ANOVA, $p > 0.1$; Figure 4.3). For specimens collected at Brine Pool NR1, the microhabitat also did not appear to have an impact on either observed ASV richness ($t = -0.37$, $p > 0.5$) or Shannon diversity ($t = -0.77$, $p > 0.05$). No significant differences were observed in community structure and composition between epibiotic and free-living *S. viridiplumi* (PERMANOVA, $p > 0.1$; Figure 4.3). Although, free-living individuals were observed to have slightly higher relative abundances of Colwelliaceae bacteria at 16.1% compared to epibiotic at 13.2% (Figure 4.2A).

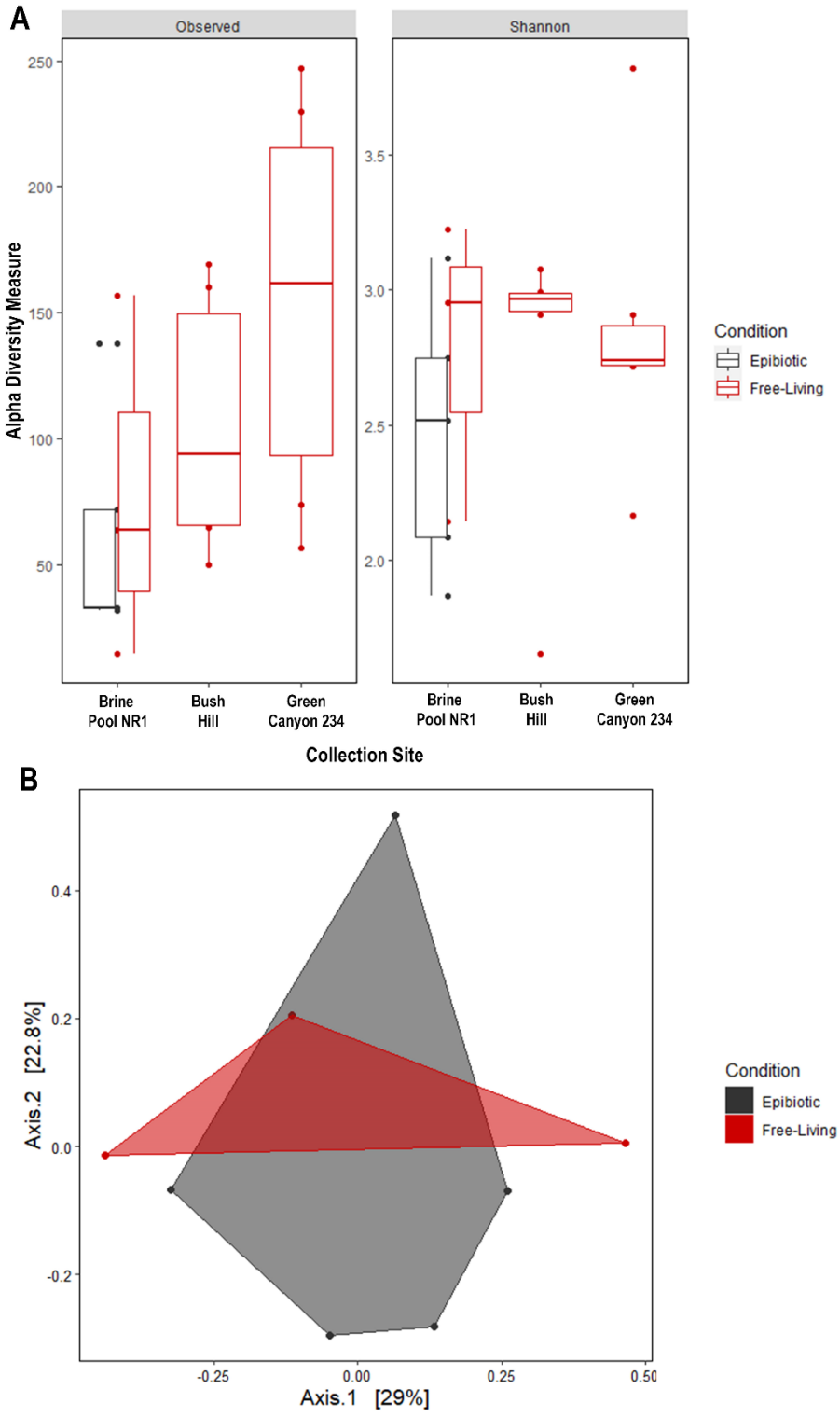

Figure 4.3. Comparisons of bacterial diversity on *Seepicola viridiplumi*. (A) Observed ASV richness and Shannon diversity, grouped by study site and colored to show microhabitat. (B) Principle Coordinate Analysis (PCoA) of the Bray-Curtis dissimilarity matrix based on microbial ASV relative abundance in each Brine Pool NR1 sample, colored by microhabitat.

3.2 Nutrient Resources

All *S. viridiplumi* individuals had isotopic ratios indicative of chemosynthetic input. Stable isotope ratios of carbon ($\delta^{13}C$) ranged between -23 to -39 ‰, $\delta^{15}N$ from 4 to 9 ‰, and $\delta^{34}S$ from -17 to 0 ‰ (Table 4.3). Individuals from Brine Pool NR1 had the lightest $\delta^{13}C$ signatures, while Bush Hill *S. viridiplumi* were consistently more enriched (Figure 4.4). Nitrogen ratios were also highly variable at each of the three sample sites, with individuals within a site often spread across the full observed range among sites (Figure 4.4). Ratios of sulfur varied among the study sites, with the samples from Bush Hill exhibiting the largest range of values (Figure 4.4). In general, Bush Hill and Green Canyon 234 were more similar to each other than either was to Brine Pool NR1.

Seasonal shifts in isotopic ratios were also observed at each of the three sites, and between collection seasons (Table 4.4A) although the patterns were inconsistent. *Seepicola viridiplumi* from Brine Pool NR1 were significantly more depleted in carbon ratios in the fall and nitrogen ratios were slightly more enriched in the summer (Supplementary Table S4.1). Bush Hill *S. viridiplumi* showed statistically different ratios of nitrogen between each collection, with ratios being the most depleted in the summer and the most enriched in the winter. While a similar trend was observed in nitrogen ratios from Green Canyon 234 sabellids, these changes were not significant (Supplementary Table S4.1). Neither Bush Hill nor Green Canyon 234 showed seasonal changes in carbon ratios. Seasonal isotopic shifts in sulfur were significant at Bush Hill (Supplementary Table S4.2), with values becoming significantly more enriched in the fall (Supplementary Table 4.3). No significant seasonal changes in sulfur were observed at either Brine Pool or Green Canyon 234 (Supplementary Table S4.2).

Table 4.3. Average isotopic values by collection ± standard error. Bolded values indicate seasons with statistically different isotopic ratios, and collections marked with an asterisk denote instances when a single comparison was significant.

		Collection		
Site	**Isotope**	**Feb 2020**	**Jun 2021**	**Oct 2022**
Brine Pool NR1	$\delta^{15}N$	6.90 ± 0.910	7.91 ± 0.351*	6.66 ± 0.212*
	$\delta^{13}C$	-31.54 ± 1.156	-30.98 ± 1.286	**-36.37 ± 1.178**
	$\delta^{34}S$	-	-3.09 ± 4.697	-2.64 ± 0.980
Bush Hill	$\delta^{15}N$	**8.93 ± 0.179**	**6.13 ± 0.607**	**8.05 ± 0.217**
	$\delta^{13}C$	-24.06 ± 0.229	-25.65 ± 0.794	-24.34 ± 0.188
	$\delta^{34}S$	-	**-10.31 ± 3.693**	**-2.75 ± 0.832**
Green Canyon 234	$\delta^{15}N$	7.18 ± 0.850	6.33 ± 0.226	6.52 ± 0.188
	$\delta^{13}C$	-26.83 ± 0.595	-26.55 ± 0.295	-25.79 ± 0.145
	$\delta^{34}S$	-	-4.77 ± 2.495	-6.83 ± 0.887

Table 4.4. Results of two-way ANOVAs. A) The effects of season, collection site, and their interaction of isotopic ratios of carbon, sulfur, and nitrogen. B) The effects of collection (site and season), microhabitat (epibiotic and free-living), and their interaction on isotopic ratios. Italicized values indicate non-significant interactions.

A

	Collection Season		Collection Site		Interaction	
Isotope	**Test Statistic (F)**	**p-value**	**Test Statistic (F)**	**p-value**	**Test Statistic (F)**	**p-value**
Carbon	24.15	< 0.0001	426.56	< 0.0001	25.21	< 0.0001
Nitrogen	23.12	< 0.0001	16.94	< 0.0001	22.88	< 0.0001
Sulfur	11.19	< 0.01	11.50	< 0.0001	14.38	< 0.0001

B

	Collection		Microhabitat		Interaction	
Isotope	**Test Statistic (F)**	**p-value**	**Test Statistic (F)**	**p-value**	**Test Statistic (F)**	**p-value**
Carbon	140.054	< 0.0001	5.892	< 0.05	2.520	*0.0661*
Nitrogen	4.752	< 0.01	74.049	< 0.0001	14.032	< 0.0001
Sulfur	35.634	< 0.0001	0.841	*0.3747*	6.287	< 0.05

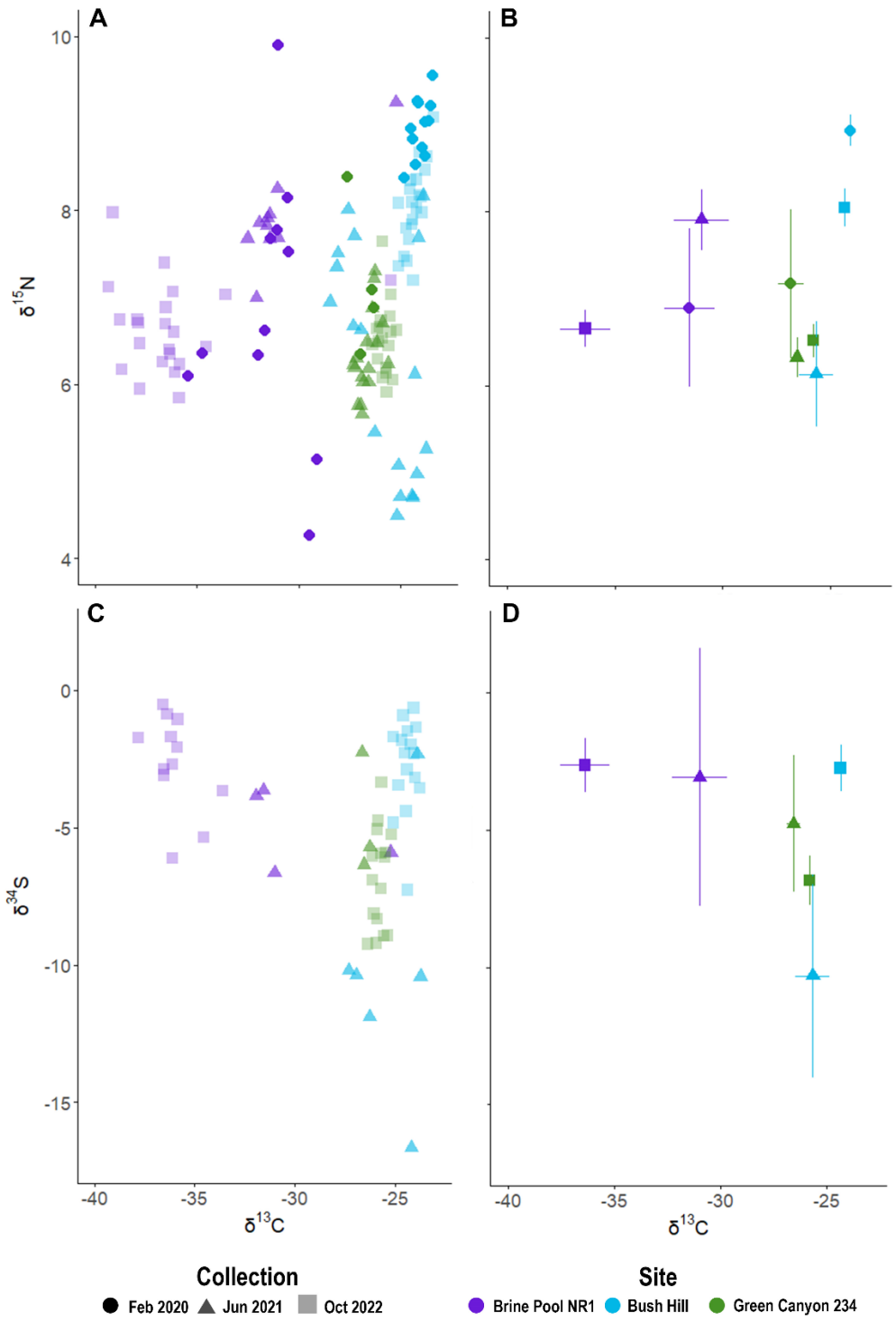

Figure 4.4. Isotopic ratios for each of the three study sites in various seasons. Ratios of $\delta^{13}C$ and $\delta^{15}N$ are shown with all data (A) as well as mean values ± 95% confidence intervals (B). Ratios of $\delta^{13}C$ and $\delta^{34}S$ are also shown with all data (C) and mean values ± 95% confidence intervals (D).

3.3 Trophic Niches for Epibiotic and Free-living *Seepicola viridiplumi*

Comparisons of isotopic ratios between paired epibiotic and free-living *S. viridiplumi* from the four times they were sampled revealed consistent patterns and differences between the two microhabitats (Table 4.4B; Figure 4.5). Free-living sabellids had significantly more enriched levels of $\delta^{15}N$ than epibiotic individuals at Brine Pool NR1 in February ($p < 0.0001$), as well as at Bush Hill (Supplementary Table S4.3; $p < 0.0001$). While a similar pattern was observed for *S. viridiplumi* at Brine Pool in October and at Green Canyon 234 in June, these were not significant (Supplementary Table S4.3). Isotopic ratios of sulfur were more similar between epibiotic and free-living individuals at both Bush Hill in June and Brine Pool in October (Supplementary Table S4.4).

SIBER ellipse analysis revealed some trophic segregation between *S. viridiplumi* from the two microhabitats, although the degree of segregation varied spatially and temporally (**Figure 4.5**). Brine Pool NR1 in February showed trophic segregation in nitrogen-carbon ellipses with an ellipse overlap of 9.26%. However, there was less trophic segregation in October with 36.72% overlap (Figure 4.5B). Green Canyon 234 also showed a higher degree of trophic niche overlap between epibiotic and free-living sabellids in June (38.91% overlap). In contrast, Bush Hill showed completely distinct isotopic niches for free-living and epibiotic *S. viridiplumi* in June (Figure 4.5C). The carbon-sulfur ellipses revealed similar patterns of varying overlap (Figure 4.5E-F). The October collection at Brine Pool NR1 had an ellipse overlap of 39.54%, while the June collection of Bush Hill only showed 10.35% ellipse overlap.

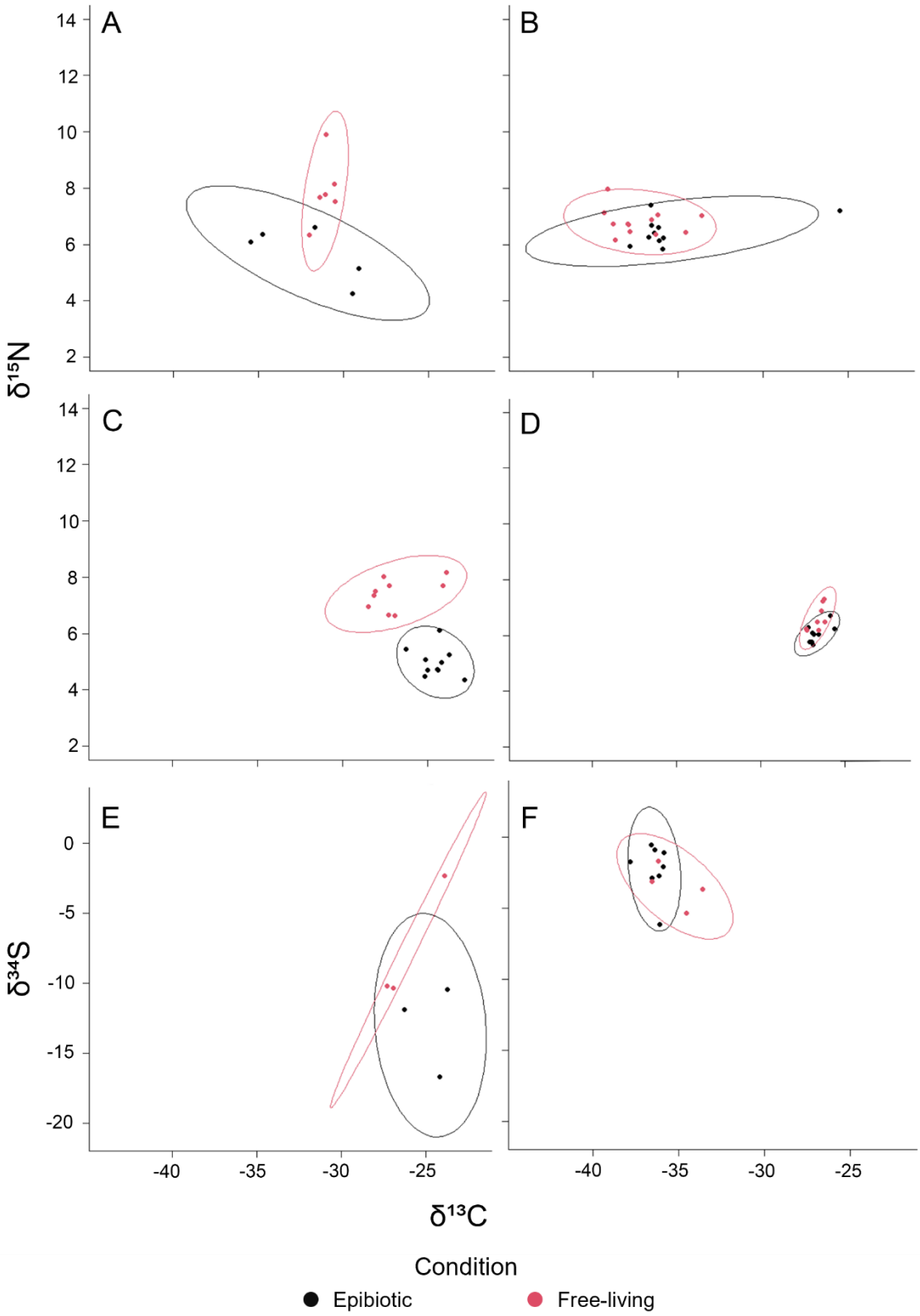

Figure 4.5. Carbon versus nitrogen (A – E) and carbon versus sulfur (E – F) isotopic niche plots of epibiotic and free-living *Seepicola viridiplumi* individuals. A) Brine Pool NR1 winter collection; B) Brine Pool NR1 fall collection; C) Bush Hill summer collection; D) Green Canyon 234 summer collection; E) Bush Hill summer collection; F) Brine Pool NR1 fall collection.

4. DISCUSSION

It has been widely accepted that hydrocarbon seep systems support high abundances of methanotrophic bacteria as well as species with sulfate-reducing and sulfite-oxidizing metabolisms (Ruff et al. 2015). However, we found that the bacterial taxa found on *Seepicola viridiplumi* radiolar crowns predominantly rely on fermentation pathways, and likely break down polysaccharides and aromatic hydrocarbons. Bacterial fermentation can be abundant at methane seep systems (Zhang et al. 2023) and is known to aid in the breakdown of organic detritus and macromolecules (Reeburgh 2007, Orcutt et al. 2010). The abundance of bacterial taxa capable of fermentation observed on *S. viridiplumi* may aid in the acquisition of nutrition from complex hydrocarbons and POM found within the methane-seep habitats.

The microbial communities associated with *S. viridiplumi* anterior regions and radiolar crowns were dominated by Bacteria in the phylum Proteobacteria, which are well known to have high abundances at chemosynthetic sites and are often observed in symbiotic associations with macrofaunal organisms (Sogin et al. 2020). Representatives of the family Colwelliaceae are also commonly observed at hydrocarbon seeps and are heterotrophic chemoorganotrophs that specialize in degrading aromatic hydrocarbon compounds through fermentation (Mason et al. 2014, Deming & Junge 2015). Recent work has indicated that Colwelliaceae are key in the initial stages of crude oil degradation, but often decrease in abundance as the degradation process continues and are succeeded by taxa like Methylococcales (Bacosa et al. 2018). In contrast, the potential role of Endozoicomonadaceae bacteria is more uncertain, although the groups that are commonly associated with marine invertebrates are heterotrophic chemoorganotrophs that utilize carbohydrates (Glaeser & Kämpfer 2020). Members belonging specifically to the genus *Endozoicomonas* have been identified in hydrothermal vent snails and polychaetes, scleractinian

corals and gorgonians, as well as sponges and tunicates (Neave et al. 2016). In *Ridgeia piscesae* tubeworms at hydrothermal vents, *Endozoicomonas* bacteria were found to aid in methane cycling and food degradation (Forget & Kim Juniper 2013). More recently, a species of *Endozoicomonas* was found in association with the gills of the file clam *Acesta excavata*, likely aiding in the breakdown of structural polysaccharides from plankton-based detritus (Jensen et al. 2021). However, free-living representatives of this group have also been suggested (Jensen et al. 2021).

Other, less abundant, bacterial taxa present on *S. viridiplumi* radiolar crowns and anterior regions are known chemoorganatrophs, including Flavobacteriaceae and Moraxellaceae (Bernardet 2015a b, Fernández-Garayzábal et al. 2022). Flavobacteriaceae also participate in fermentation pathways to breakdown polysaccharides and organic matter (Liu & Liu 2013, Bernardet 2015a). The potential role of Moraxellaceae is less clear but species in this group are known to assist in denitrification and acetate metabolism (Ji et al. 2015, Li et al. 2023, Fu et al. 2024). Strains of Vibrionaceae, which were most abundant in the Brine Pool NR1 sabellids, are also known to participate in oil degradation pathways (Liu & Liu 2013, Bacosa et al. 2018). The lack of recovered Archaeal ASVs was surprising but could have been caused by a low abundance of Archaea on the radiolar crowns of the *Seepicola viridiplumi* examined in this study, or a failure of the Archaeal primers used in the amplification process.

Typically, macrofaunal invertebrate species engaging in symbiotic relationships with microbes associated with a single or a few microbial taxa that dominate the host microbiome (Sogin et al. 2020). Such a trend was not observed in *S. viridiplumi*. While the same Bacterial families were present across all individuals, the relative abundances for each group showed a high degree of variability within and between sample sites. It is more likely that *S. viridiplumi* are acting as opportunistic grazers, feeding on free-living bacteria present within their immediate

environment. Sabellids have been hypothesized to act as opportunistic generalist feeders at hydrocarbon seeps (Becker et al. 2009, Cordes et al. 2010a), and are known as efficient suspension-feeders capable of consuming bacteria and resuspended material (Jumars et al. 2015).

The hypothesis that *S. viridiplumi* are acting as opportunistic grazers of the hydrocarbon seep bacterial community and POM derived from both surface photosynthetic productivity and local chemosynthetic productivity is supported by the observed isotopic values. While methanotrophic and thiotrotrophic bacterial taxa were rare on the radiolar crowns and anterior regions of *S. viridiplumi*, the isotopic ratios strongly implied thiotrophic input. Bacterial mats, common in hydrocarbon seep systems, are usually composed of sulfur-oxidizing bacteria (Paul et al. 2017, Leprich et al. 2021). These mats can be extensive within the Gulf of Mexico (MacDonald et al. 1989) and are known as potential nutrient sources on the benthos (Kelley & Coffin 1998). Bacterial mats frequently grow on authigenic carbonate outcrops and can be resuspended due to currents (Grant & Bathmann 1987) or mobile benthic fauna. Epibiotic *S. viridiplumi* sabellids may still be able to graze on thiotrophic bacteria free-living in the water column above the seep.

The strongest signal of thiotrophy was seen in the depleted $\delta^{34}S$ ratios observed in all sabellids, but the $\delta^{13}C$ ratios also broadly correspond to Calvin-Benson-Bassham thiotrophy (Hügler & Sievert 2011). We observed differences in $\delta^{13}C$ ratios between sites, which was expected due to differences in the supplying methane pools (Becker et al. 2013, Carney et al. 2015). Carbon ratios were consistently more enriched at Bush Hill and Green Canyon 234 than at Brine Pool, but remained more depleted than the values of surface-derived photosynthetic material in the Gulf of Mexico (-16.4 to -22.7 ‰ $\delta^{13}C$; Wells & Rooker 2009). *Seepicola viridiplumi* at these two sites are likely consuming more nutrition derived from thiotrophy or thermogenic methanotrophy (Carney et al. 2015). In contrast, *S. viridiplumi* at Brine Pool NR1 likely rely more

on biogenic methanotrophic material.

Interestingly, *S. viridiplumi* at Brine Pool NR1 showed a seasonal shift in carbon ratios, with more depleted values observed in the fall. The Gulf of Mexico is known to have peaks in sea surface productivity and POC flux in the winter (Biggs et al. 2008). While this pattern does correspond with the change in carbon ratios at Brine Pool NR1, this pattern was not observed at Green Canyon 234 or Bush Hill. The three study sites are in close geographic proximity, but Green Canyon 234 and Bush Hill are slightly shallower in depth. Bush Hill and Green Canyon 234 may receive a more stable influx of POC throughout the year because of this difference in depth. Being at a deeper site, the sabellids at Brine Pool NR1may experience and reduction in POC availability in the fall. Bush Hill and Green Canyon 234 both showed similar seasonal shifts in nitrogen ratios and may indicate a change in the availability of heavily recycled detritus throughout the year at these two sites. Topography could also be an underlying factor influencing these observed patterns. Bush Hill is a known topographic high topped by large authigenic carbonate outcroppings while Green Canyon 234 also has extensive tubeworm fields and carbonate outcrops. These structures may cause a localized acceleration of currents and increase the flux of POM and detrital resuspension from the seafloor (Becker et al. 2009).

Broadly, epibiotic settlement was also found to affect the diet of *S. viridiplumi* sabellids, although the microbiome did not appear to shift. Trophic niches for epibiotic and free-living *S. viridiplumi* generally showed overlap, indicating both groups shared access to some nutritional resources. However, free-living sabellids consistently had more enriched nitrogen values than epibiotic individuals, potentially indicating improved access to a wider variety of detritus and recycled material. The complete trophic niche separation between microhabitats at Bush Hill suggests that epibiotic *S. viridiplumi* were feeding heavily on POM from the surface, while free-

living relied more on localized bacterial trophic input.

5. CONCLUSIONS

This study is the second to examine the microbial communities associated with hydrocarbon seep sabellids. While sabellids have been recently identified as a potential group harboring chemosynthetic microbial symbionts (Goffredi et al. 2020), our results indicate that this is not true for all sabellid species at hydrocarbon seeps. *Seepicola viridiplumi* was found to have a microbiome dominated by hydrocarbon-degrading Bacterial taxa with fermentation metabolic pathways and lacked an obvious candidate for a chemosymbiotic association. We also found an apparent lack of Archaeal taxa on the radiolar crowns of *S. viridiplumi*, which may have been caused by low abundance or by failure of the Archaeal primers used during PCR. Instead, the sabellid acts as a generalist suspension feeder, with body tissue isotopic ratios suggesting input from thiotrophic and photosynthetic sources. Very little is known about sabellids in chemosynthetic systems (Capa et al. 2021), and the work presented here helps to better encapsulate the ecological roles sabellids play in these habitats.

Furthermore, this study revealed the potential impact of epibiotic settlement on diet at a chemosynthetic system. We found that *S. viridiplumi* sabellids access different nutritional resources depending on microhabitat within the methane seep system, with epibiotic individuals even having complete trophic niche separation in some instances. As epifauna and epibiotic settlement on habitat-forming species are common within hydrocarbon seep systems, the number of trophic pathways within seeps has likely been underestimated, and the importance of small-scale spatial changes within a seep has been overlooked. As the need for impact assessment and deep-sea resource management continues to grow, the knowledge of the trophic structure for

chemosynthetic systems like hydrocarbon seeps is becoming increasingly important (Levin et al. 2016). Thus, examining the epibiotic and epifaunal communities that are often abundant yet poorly identified is vital.

BRIDGE

In Chapter IV, I described the trophic ecology of *Seepicola viridipluumi* from methane seeps in the Gulf of Mexico and identified that they are generalist suspension feeders that do not rely on chemosynthetic symbionts. Additionally, *S. viridiplumi* have differing trophic niches depending on whether individuals are epibiotic or free-living. In the next chapter, I consider how the observed differences impact the reproductive output of both epibiotic and free-living *S. viridiplumi* individuals.

CHAPTER V

IMPACTS OF EPIBIOSIS ON THE REPRODUCTIVE PATTERNS OF A SABELLID POLYCHAETE FROM GULF OF MEXICO METHANE SEEPS

This work includes coauthor Dr. Craig Young as contributor to manuscript preparation.

1. INTRODUCTION

Polychaetes in the family Sabellidae are remarkably adept at colonizing new environments (Lee et al. 2018) and can be found in most marine realms and even freshwater habitats (Capa et al. 2021). Many species have been identified from shallow-water and coastal systems, and representatives of various genera have been reported to depths of 6000 m (Capa et al. 2021). One species, *Jasmineira filitovae*, was identified from a depth of 9735 m (Levenstein 1961). Recent work has also identified sabellid polychaetes as consistent members of chemosynthetic communities, including hydrothermal vents (Capa et al. 2013), hydrocarbon methane seeps (Cordes et al. 2010a, Vestheim & Kaartvedt 2016), and whale falls (Amon et al. 2013).

One reason sabellids are able to colonize diverse habitats successfully is the wide diversity of reproductive strategies and patterns within the family (Patti et al. 2003, Dávila-Jiménez et al. 2017). While all sabellid species undergo lecithotrophic larval development, egg sizes among species can range from 82 to 600 μm (Rouse & Fitzhugh 1994). Reproductive modes also include broadcast spawning and ovoviviparity, although intra- and extratubular brooding has also been reported (Rouse & Fitzhugh 1994). Most species are also gonochoristic and iteroparous, but some taxa demonstrate simultaneous hermaphroditism (Capa et al. 2019) or semelparous reproduction (Yun & Kikuchi 1991). Smaller species tend to have a prolonged reproductive season compared to larger taxa (Rouse & Fitzhugh 1994, Capa et al. 2019). However, much of this information comes

from shallow-water systems, and the biology and ecology of species below mesophotic depths remain unstudied. Furthermore, only 13 species from depths below 1000 meters have been coarsely identified (Capa et al. 2021).

At hydrocarbon methane seeps, sabellids are often observed but are rarely identified below the family level (Cordes et al. 2010a, Vestheim & Kaartvedt 2016, Capa et al. 2021). Similar to their shallow-water counterparts, sabellids at chemosynthetic habitats are hypothesized to act primarily as opportunistic grazers, taking advantage of the available hard substrate and increased local productivity (Capa et al. 2019). A newly-described sabellid species, *Seepicola viridiplumi*, has been identified within the Upper Louisiana Slope hydrocarbon methane seeps of the Gulf of Mexico (chapter 3). Individuals burrow into authigenic carbonate cements along the seafloor within the seep systems or act as hyper-epibionts on *Acesta oophaga* file clams. *Acesta oophaga* are obligate epibionts on tubes of the siboglinid polychaete *Lamellibrachia luymesi* (Järnegren et al. 2005, Cordes et al. 2010b, Burris et al. 2014), meaning *S. viridiplumi* individuals can be separated vertically by as much as two meters, depending on their substratum. Epibiotic *S. viridiplumi* appear to consume a higher level of surface-derived particulate organic matter (POM) compared to free-living individuals, which rely more heavily on free-living bacteria resuspended from the seafloor and within the water column (chapter 4).

The implications of epibiotic settlement on facultatively epibiotic species is understudied in comparison to the host species (Wahl & Mark 1999). The changes in diet caused by epibiotic settlement of *S. viridiplumi* may also impact other aspects of sabellid biology, including reproductive output. Food quantity and quality have been widely recognized as important variables that can impact an organism's ability to reproduce (Sokolova et al. 2012). Increases in food availability can increase female size, per-segment fecundity, and egg size in capitellid polychaetes

(Grémare et al. 1988, Qian & Chia 1991, Linton & Taghon 2000). Similarly, diet impacts the body size and size-at-reproductive maturity in the sabellid *Terebrasabella heterouncinata* (Simon et al. 2005).

This study aims to examine and describe the gametogenic and reproductive patterns exhibited by populations at shallow hydrocarbon seeps of the Gulf of Mexico. We sampled three populations over three seasons to examine spatial and temporal differences. As there are currently no reproductive data for sabellids from the deep sea or from any chemosynthetic habitat, we also provide information on gamete size. Additionally, the facultative nature of the epibiotic association between *S. viridiplumi* and *A. oophaga* makes this an ideal system to investigate the consequences of epibiosis on an epibiotic species. To this end, we collected and examined reproductive output for both free-living and epibiotic *S. viridiplumi* individuals to determine if there are any reproductive consequences of epibiotic settlement, potentially caused by the differing trophic niches (chapter 4).

2. MATERIALS AND METHODS

2.1 Study Sites

The three sample sites targeted for this study are located along the upper continental slope of Louisiana, USA (**Figure 5.1**). Brine Pool NR-1 (Brine Pool) lies at a depth of 700 meters in the oil-extraction lease site Green Canyon 233. The site is notable for its large pool of brine surrounded by a dense band of *Gigantidas childressi* mussels. Approximately 200 meters to the south-southwest from the pool are outcroppings of authigenic carbonate rock and *Lamellibrachia luymesi* tube worms with observed sabellids and *Acesta oophaga*. Bush Hill is a conical hill rising approximately 40 meters from its base at a depth of 580 meters. The summit of the hill is

dominated by scattered siboglinid tube worm aggregations, small patches of bathymodiolian mussel beds, authigenic carbonate outcroppings, and active oil and gas seepage. The third sample site is located at the fault-scarp seep at Green Canyon 234. This seep lies at a depth of 580 meters and has extensive *L. luymesi* aggregations and carbonate outcrops.

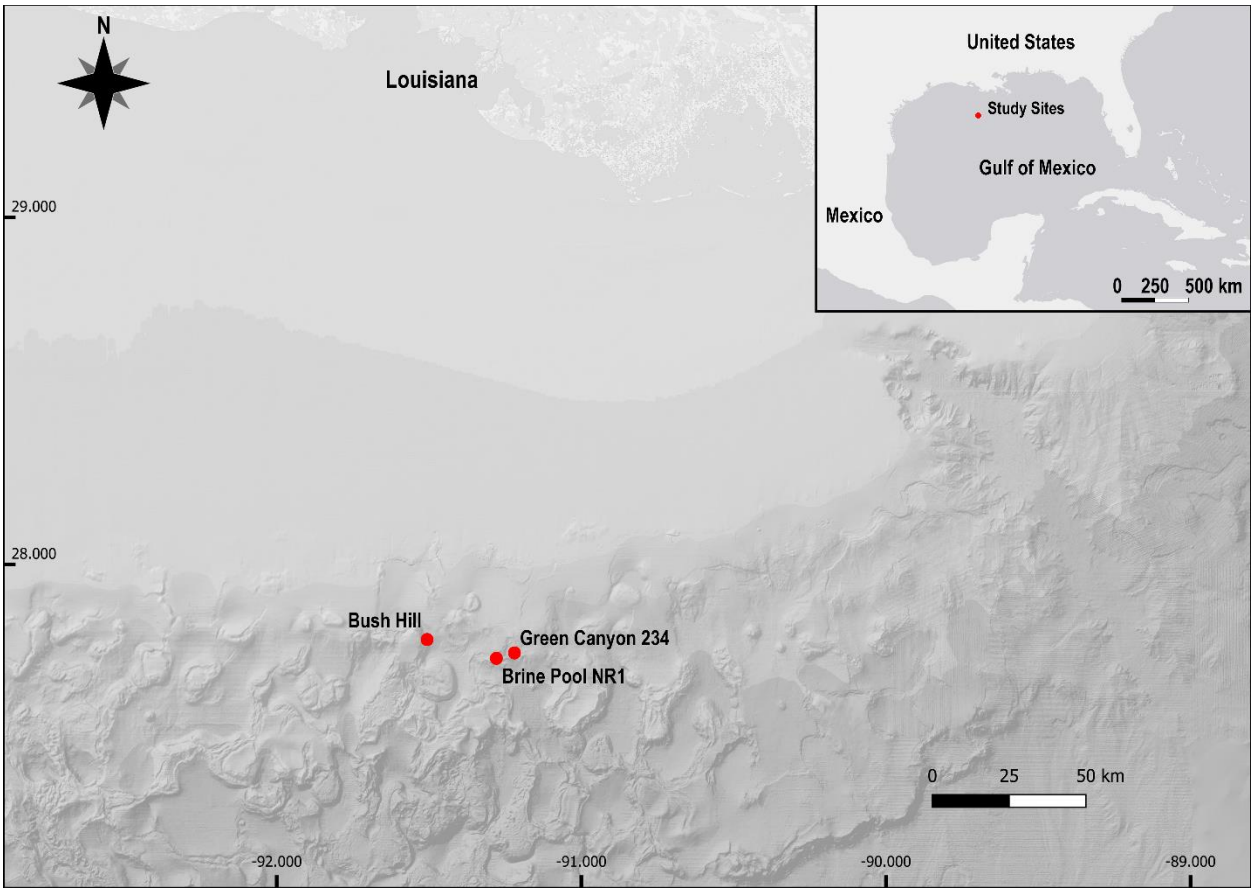

Figure 5.1. The study area in the Gulf of Mexico showing the three methane seep sites where *Seepicola viridiplumi* were collected in 2020 to 2022 in relation to the local bathymetry. Inset shows the position of the seep sites in within the Gulf of Mexico.

2.2 Sample Collection

Samples of *Seepicola viridiplumi* sabellids and their associated substrata were collected from Brine Pool, Bush Hill, and Green Canyon 234 using either HOV *Alvin* deployed from the R/V *Atlantis* (expeditions AT42-24 and AT50-04) or ROV *Jason* deployed from the R/V *Thomas*

G. Thompson (expedition TN391). Collections were made in three different seasons (spring, summer, fall) between 2020 and 2022 (Table 5.1). In each instance, we sought to sample the two microhabitats utilized by *S. viridiplumi*: authigenic carbonate outcroppings and the epizoic file clam *A. oophaga* (Figure 5.2). To minimize damage to the populations of the file clam, collections for epibiotic were only conducted if more than 10 file clams were observed. Whole file clams and pieces of carbonate rock were obtained with the vehicle manipulator arm and were transported to the surface in insulated collection boxes of high-density polyethylene plastic.

Table 5.1. Sample collection details for each site and time point. Italicized collections represent those that were used in comparisons of reproductive output between epibiotic and free-living individuals. The numbers in parentheses indicate the number of stage 4 females used in the microhabitat comparisons for each paired collection.

					Sabellids Sampled		
Site	**Depth (m)**	**Latitude**	**Longitude**	**Collection**	**Total**	**Epibiotic**	**Free-living**
Brine Pool NR-1	658	27.72347544	-91.27924444	*Feb, 2020*	*46*	*36 (13)*	*10 (3)*
				Jun, 2021	11	-	11
				Oct, 2022	51	35	16
Bush Hill	540	27.78237117	-91.50830855	Feb, 2020	15	-	15
				Jun, 2021	*63*	*40 (5)*	*23 (5)*
				Oct, 2022	39	-	39
Green Canyon 234	528	27.74614894	-91.22191704	Feb, 2020	4	2	2
				Jun, 2021	*61*	*26 (6)*	*35 (3)*
				Oct, 2022	27	-	27

Once recovered to the ship, substrata bearing *S. viridiplumi* were transferred to cold rooms (7^{o}C) and kept in aerated, filtered seawater until processing. Ship-board processing occurred as soon as possible (<48 hours). Collected carbonate slabs were carefully broken into smaller fragments using a hammer and chisel, and worms were then removed using dental picks. After obtaining morphometrics for the host file clams, *A. oophaga* individuals were shucked and the number of sabellid tubes on the valves were counted. *Seepicola viridiplumi* individuals were then

carefully isolated using dental picks. Upon removal from the substrate, worms were cut from their parchment tubes and measured for total length.

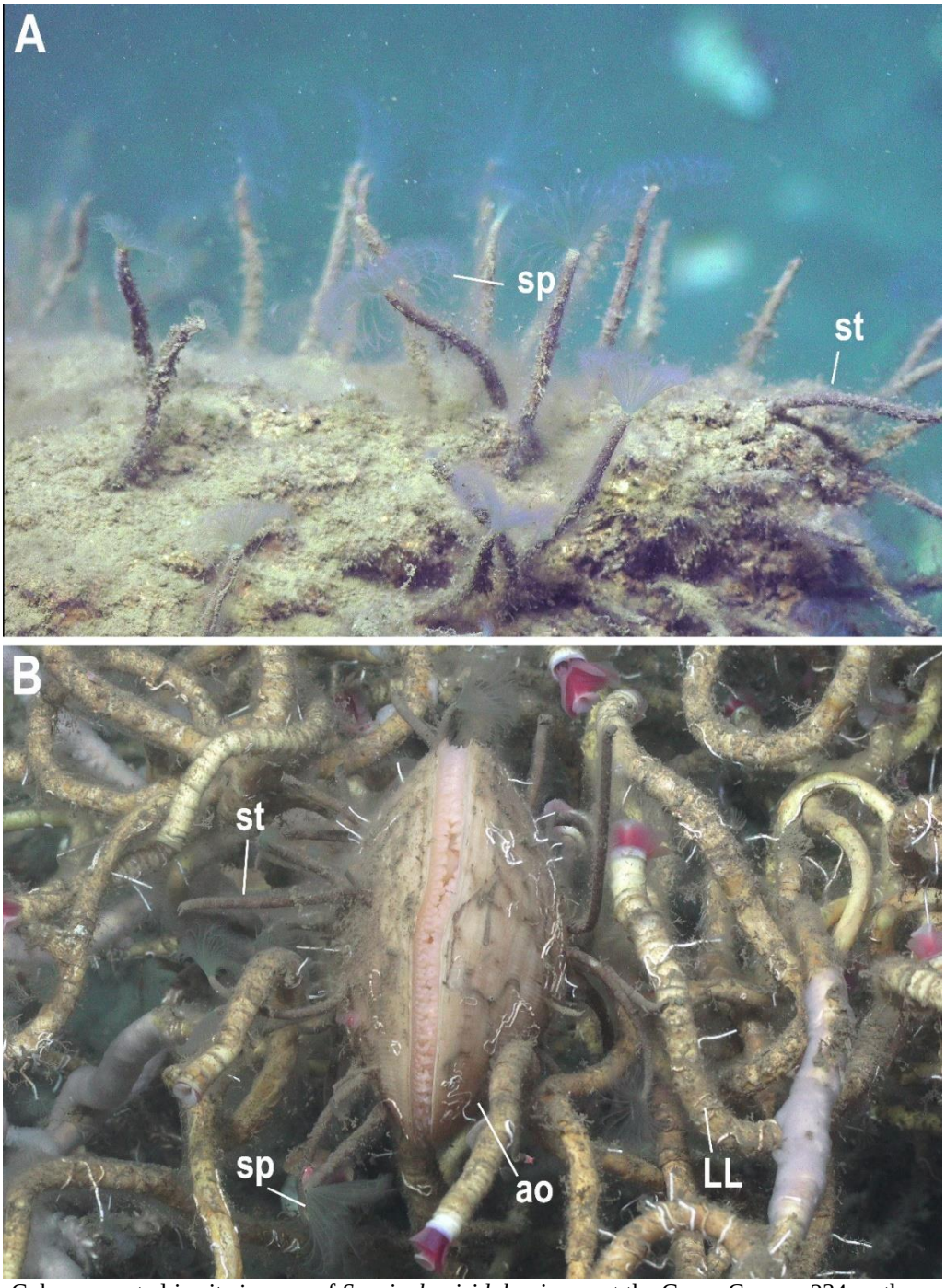

Figure 5.2. Color-corrected *in situ* images of *Seepicola viridplumi* seen at the Green Canyon 234 methane seep site showing (A) free-living and (B) epibiotic individuals. st = sabellid tube; sp = extended sabellid plume; ao = *Acesta oophaga*; LL = *Lamellibrachia luymesi* tube.

2.3 Histology

Extracted *S. viridiplumi* sabellids were preserved at sea using 10% buffered formalin before being transferred to 70% ethanol. All *S. viridiplumi* specimens were cut into smaller fragments along their lengths prior to tissue dehydration to ensure that all samples would fit within the histological molds. The dehydration process consisted of 20-minute graded ethanol baths, progressing from 70 to 100% ethanol with a 5 to 10% increase between baths before being left in 100% ethanol overnight (~18 hours). Tissue samples were then rinsed in a final 100% ethanol bath for 20 minutes before being cleared in toluene for two hours. Tissue samples were then transferred to molten paraffin and left to infiltrate in a 60ºC oven for at least 48 hours prior to being embedded in paraffin blocks.

Wax blocks were sectioned on an AO Spencer 820 Rotary Microtome at 7 µm. Approximately 100 oocytes from one stage-4 female were selected randomly and measured to determine nucleus size to set the slicing interval for serial sectioning. An average nuclear diameter of 32.4 µm was determined and thus a sectioning interval of 28 µm was implemented between slides. This spacing reduced the possibility of double-counting oocytes when quantifying fecundity. Only oocytes with observed nucleoli were counted. Sectioned tissue was allowed to expand in a warm water bath before being mounted onto glass slides and dried for at least 24 hours. Slides were stained using a modified version of Masson's Trichrome (Presnell & Schreibman 1997) in which Mayer's Haematoxylin was used to stain nucleic acids, Ponceau de Xylidine was used to stain cytoplasmic constituents, and connective tissue was stained using Fast Green. All stained slides were viewed under an Olympus BX-50 compound light microscope and imaged at 100x magnification using a microscope-mounted Flea3 camera.

2.4 Reproductive Analysis

All individuals examined histologically were categorized into gametogenic stages to maintain consistency when determining reproductive maturity (Figure 4.3). *Seepicola viridiplumi* individuals commonly showed a mix of reproductive stages along the length of the body, so gametogenic stages were assigned based on the characteristics most observed within abdominal segments. The following descriptions, modified from Bybee et al. (2007), were used to maintain consistency in assigning gametogenic stages.

Stage 1: Coelomic cavity empty and no observable evidence of gametogenesis; sex cannot be determined

Stage 2: Coelomocytes present within the coelomic cavity but no gametes observed; sex cannot be determined

Stage 3: Gametes present in the coelom but the coelom is not filled and most of the gametes are immature; males mainly have spermatids, females with previtellogenic oocytes and dispersed ovaries (proliferative regions) are visible

Stage 4: Coelomic cavity densely filled with mature gametes; male coelomic cavities filled mainly with mature spermatozoa, females with vitellogenic oocytes

Stage 5: Post-spawning, where the coelomic cavity has a small number of both mature and immature gametes; no proliferative regions observed in female coelomic cavities

We took three to five representative images of the abdominal coelomic cavity in male and non-reproductive individuals. For female *S. viridiplumi*, photographs were taken of 20 to 100 random oocytes, depending on availability, and the number of segments containing oocytes were counted. Oocytes were measured using ImageJ (NIH) and Feret diameters were calculated from the

area of each oocyte. Both previtellogenic and vitellogenic oocytes were included in fecundity counts.

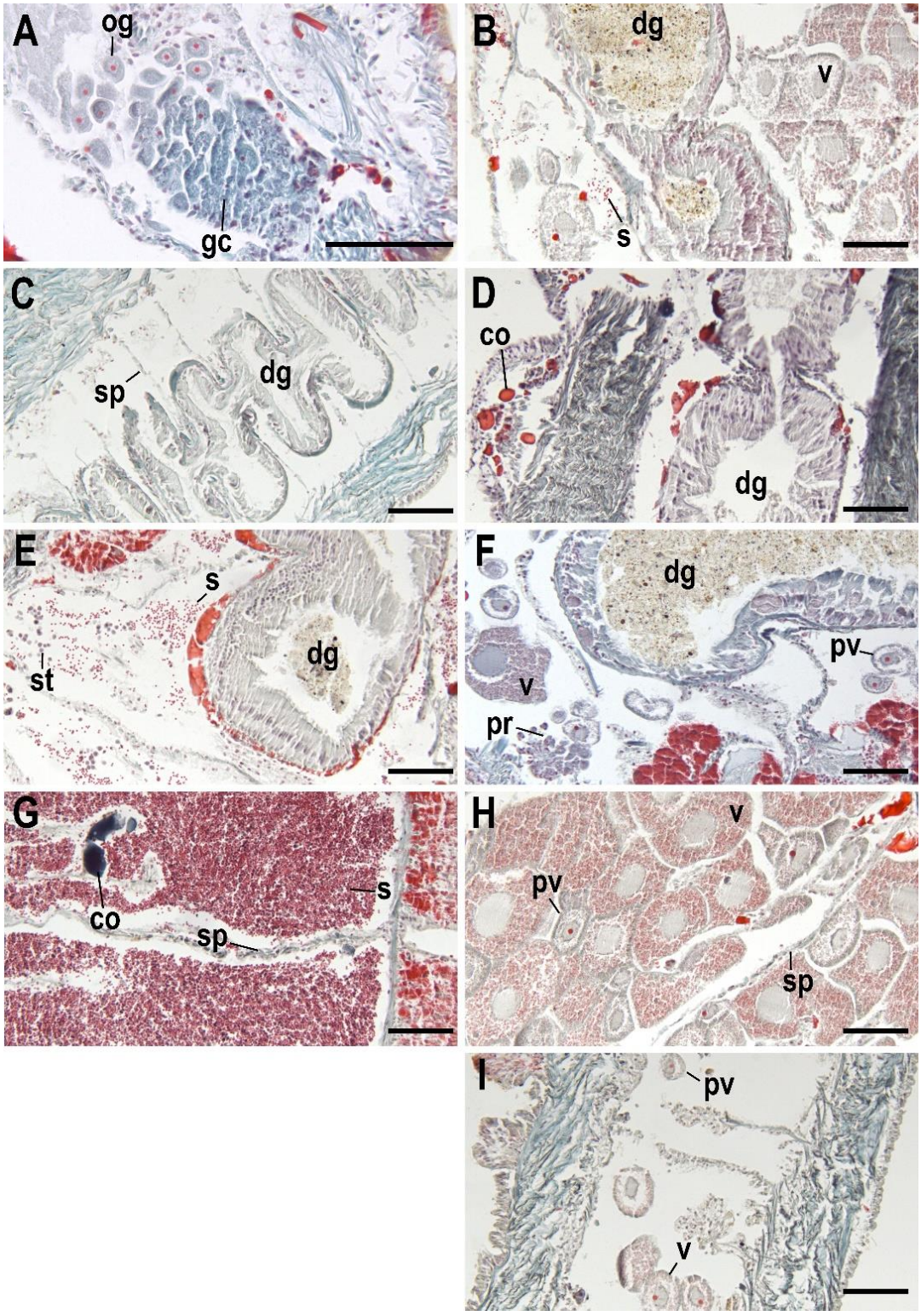

Figure 5.3. Gametogenic stages for *Seepicola viridiplumi*, showing both male and female stages. (A) Proliferative region in a female with germ cells (gc) and oogonia (og) present. (B) Simultaneous hermaphrodite with intermingled vitellogenic oocytes (v) and spermatozoa (s). (C) Stage 1 coelomic cavity with septa (sp) and the digestive tract (dg) visible. (D) Stage 2 coelomic cavity with coelomecytes present. (E) Stage 3 male with both spermatids (st) and spermatozoa. (F) Stage 3 female with previtellogenic oocytes (pv), a vitellogenic oocyte, and a proliferative region (pr) in view. (G) Stage 4 male with abundant spermatozoa. (H) Stage 4 female. (I) Stage 5 female. No stage 5 male was observed in this study. No Representative images of proliferative regions and a simultaneous hermaphrodite are also provided. All scale bars represent 100 μm.

2.5 Statistical Analysis

All data were analyzed using RStudio version 4.2.3 (R Core Team 2023), and the map of collection sites was created using QGIS. Data were first tested using the Shapiro-Wilk test to check for normality of distributions and the Levene's test to check for homogeneity of variances.

The effects of seasonality on the reproduction of *S. viridiplumi* were examined at each of the three study sites. For each site, population-level differences in the frequency of gametogenic stages were examined across time using chi-square contingency table tests. A Kruskal-Wallis test followed by a Dunn's *post hoc* test was used to check for differences in population-level oocyte size distributions between collection times at each sample site. Calculated p-values were adjusted using the Holm method. An additional Kruskal-Wallis test and Dunn's *post hoc* test were used to compare the individual oocyte size distributions within each collection. A $\eta^2[H]$ effect size was calculated to compare the synchronicity of oocyte size distributions of females within each collection.

To determine the potential advantages of epibiosis, we compared body lengths, oocyte sizes, and fecundity between individuals from the two microhabitats. For each collection site, body lengths of intact sabellids (male, female, and non-reproductive) were pooled across collection season to compare differences between the two microhabitats. Differences were examined using a Kolmogorov-Smirnov test. Only collections with paired epibiotic and free-living sabellid samples were included in the comparisons of oocyte size and fecundity (Table 5.1). Additionally, only stage

4 females from the paired collections were included in comparisons of oocyte size and fecundity to ensure all oocyte sizes could be assessed and that measurements of fecundity were more accurate. Fecundity counts were standardized to the number of oocytes per abdominal segment to compare across *S. viridiplumi* females of various sizes. Following a logarithmic transformation, the counts of fecundity per segment within each paired collection were compared using a two-sample *t*-Test. Comparisons of oocyte sizes between epibiotic and free-living individuals from paired collections were conducted using Mann-Whitney U tests.

3. RESULTS

Seepicola viridiplumi sabellids averaged 53 mm in length (SE ± 3.21). Significant differences between the body length of free-living and epibiotic individuals were observed at Brine Pool ($D = 1.16$, $p < 0.0001$) but not at Bush Hill or Green Canyon 234 (Figure 5.4). Reproductive individuals were observed across the full-size range of collected specimens, with both the smallest (11.5 mm) and the largest (117.7 mm) individuals identified as reproductive males. *Seepicola viridiplumi* displayed gonochorism, and only 1.9% of examined individuals were simultaneous hermaphrodites. In hermaphroditic individuals, most segments were dedicated to either spermatogenesis or oogenesis although some intermingling of gametes were observed in segments at transition points (Figure 5.3B). A total of 109 females and 115 males were observed with male:female sex ratios varying among sites (Brine Pool: 1:1.4, Bush Hill: 1:0.84, Green Canyon 234: 1:0.93). When all collections are pooled, the species has an even ratio of males to females (1:1.05). Nonreproductive individuals were observed at all sites and in all collections. The smallest nonreproductive individual was 13.4 mm and the largest was 83.7 mm.

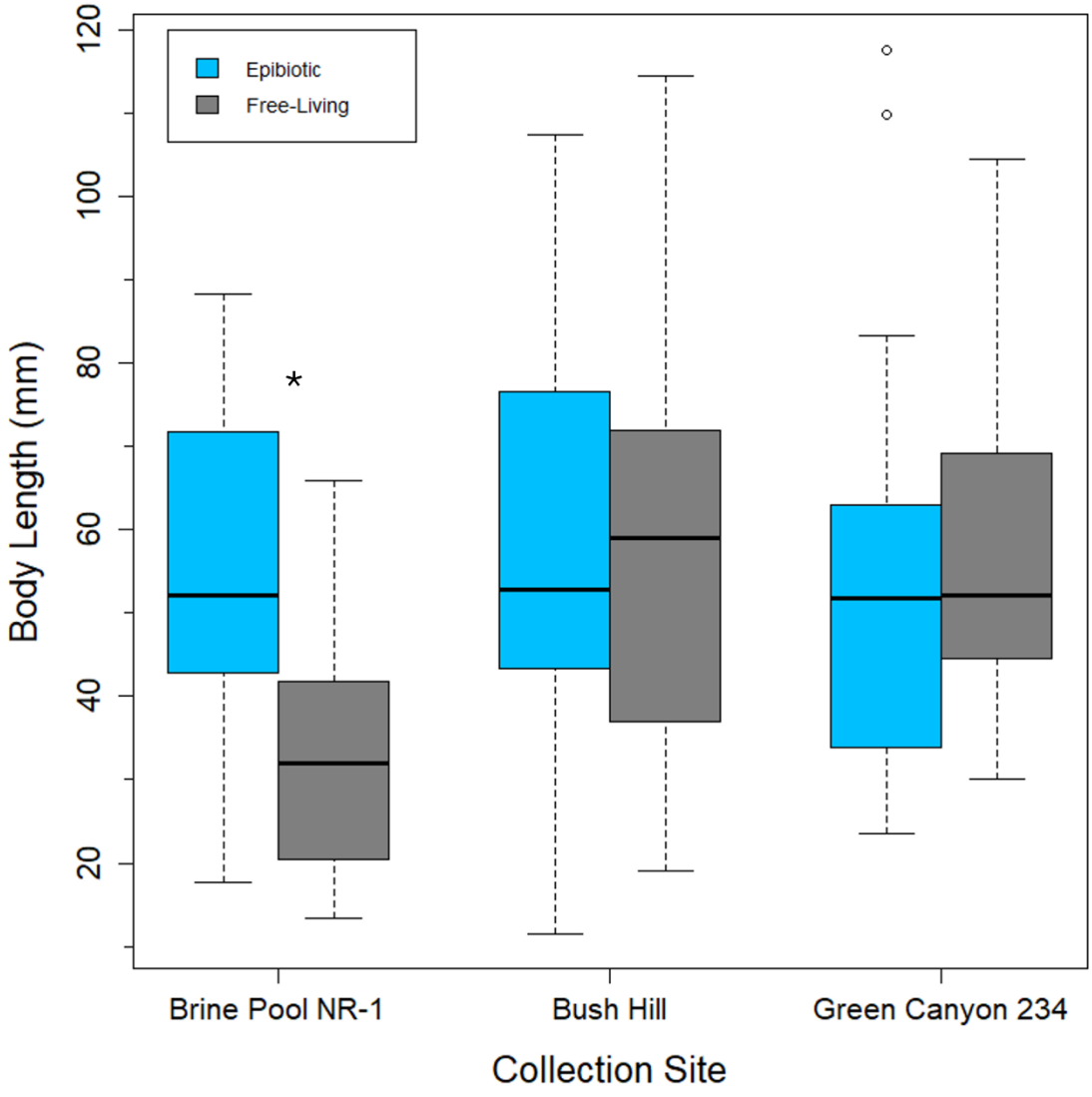

Figure 5.4. Comparisons in pooled body length measurements between all epibiotic and free-living *Seepicola viridiplumi* sabellids from each sample site. Asterisks note statistically significant differences.

Spermatids and spermatozoa were both visible on histologically prepared slides, although flagella were not observed (Figure 5.3). Spermatids had a diameter of approximately 5 μm while spermatozoa were smaller, around 2.5 μm. In stage three and four females, proliferative regions with densely clustered germ cells and oogonia were frequently observed along the ventral side of the coelomic cavity (Figure 5.3A). Maximum oocyte sizes for *S. viridiplumi* reached approximately 200 μm in diameter. Oocyte size distributions between females during all

collections were roughly synchronous, meaning the peaks of oocyte size frequencies aligned between females within each collection (Supplementary Figures S5.1, S5.2, S5.3). Although, there were inconsistent seasonal differences marked by decreased synchronicity between females (Table 5.2). Population level oocyte size distributions were consistently bimodal across all collections (Figure 5.5). Despite these variances, there were few differences in mean oocyte diameter between collection seasons at each site, although the diameters from the October collection at Brine Pool were notably larger ($p < 0.01$) and the February collections at both Bush Hill ($p < 0.0001$) and Green Canyon 234 ($p < 0.0001$) were significantly smaller (Table 5.3). Fecundity measurements for mature, stage 4 females was variable, with one 48.8 mm long female having 29.8 oocytes/segment (1227 oocytes total) and a 68.9 mm female with 98.7 oocytes/segment (6712 oocytes total). The mean per segment fecundity for mature, stage 4 females was 42.7 oocytes per segment (SE ± 10.14).

Table 5.2. Kruskal-Wallis test results comparing oocyte size distribution synchronicity among individuals within each sabellid collection. $\eta^2[H]$ indicates effect size where 1 is fully asynchronous and 0 indicates fully synchronous.

		Sample Size		Kruskal-Wallis		
Site	**Collection**	**Females**	**Oocytes**	**H**	**p-value**	**$\eta^2[H]$**
Brine Pool NR – 1	Feb, 2020	20	1855	340	<0.0001	0.173
	Jun, 2021	2	21	9.36	<0.001	0.005
	Oct, 2022	11	417	43.6	<0.0001	0.018
Bush Hill	Feb, 2020	5	506	56.0	<0.0001	0.037
	Jun, 2021	18	1425	321	<0.0001	0.217
	Oct, 2022	10	320	18.5	<0.01	0.007
Green Canyon 234	Feb, 2020	1	101	-	-	-
	Jun, 2021	18	1355	276	<0.0001	0.194
	Oct, 2022	5	128	2.52	0.641	-

Table 5.3. Mean oocyte sizes ± standard error for each site and collection. Bolded means indicate collections that were statistically different within each site based on the Dunn's post-hoc test.

	Mean Oocyte Diameter (µm)			Kruskal-Wallis	
Site	**Feb 2020**	**Jun 2021**	**Oct 2022**	**H**	**p-value**
Brine Pool NR-1	89.4 ± 1.7	75.6 ± 13.1	**102.5 ± 3.7**	16.07	<0.001
Bush Hill	**75.5 ± 3.0**	95.4 ± 2.0	90.5 ± 3.5	94.93	<0.0001
Green Canyon 234	**75.5 ± 5.2**	97.2 ± 2.0	96.4 ± 5.9	28.38	<0.0001

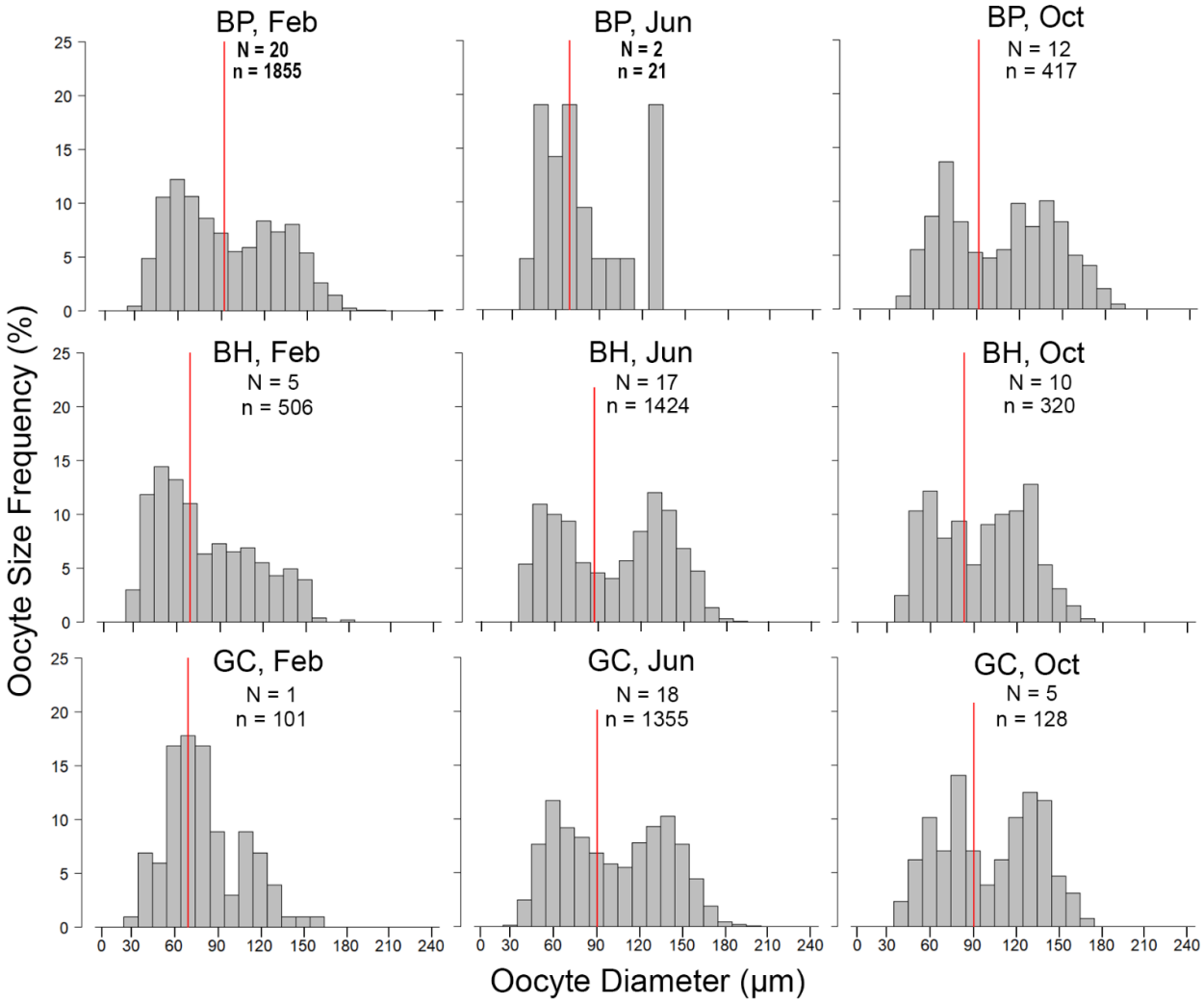

Figure 5.5. Oocyte size frequency histograms for each site (arranged in columns) and sampling period (arranged in rows). Red lines indicate the mean oocyte size. Scales are identical for each plot. N represents the number of sabellids examined; n is the number of oocytes circled.

Seepicola viridiplumi sabellids appeared to lack any strong seasonal gametogenic pattern.

Males and females with developing gametes, represented by stages three and four, were observed frequently during each of the collections (Figure 5.6)**.** Similarly, nonreproductive individuals with coelomocytes (stage 2) were also commonly observed. No statistically significant differences were found in gametogenic stages between collections at each site except for the June collection at Brine Pool NR (χ^2 = 3.4604, p <0.0001), when stages two and five were more readily observed (p <0.01) and stage 4 was more infrequent (p <0.01).

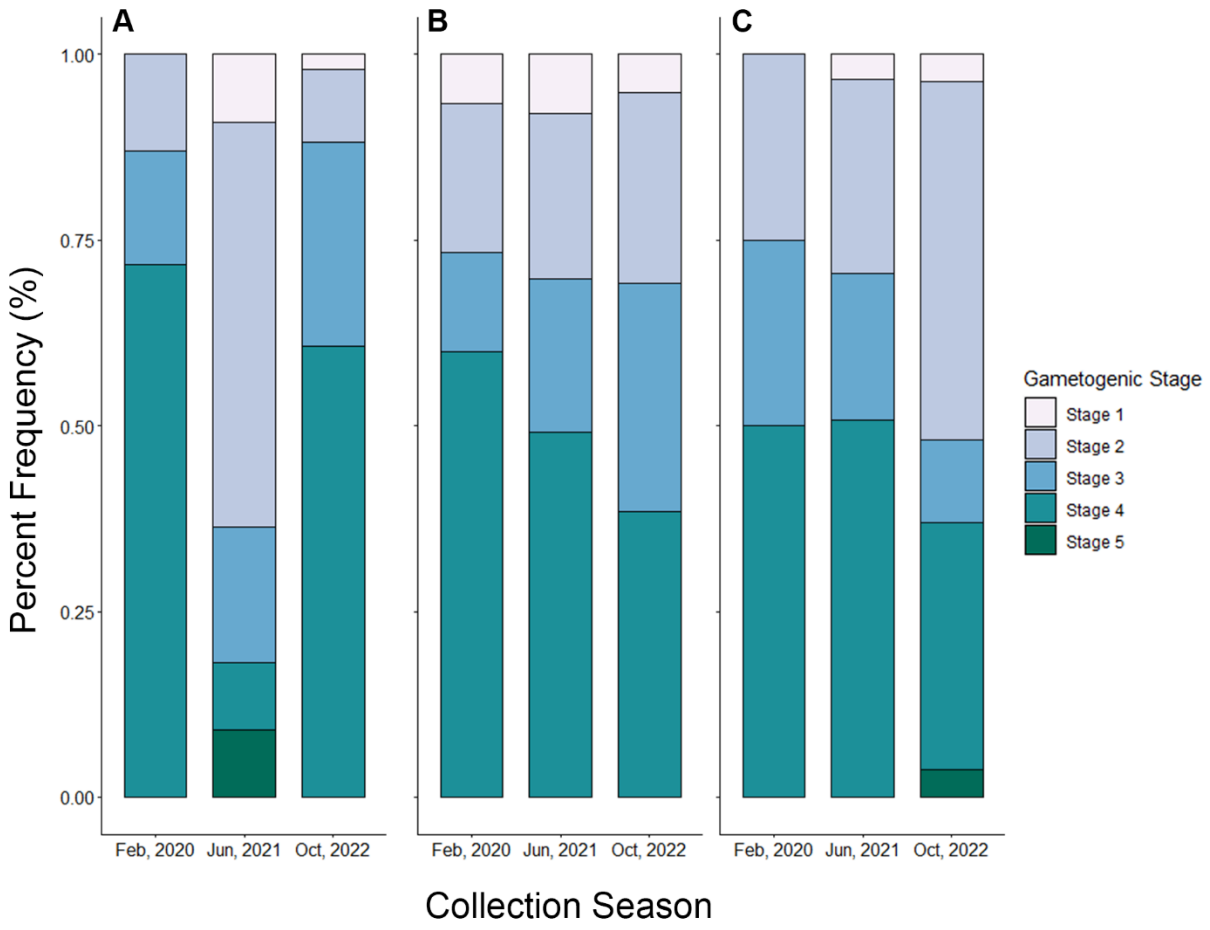

Figure 5.6. Percent frequency distributions of pooled gametogenic stages from all *Seepicola viridiplumi* individuals examined from (A) Brine Pool NR1, (B) Bush Hill, and (C) Green Canyon 234.

When comparing between epibiotic and free-living *S. viridiplumi*, fecundity was consistently higher in epibiotic individuals (Figure 5.7A), although it was only significant at Bush

Hill ($t = -3.642$, $p < 0.05$). Mean oocyte sizes between the two microhabitats were similar at Brine Pool (epibiotic = 95.1 μm ± 2.04 SE, free-living = 105.4 μm ± 3.25 SE, Figure 5.7B) and Green Canyon 234 (epibiotic = 103.7 μm ± 3.03 SE, free-living = 107.3 μm ± 3.74 SE, Figure 5.7D). Differences in mean oocyte sizes between individuals from each microhabitat were only statistically significant at Bush Hill, where epibiotic oocytes averaged 105.4 μm (±3.25 SE) and free-living oocytes averaged 94.3 μm (± 3.43 SE) ($W = 160213$, $p < 0.001$; Figure 5.7C). Additionally, while not statistically significant, the range of oocyte sizes was consistently greater in epibiotic individuals than free-living individuals (Figure 5.7B–D).

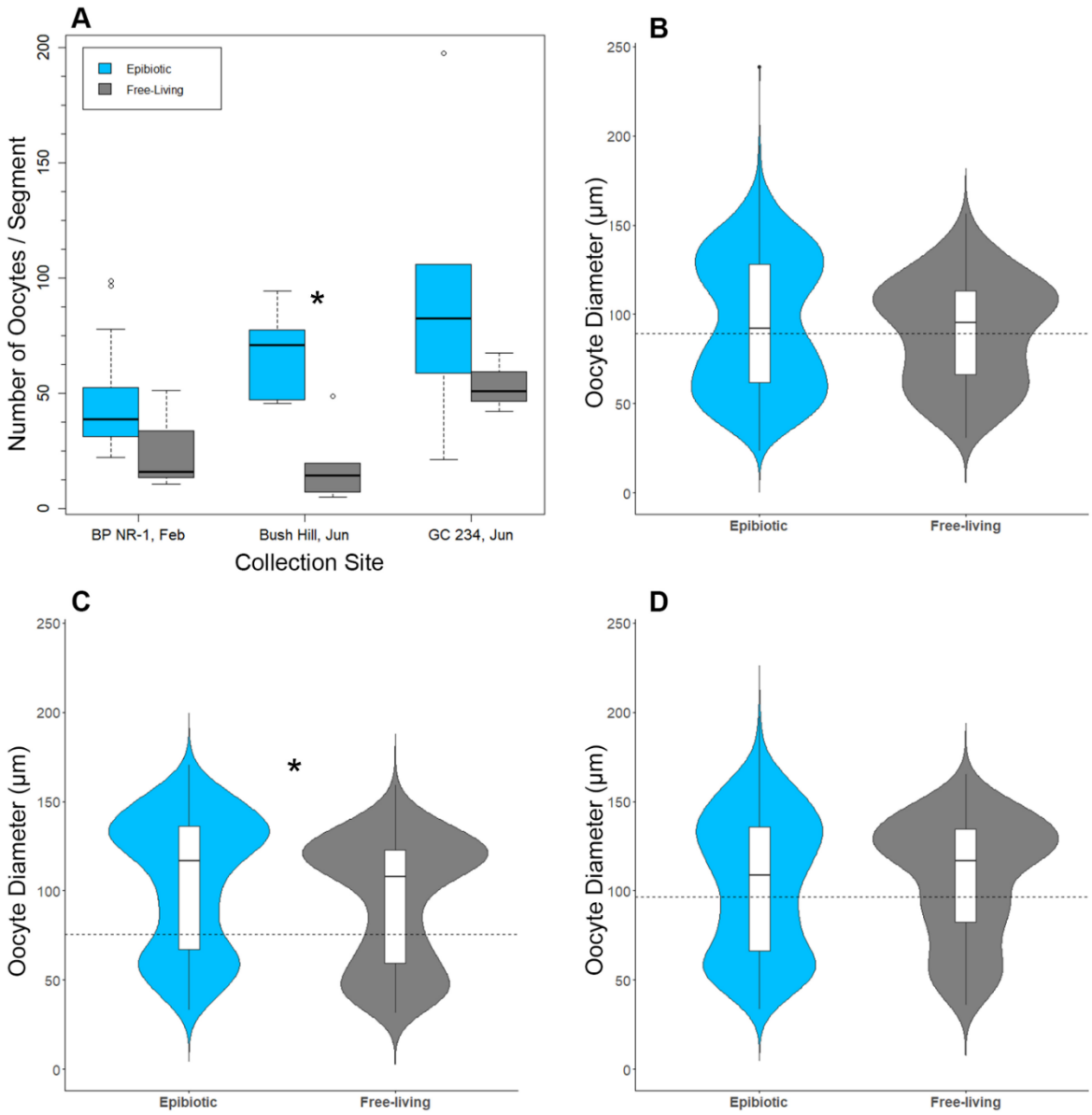

Figure 5.7. Comparisons in reproductive output between epibiotic and free-living *Seepicola viridiplumi* sabellids from each of the paired collections. All epibiotic data are shown in blue, free-living in grey. (A) Boxplot showing the number of oocytes per chaeitger. Comparisons in oocyte size frequency distributions between epibiotic and free-living sabellids from (B) Brine Pool NR-1, (C) Bush Hill, and (D) Green Canyon 234. Asterisks denote statistically significant differences.

4. DISCUSSION

The reproductive characteristics of *Seepicola viridiplumi* follow the general patterns observed within the subfamily Sabellinae, including gonochorism, iteroparity (Patti et al. 2003),

and extraovarian oogenesis, where oocytes are released into the coelom prior to vitellogenesis (Eckelbarger 1994, Giangrande et al. 2000, Eckelbarger & Hodgson 2021). As brooded larvae were not observed within the radioles or tubes of any individual, this species likely broadcast spawns similar to other members of the subfamily (McEuen et al. 1983, Giangrande & Petraroli 1994, Bybee et al. 2007). Furthermore, the maximum oocyte sizes around 200 μm indicate the potential for lecithotrophy, a form of larval development commonly observed in Sabellinae (Rouse et al. 2006).

We observed relatively high levels of synchronicity in oocyte sizes among females, and oocyte size distributions for each collection had a distinct bimodal appearance. This, when taken with the high presence of mature females at every site and collection season, can indicate that *S. viridiplumi* lacks a seasonal reproductive pattern and produces gametes semi-continuously. Semi-continuous gametogenesis, where individuals produce gametes continuously over an extended reproductive season has been described in smaller sabellid species (Rouse & Fitzhugh 1994). This pattern is usually attributed to the smaller body volumes of these species (Patti et al. 2003, Capa et al. 2019). Larger sabellid species tend to reproduce seasonally, undergoing gametogenesis and spawning once or twice a year (Giangrande 1997, Gambi & Patti 1999, Bybee et al. 2007, Murray et al. 2011, Capa et al. 2019). *Seepicola viridiplumi* is comparable in size to shallow-water species with reproductive seasonality (chapter 3), meaning that body volume is likely not a factor influencing the observed lack of seasonality. It is possible that the food resources present within the methane-seep habitat (i.e. free-living bacteria, resuspended organic matter from the seafloor, POM from the surface) may be consistent enough to enable *S. viridiplumi* sabellids to undergo an extended period of gametogenesis.

The consistently bimodal distribution of oocytes, as seen here, is caused by the

asynchronous development of oocytes within individual females, which has been described in the sabellid species *Perkinsiana schizogenica* (Tovar-Hernández & Dean 2014) and *Bispira bairdi* (Tovar-Hernández et al. 2009). Similar patterns where multiple cohorts of oocytes develop simultaneously have also been reported in various serpulid species, where oocyte sizes only become synchronous right before and after a spawning event (Kupriyanova et al. 2001). With reproductively mature females being observed during each collection, there is the potential for a lengthy spawning season in this species. However, the sampling intervals employed in this study might not have been fine enough to capture peaks in post-spawning individuals (if they occur). Lengthy spawning periods have been described for other sabellid species, such as *Sabellastarte spectabilis* (Bybee et al. 2007). The instances in this study where oocyte diameters were significantly smaller at Bush Hill and Green Canyon 234 in February 2020 were likely influenced by the low sample sizes. Similarly, the low number of reproductive individuals observed at Brine Pool in June 2021 was influenced by a small collection where only four reproductive individuals were identified.

This species also showed no evidence of sexual dimorphism in body sizes, as evidenced by the wide range of lengths in both sexes. While there were differences among the three sites, there were few differences among individuals living in the different microhabitats. Epibiotic individuals were larger than free-living specimens only at Brine Pool, suggesting that epibiosis itself does not confer a body size advantage in this species. While the exact cause for this difference is unknown, it could be due to factors only present at that site, such as differential recruitment or nutrient availability.

When comparing reproductive output between epibiotic and free-living individuals, we observed that epibiotic individuals had greater ranges of oocyte sizes and slightly higher

fecundities. Epibiotic individuals were slightly more advanced in oogenic development than their free-living counterparts at each site, though the difference was only statistically significant at Bush Hill, the site with the largest sample size. The consistently higher fecundities and larger oocyte sizes observed across the three paired collections could indicate that there is a slight advantage to epibiotic life for *S. viridiplumi*. While the fecundity comparisons may have been affected by low sample size, these results could also indicate that the diet for epibiotic individuals may be of higher nutritional quality. Higher-quality diets have been shown to increase fecundity in polychaetes with lecithotrophic development (Ramirez-Llodra 2000). It has also been suggested that polychaete species with opportunistic diets have heightened genetic variation for reproductive traits like fecundity and oocyte size (Qian & Chia 1991). This would allow a species to have reproductive flexibility to accommodate environmental variation and may be supported by specialized vitellogenic pathways that rapidly allocate excess energy into reproduction (Eckelbarger 1994, Linton & Taghon 2000, Eckelbarger & Hodgson 2021). Whether the magnitude of difference in oocyte size and fecundity observed in this study has biological and ecological significance is uncertain.

In addition to impacting the diet available to *S. viridiplumi* individuals (chapter 4), settlement on *A. oophaga* hosts could reduce competition for access to settlement surfaces (Wahl 1989). *Seepicola viridiplumi* is gregarious and approximately 330 individuals can be found within a square meter of authigenic carbonate (chapter 3). Settlement on *A. oophaga* valves could also reduce the risk of predation via associational defense (Young 1986, Wahl 1989). An unidentified sabellid species at the Green Canyon 234 methane seep site are known prey for the shrimp *Alvinocaris stactophila* and *Munidopsis* squat lobsters (Cordes et al. 2010a). Settling on a host located above the seafloor and surrounded by a *Lamellibrachia luymesi* bush could make the

epibiotic *S. viridiplumi* individuals more difficult to reach than the free-living individuals.

The presence of epibiotic sabellids likely impacts the host, *Acesta oophaga.* We routinely observed blister-like formations on the interior layers of the *A. oophaga* file clam valves underneath the *S. viridiplumi* burrows, indicating additional nacreous layers had been deposited. Calcareous-burrowing polychaetes including spionids and *Terebrasabella* sabellids in shallow water systems are known to embrittle host shells (Bergman et al. 1982, Oakes & Fields 1996) and hinder growth rates (McDiarmid et al. 2004, Riascos et al. 2008). In particularly heavy infestations, host shellfish have also been observed to have reduced spawning efforts (Wargo & Ford 1993) and lowered body conditions (McDiarmid et al. 2004, Riascos et al. 2008). As *A. oophaga* consume *Lamellibrachia luymesi* eggs, the burrowing action of the epibiotic *S. viridiplumi* could influence other aspects of the methane seep trophic structure by reducing *A. oophaga* fitness. The observed scarcity of *Acesta oophaga* file clams was surprising, given the historically high abundances at these sites (Burris et al. 2014). During this study however, the number of *A. oophaga* at each of the sample sites was low, and many lacked observable sabellid tubes. The cause for the decreased population of *A. oophaga* is unknown but could have been influenced by predation events, a lack of recruitment, over collecting, or slow growth rates leading to a scarcity of observable adults.

5. CONCLUSIONS

This study presents the reproductive patterns of a deep-sea sabellid, or for a sabellid species from any chemosynthetic system. *Seepicola viridiplumi* is gonochoristic, but some individuals appear to be simultaneous hermaphrodites. Oocyte sizes are comparable to those of other sabellid species and are indicative of lecithotrophic larval development. While many large sabellid species from shallow-water systems have reproductive seasonal patterns, S. viridiplumi appears to undergo

semi-continuous gametogenesis without a true seasonal signal. Our results also indicate that epibiotic settlement slightly increases oocyte size and per-segment fecundity. The findings presented here help shed light on how Sabellidae adapt to deep-water habitats, for which there is little known (Capa et al. 2021). Furthermore, as epibiotic organisms are ubiquitous in marine communities (Wahl 2009) and broadly understudied (Chen et al. 2021), our results provide additional insights into potential drivers behind this association.

CHAPTER VI

CONCLUSION

This dissertation highlights some of the ways epizoic species have adapted to and are impacted by epibiotic settlement. As the work presented here shows, directly examining the biology and ecology of epibiotic species can help address gaps in estimates of species diversity and elucidate potential biological drivers for these associations.

Chapter II described the reproductive patterns of *Solidobalanus hesperius* and revealed adaptations that have led to the success of this species in colonizing ephemeral biological substratum. I found that *S. hesperius* has an accelerated life history and year-round reproduction. As many barnacles perish during the annual molt of the host crab species, the rapid onset of reproduction and continuous production of offspring at all times of the year helps to ensure that some members of the population are able to reproduce successfully. This is further bolstered by *S. hesperius* larval settlement correlating with the molting patterns of the host crabs. Furthermore, I found that spatial distributions of the barnacles tightly followed the morphology of the host exoskeleton, likely helping individual barnacles persist despite host behavior such as burial.

While Chapter II focused on how an epizoic species specialized in life on ephemeral substrata, Chapters III, IV, and V examined how epibiotic settlement can impact an organism in a specialized environment. By describing a new genus and species of sabellid polychaete, Chapter III also helped to address the underexamined diversity of this taxa within chemosynthetic habitats (Capa et al. 2021). Hundreds of sabellid species have been described from shallow-water systems, but a single species has been named from hydrothermal vents (Capa et al. 2013), and only one has been identified to genus-level at methane seeps (Goffredi et al. 2020).

Sabellids have been observed at whale falls (Amon et al. 2013), methane seeps around the world (Cordes et al. 2010a, Vestheim & Kaartvedt 2016), and up to depths over 9,000 meters (Levenstein 1961). By finding a new genus at some of the most well-studied methane seeps sites (Levin et al. 2016), our work highlights the under described sabellid diversity in deep-sea ecosystems.

As the newly described sabellid *Seepicola viridiplumi*, is facultatively hyper-epibiotic and was observed with aggregations of brown material within the radiolar crown, I examined the microbiome and trophic ecology of this species in Chapter IV. I identified high abundances of Bacterial taxa that specialize in degrading hydrocarbon compounds and no obvious bacterial candidate for a symbiotic relationship. Additionally, examining the stable isotopic ratios showed that *S. viridiplumi* rely on nutrients from thiotrophic and phototrophic sources, although specific trophic niches can vary between epibiotic and free-living individuals. With the high abundance of epizoic species within methane seep systems, the findings presented here could indicate that the number of potential trophic pathways has been underestimated for these habitats. A species of intertidal barnacle has also been shown to have differing diets depending on whether an individual is epibiotic or free-living (Puccinelli & McQuaid 2021). Epibiotic settlement could routinely alter the nutrients available to individuals of facultatively epibiotic species, although more research is required to confirm this trend.

In Chapter V, I further investigated the potential impacts of epibiotic settlement on the biology of *S. viridiplumi*. Using histological methods, I was able to determine that epibiotic individuals consistently had slightly increased oocyte sizes and levels of fecundity. These results could indicate differences in energy investment due to changes in diet quality between epibiotic and free-living individuals. This finding could highlight a potential biological driver behind epibiotic associations. I also found that while oocyte sizes were comparable to other sabellid

species, gametogenesis in *S. viridiplumi* lacked a clear seasonal signal and could indicate a prolonged spawning season. However, as larger sabellid species tend to reproduce seasonally, the abundance of food resources within methane seep habitats may be the driver sustaining the increased investment in reproduction for this species.

As shown in this dissertation, examining epibiosis from the lens of epizoans can provide quantitative evidence for how certain organismal relationships develop and are able to persist. The nature of epibiotic associations has a high degree of plasticity and can shift depending on numerous external factors and the condition of the host basibiont (Fernandez-Leborans 2010, McLeod et al. 2020). For example, epibiotic settlement can increase in prevalence when hosts are parasitized (Yoshioka et al. 2023). Such plasticity can make the impacts of epibiosis for the host difficult to predict (Fernandez-Leborans 2010), but a better understanding of the biology of epizoic species could mitigate uncertainty. Future work should continue to give attention to epibiotic species. With the number of epibiotic associations within the marine realm, the resulting insights of such research could aid in obtaining a more accurate understanding of community functioning and biodiversity.

REFERENCES CITED

Abelló P, Villanueva R, Gili JM (1990) Epibiosis in deep-sea crab populations as indicator of biological and behavioural characteristics of the host. J Mar Biol Assoc United Kingdom 70:687–695.

Aharon P, Fu B (2003) Sulfur and oxygen isotopes of coeval sulfate-sulfide in pore fluids of cold seep sediments with sharp redox gradients. Chem Geol 195:201–218.

Amon DJ, Glover AG, Wiklund H, Marsh L, Linse K, Rogers AD, Copley JT (2013) The discovery of a natural whale fall in the Antarctic deep sea. Deep Res Part II Top Stud Oceanogr 92:87–96.

Arellano SM, Lee OO, Lafi FF, Yang J, Wang Y, Young CM, Qian PY (2013) Deep sequencing of Myxilla (Ectyomyxilla) methanophila, an epibiotic sponge on cold-seep tubeworms, reveals methylotrophic, thiotrophic, and putative hydrocarbon-degrading microbial associations. Microb Ecol 65:450–461.

Babu MY, Durgekar R, Devi VJ, Ramakritinan CM, Kumaraguru AK (2012) Influence of ciriped barnacles *Chelonibia patula* (Ranzani) on commercial crabs from Gulf of Mannar and Palk bay coastal waters. Res Environ Life Sci 5:109–116.

Bacosa HP, Erdner DL, Rosenheim BE, Shetty P, Seitz KW, Baker BJ, Liu Z (2018) Hydrocarbon degradation and response of seafloor sediment bacterial community in the northern Gulf of Mexico to light Louisiana sweet crude oil. ISME J 12:2532–2543.

Barnes H, Barnes M (1959) The naupliar stages of *Balanus hesperius* Pilsbry. Can J Zool 37:237–244.

Becker EL, Cordes EE, Macko SA, Fisher CR (2009) Importance of seep primary production to *Lophelia pertusa* and associated fauna in the Gulf of Mexico. Deep Res Part I Oceanogr Res Pap 56:786–800.

Becker EL, Cordes EE, Macko SA, Lee RW, Fisher CR (2013) Using stable isotope compositions of animal tissues to infer trophic interactions in Gulf of Mexico lower slope seep communities. PLoS One 8:1–16.

Becker K, Wahl M (1996) Behaviour patterns as natural antifouling mechanisms of tropical marine crabs. J Exp Mar Bio Ecol 203:245–258.

Bellwood O (2002) The occurrence, mechanics and significance of burying behaviour in crabs (Crustacea: Brachyura). J Nat Hist 36:1223–1238.

Bergman KM, Elner RW, Risk MJ (1982) The influence of *Polydora websteri* borings on the

strength of the shell of the sea scallop, *Placopecten magellanicus*. Can J Zool 60:2551–2556.

Bergquist DC, Ward T, Cordes EE, McNelis T, Howlett S, Kosoff R, Hourdez S, Carney R, Fisher CR (2003) Community structure of vestimentiferan-generated habitat islands from Gulf of Mexico cold seeps. J Exp Mar Bio Ecol 289:197–222.

Bernardet J (2015a) Flavobacteriaceae . Bergey's Man Syst Archaea Bact:1–18.

Bernardet J (2015b) Flavobacteriales ord. nov . Bergey's Man Syst Archaea Bact:1–2.

Biggs DC, Hu C, Müller-Karger FE (2008) Remotely sensed sea-surface chlorophyll and POC flux at Deep Gulf of Mexico Benthos sampling stations. Deep Res Part II Top Stud Oceanogr 55:2555–2562.

Brooks JM, Kennicutt MC, Fisher CR, Macko SA, Cole K, Bidigare RR, Vetter RD (1987) Deep-sea hydrocarbon seep communities: Evidence for energy and nutritional carbon sources. Science (80-) 238:1138–1142.

Bruguière LG (1789) Encyclopédie Méthodique. Histoire naturelle des vers Vol. I, Part I. Chez Panckoucke, imprimeur- libraire, hôtel de Thou, rue des Poitevins, Paris.

Buhl-Mortensen L, Vanreusel A, Gooday AJ, Levin LA, Priede IG, Buhl-Mortensen P, Gheerardyn H, King NJ, Raes M (2010) Biological structures as a source of habitat heterogeneity and biodiversity on the deep ocean margins. Mar Ecol 31:21–50.

Burris ZP, Lord JP, Young CM (2014) Effects of the oophagous bivalve Acesta oophaga on the morphology and fecundity of its deep-sea tubeworm host, *Lamellibrachia luymesi*. Mar Ecol 35:106–111.

Bush KJ (1905) Tubicolous annelids of the tribes Sabellides and Serpulides from the Pacific Ocean. Harriman Alaska Exped 12:169–355.

Bybee DR, Bailey-Brock JH, Tamaru CS (2007) Gametogenesis and spawning periodicity in the fan worm *Sabellastarte spectabilis* (Polychaeta: Sabellidae). Mar Biol 151:639–648.

Callahan BJ, McMurdie PJ, Rosen MJ, Han AW, Johnson AJA, Holmes SP (2016) DADA2: High-resolution sample inference from Illumina amplicon data. Nat Methods 13:581–583.

Campos J, Ribas F, Bio A, Freitas V, Souza AT, van der Veer HW (2022) Body condition and energy content of the shore crab *Carcinus maenas* L. in a temperate coastal system: the cost of barnacle epibiosis. Biofouling 38:764–777.

Cao Y, Dong Q, Wang D, Zhang P, Liu Y, Niu C (2022) MicrobiomeMarker: an R/Bioconductor package for microbiome marker identification and visualization. Bioinformatics btac438.

Capa M (2007) Taxonomic revision and phylogenetic relationships of apomorphic sabellids (Polychaeta) from Australia.

Capa M, Giangrande A, Nogueira JMM, Tovar-Hernández MA (2019) Sabellidae Latrielle, 1824. In: *Handbook of Zoology, Volume 2: Pleistoannelida, Sedentaria II*. Purschke G, Böggermann M, Wesheide W (eds) De Gruyter, Berlin, Germany, p 164–212.

Capa M, Hutchings P, Teresa Aguado M, Bott NJ (2011) Phylogeny of Sabellidae (Annelida) and relationships with other taxa inferred from morphology and multiple genes. Cladistics 27:449–469.

Capa M, Kupriyanova E, Nogueira DM, Bick A, Tovar-Hernández MA (2021) Fanworms: yesterday, today and tomorrow. Diversity 13.

Capa M, Nishi E, Tanaka K, Fujikura K (2013) First record of a *Bispira* species (Sabellidae: Polychaeta) from a hydrothermal vent. Mar Biodivers Rec 6:1–6.

Carlton JT (2007) The Light and Smith Manual: Intertidal Invertebrates from Central California to Oregon, 4th ed. Carlton JT (ed) University of California Press, Los Angeles.

Carney RS, Riekenberg P, Fry B (2015) Biomass and mass-balance isotope content of seep populations on the Upper Slope Gulf of Mexico, determined from archived samples. New Orleans.

Chen Y-Y, Edgar GJ, Fox RJ (2021) The Nature and Ecological Significance of Epifaunal Communities within Marine Ecosystems. Oceanogr Mar Biol an Annu Rev 59:585–720.

Chughtai I, Knight-Jones EW (1988) Burrowing into limestone by sabellid polychaetes. Zool Scr 17:231–238.

Comeau AM, Li WKW, Tremblay JÉ, Carmack EC, Lovejoy C (2011) Arctic ocean microbial community structure before and after the 2007 record sea ice minimum. PLoS One 6.

Cordes EE, Becker EL, Fisher CR (2010a) Temporal shift in nutrient input to cold-seep food webs revealed by stable-isotope signatures of associated communities. Limnol Oceanogr 55:2537–2548.

Cordes EE, Bergquist DC, Fisher CR (2009) Macro-ecology of Gulf of Mexico cold seeps. Ann Rev Mar Sci 1:143–168.

Cordes EE, Carney SL, Hourdez S, Carney RS, Brooks JM, Fisher CR (2007) Cold seeps of the deep Gulf of Mexico: Community structure and biogeographic comparisons to Atlantic equatorial belt seep communities. Deep Sea Res Part I Oceanogr Res Pap 54:637–653.

Cordes EE, Hourdez S, Predmore BL, Redding ML, Fisher CR (2005) Succession of hydrocarbon seep communities associated with the long-lived foundation species *Lamellibrachia luymesi*. Mar Ecol Prog Ser 305:17–29.

Cordes EE, Hourdez S, Roberts HH (2010b) Unusual habitats and organisms associated with the cold seeps of the Gulf of Mexico. In: *The Vent and Seep Biota: Aspects from Microbes to Ecosystems*. p 315–332.

Crisp DJ (1974) Factors influencing the settlement of marine invertebrate larvae. In: *Chemoreception in Marine*. Grant A, Mackie (eds) Academic Press, London, p 177–265.

Crisp DJ, Barnes H (1954) The orientation and distribution of barnacles at settlement with particular reference to surface contour. J Anim Ecol 23:142–162.

Dávila-Jiménez Y, Tovar-Hernández MA, Simões N (2017) The social feather duster worm Bispira brunnea (Polychaeta: Sabellidae): aggregations, morphology and reproduction. Mar Biol Res 13:782–796.

DeChaine EG, Cavanaugh CM (2005) Symbioses of methanotrophs and deep-sea mussels (Mytilidae: Bathymodiolinae). In: *Molecular Basis of Symbiosis*. Overmann J (ed) Springer-Verlag Berlin Heidelberg, Berlin, p 227–249.

Deming JW, Junge K (2015) *Colwellia*. In: *Bergey's Manual of Systematics of Archaea and Bacteria*. p 1–12.

Du X, Peterson WT (2014) Seasonal cycle of phytoplankton community composition in the coastal upwelling system off central Oregon in 2009. Estuaries and Coasts 37:299–311.

Dunn O (1964) Multiple comparisons using rank sums. Techometrics 6:241–252.

Dvoretsky AG, Dvoretsky VG (2023) Epibionts of an introduced king crab in the Barents Sea: A second five-year study. Diversity 15.

Dvoretsky AG, Dvoretsky VG (2022) Epibiotic communities of common crab species in the coastal barents sea: Biodiversity and infestation patterns. Diversity 14.

Eckelbarger KJ (1994) Diversity of metazoan ovaries and vitellogenic mechanisms: Implications for life history theory. Proc Biol Soc Washingt 107:193–218.

Eckelbarger KJ, Hodgson AN (2021) Invertebrate oogenesis–a review and synthesis: comparative ovarian morphology, accessory cell function and the origins of yolk precursors. Invertebr Reprod Dev 65:71–140.

Enrichetti F, Baldrighi E, Bavestrello G, Betti F, Canese S, Costa A, del Pasqua M, Giangrande A, Langeneck J, Misic C, Putignano M, Toma M, Bo M (2022) Ecological role and phylogenetic position of a new habitat-forming species (Canalipalpata, Sabellidae) from the Mediterranean mesophotic soft bottoms. Estuar Coast Shelf Sci 265.

Eschweiler N, Buschbaum C (2011) Alien epibiont (*Crassostrea gigas*) impacts on native periwinkles (*Littorina littorea*). Aquat Invasions 6:281–290.

Esteban GF, Fenchel TM (2020) Symbiosis. In: *Ecology of Protozoa*. Springer, p 87–105.

Farrapeira CMR (2010) Shallow water Cirripedia of the northeastern coast of Brazil: the impact of life history and invasion on biogeography. J Exp Mar Bio Ecol 392:210–219.

Fernández-Garayzábal JF, Miguela-Villoldo P, Vela AI (2022) Moraxellaceae. In: *Bergey's Manual of Systematics of Archaea and Bacteria*. Whitman WB (ed) John Wiley & Sons, Ltd.

Fernandez-Leborans G (2010) Epibiosis in Crustacea: An overview. Crustaceana 83:449–640.

Fitzhugh K (1989) A systematic revision of the Sabellidae-Caobangiidae-Sabellongidae complex (Annelida: Polychaeta). Bull Am Museum Nat Hist 192:1–104.

Folmer O, Black M, Hoeh W, Lutz R, Vrijenhoek R (1994) DNA primers for amplification of mitochondrial cytochrome c oxidase subunit I from diverse metazoan invertebrates. Mol Mar Biol Biotechnol 3:294–299.

Forget NL, Kim Juniper S (2013) Free-living bacterial communities associated with tubeworm (*Ridgeia piscesae*) aggregations in contrasting diffuse flow hydrothermal vent habitats at the main Endeavour field, Juan de Fuca Ridge. Microbiologyopen 2:259–275.

Frick MG, Ross A (2002) Happenstance or design: an unusual association between a sea turtle, octocoral and barnacle. Mar Turt Newsl 97:10–11.

Fu L, Liu Y, Wang M, Lian C, Cao L, Wang W, Sun Y, Wang N, Li C (2024) The diversification and potential function of microbiome in sediment-water interface of methane seeps in South China Sea. Front Microbiol 15:1–14.

Gabaev DD (2013) Effects of fouling on the Japanese scallop *Mizuhopecten yessoensis* (Jay) in Peter the Great Bay (Sea of Japan). Oceanology 53:183–191.

Gambi MC, Patti FP (1999) Reproductive biology of *Perkinsiana antarctica* (Kinberg) (Polychaeta, Sabellidae) in the Straits of Magellan (south America): Systematic and ecological implications. Sci Mar 63:253–259.

Gearing JN, Gearing PJ, Rudnick DT, Requejo AG, Hutchins MJ (1984) Isotopic variability of organic carbon in a phytoplankton-based, temperate estuary. Geochim Cosmochim Acta 48:1089–1098.

Giangrande A (1997) Polychaete Reproductive Patterns, Life Cycles, and Life Histories: An Overview. Oceanogr Mar Biol An Annu Rev 35:323–386.

Giangrande A, Licciano M, Pagliara P, Gambi MC (2000) Gametogenesis and larval development in Sabella spallanzanii (Polychaeta: Sabellidae) from the Mediterranean Sea. Mar Biol 136:847–861.

Giangrande A, Petraroli A (1994) Observations on reproduction and growth of Sabella spallanzanii (Polychaeta, Sabellidae) in the Mediterranean Sea. In: *Actes de la Conference internationale des Polychetes*. Dauvin JC, Laubier L, Reish DJ (eds) Mémoires du Muséum national D'histoire naturelle, Paris, p 51–56.

Gili JM, Abello P, Villanueva R (1993) Epibionts and intermoult duration in the crab *Bathynectes piperitus*. Mar Ecol Prog Ser 98:107–113.

Glaeser SP, Kämpfer P (2020) Endozoicomonadaceae. In: *Bergey's Manual of Systematics of Archaea and Bacteria*. p 1–4.

Glass G V., Peckhan PD, Sanders JR (1972) Consequences of Failure to Meet Assumptions Underlying the Fixed Effects Analyses of Variance and Covariance. Rev Educ Res 42:237–288.

Goffredi SK, Tilic E, Mullin SW, Dawson KS, Keller A, Lee RW, Wu F, Levin LA, Rouse GW, Cordes EE, Orphan VJ (2020) Methanotrophic bacterial symbionts fuel dense populations of deep-sea feather duster worms (Sabellida, Annelida) and extend the spatial influence of methane seepage. Sci Adv 6:eaay8562.

Govenar B (2010) Shaping vent and seep communities: habitat provision and modification by foundation species. In: *The Vent and Seep Biota: Aspects from Microbes to Ecosystems*. Kiel S (ed) Springer, London, p 423–432.

Grant J, Bathmann U V (1987) Swept away: Resuspension of bacterial mats regulates benthic-pelagic exchange of sulfur. Science (80-) 236:1472–1474.

Grémare A, Marsh AG, Tenore KR (1988) Short-term reproductive responses of *Capitella* sp. I (Annelida: Polychaeta) fed on different diets. J Exp Mar Bio Ecol 123:147–162.

Harder T (2009) Marine Epibiosis: Concepts, ecological consequences and host defense. In: *Marine and Industrial Biofouling*. Flemming H-C, Venkatesan R, Murthy S, Cooksey K, Costerton WJ (eds) Springer-Verlag Berlin Heidelberg, Berlin, p 219–232.

Harwell MR, Rubinstein EN, Hayes WS, Olds CC (1992) Summarizing Monte Carlo Results in Methodological Research : The One- and Two-Factor Fixed Effects ANOVA Cases. J Educ Stat 17:315–339.

Heath DJ (1976) The distribution and orientation of epizoic barnacles on crabs. Zool J Linn Soc 59:59–67.

Hines AH (1976) Comparative reproductive ecology of three species of intertidal barnacles. University of California, Berkley.

Hoagland RA (1919) Polychaetous annelids from Porto Rico, the Florida Keys, and Bermuda. Bull Am Museum Nat Hist 41:571–591.

Hoeg JT, Illg PL, Strathmann RR, Wethey DS (1987) Phylum Crustacean, Class Mmaxillopoda, Subclass Cirripedia. In: *Reproduction and Development of Marine Invertebrates of the Northern Pacific Coast*. Strathmann MF (ed) University of Washington Press, Seattle, p 370–392.

Holm S (1979) A simple sequentially rejective multiple test procedure. Scandanavian J Stat 6:65–70.

Hügler M, Sievert SM (2011) Beyond the Calvin cycle: Autotrophic carbon fixation in the ocean. Ann Rev Mar Sci 3:261–289.

Jackson AL, Inger R, Parnell AC, Bearhop S (2011) Comparing isotopic niche widths among and within communities: SIBER - Stable Isotope Bayesian Ellipses in R. J Anim Ecol 80:595–602.

Jackson JBC (1977) Competition on marine hard substrata: The adaptive significance of solitary and colonial strategies. Am Nat 111:743–767.

Järnegren J, Rapp HT, Young CM (2007) Similar reproductive cycles and life-history traits in congeneric limid bivalves with different modes of nutrition. Mar Ecol 28:183–192.

Järnegren J, Tobias CR, Macko SA, Young CM (2005) Egg predation fuels unique species association at deep-sea hydrocarbon seeps. Biol Bull 209:87–93.

Jensen S, Frank JA, Arntzen M, Duperron S, Vaaje-Kolstad G, Hovland M (2021) Endozoicomonadaceae symbiont in gills of *Acesta* clam encodes genes for essential nutrients and polysaccharide degradation. FEMS Microbiol Ecol 97:1–13.

Ji B, Yang K, Zhu L, Jiang Y, Wang H, Zhou J, Zhang H (2015) Aerobic denitrification: A review of important advances of the last 30 years. Biotechnol Bioprocess Eng 20:643–651.

Johansson KE (1922) On some new tubicolous annelids from Japan, the Bonin Islands, and the Antarctic. Ark för Zool 15:1–11.

Jumars PA, Dorgan KM, Lindsay SM (2015) Diet of worms emended: An update of polychaete feeding guilds - Supplemental Material. Ann Rev Mar Sci 7:497–520.

Kelley CA, Coffin RB (1998) Stable isotope evidence for alternative bacterial carbon sources in the Gulf of Mexico. Limnol Oceanogr 43:1962–1969.

Key MM, Jeffries WB, Voris HK, Yang CM (1996) Epizoic bryozoans and mobile ephemeral host substrata. In: *Bryozoans in Space and Time. Proceedings of the 10th International Byrozoology Conference*. Gordon D., Smith AM, Grant-Mackie JA (eds) National Institute of Water and Atmospheric Research, Ltd, Wellington, New Zealand, p 157–165.

Key MM, Volpe JW, Jeffries WB, Voris HK (1997) Barnacle fouling of the blue crab Callinectes

sapidus at Beaufort, North Carolina. J Crustac Biol 17:424–439.

Kiel S, Tyler PA (2010) Chemosynthetically-driven ecosystems in the deep sea. In: *The Vent and Seep Biota: Aspects from Microbes to Ecosystems*, 33rd ed. Landman NH, Harries PJ, Kiel S (eds) Springer US, New York, p 1–14.

Knight-Jones P (1983) Contributions to the taxonomy of Sabellidae (Polychaeta). Zool J Linn Soc 79:245–295.

Knight-Jones P, Darbyshire T, Petersen ME, Tovar-Hernández MA (2017) What is *Pseudopotamilla reniformis* (Sabellidae)? Comparisons of populations from Britain, Iceland and Canada with comments on *Eudistylia* and *Schizobranchia*. Zootaxa 4254:201–220.

Knudsen JW (1964) Observations of the reproductive cycles and ecology of the common Brachyura and crablike anomura of Pugent Sound, Washington. Pacific Sci 18:3–33.

Korn OM (1999) Distribution of cirripede larvae iin Nakhodka Bay (Sea of Japan). Russ J Mar Biol 25:365–371.

Korn OM, Scherbakova N V. (2012) The distribution of cirripede larvae (Cirripedia: Thoracica) in the Amursky and Ussuriisky bays of the Sea of Japan. Russ J Mar Biol 38:166–178.

Krøyer H (1856) Meddelelser af en Afhandling om Ormeslaegten Sabella Linn., isaer med Hensyn til dens nordiske Arter. In: *Översigt over del Kongelige danske Videnskabemes Selskabs Forhandlinger 1856*. p 1–36.

Kruskal W, Wallis W (1952) Use of rankks in one-criterion variance analysis. J Am Stat Assoc 47:583–621.

Kumar S, Stecher G, Li M, Knyaz C, Tamura K (2018) MEGA X: Molecular evolutionary genetics analysis across computing platforms. Mol Biol Evol 35:1547–1549.

Kupriyanova EK, Nishi E, Hove HA ten, Rzhavasky AV (2001) Life-history patterns in serpulimorph polychaetes: ecological and evolutionary perspectives. Oceanogr Mar Biol An Annu Rev 39:1–23.

Lee AL, Dafforn KA, Hutchings PA, Johnston EL (2018) Reproductive strategy and gamete development of an invasive fanworm, *Sabella spallanzanii* (polychaeta: Sabellidae), a field study in Gulf St. Vincent, South Australia. PLoS One 13:1–13.

Leprich DJ, Flood BE, Schroedl PR, Ricci E, Marlow JJ, Girguis PR, Bailey J V. (2021) Sulfur bacteria promote dissolution of authigenic carbonates at marine methane seeps. ISME J 15:2043–2056.

Levene H (1960) Robust Tests for Equality of Variances. In: *Contributions to Probability and Statistics*. Olkin I, Ghurye SG, Hoeffding W, Madow W., Mann HB (eds) Stan, Stanford,

California, p 278–292.

Levenstein RY (1961) Polychaeta from deep water in the Berin Sea. Proc from Inst Oceanol USSR Acad Sci 46:147–178.

Levin LA, Baco AR, Bowden DA, Colaco A, Cordes EE, Cunha MR, Demopoulos AWJ, Gobin J, Grupe BM, Le J, Metaxas A, Netburn AN, Rouse GW, Thurber AR, Tunnicliffe V, Van Dover CL, Vanreusel A, Watling L (2016) Hydrothermal Vents and Methane Seeps : Rethinking the Sphere of Influence. Front Mar Sci 3:1–23.

Levin LA, Mendoza GF, Grupe BM, Gonzalez JP, Jellison B, Rouse G, Thurber AR, Waren A (2015) Biodiversity on the rocks: Macrofauna inhabiting authigenic carbonate at Costa Rica methane seeps. PLoS One 10.

Lewis JB (1992) Recruitment, growth and mortality of a coral-inhabiting barnacle *Megabalanus stultus* (Darwin) upon the hydrocoral *Millepora complanata* Lamarck. J Exp Mar Bio Ecol 162:51–64.

Li C, Feng J, Zhang S, Liang J (2023) Methane anaerobic oxidation on carbonate in cold seep environments with high-pressure enrichment cultivation. Energy Proc 36.

Lim CS, Tan LJX, Neo ML, Teo SLM, Beng SSL, Nadaranjan S, Tun K (2021) A preliminary investigation of epibiotic macrofauna on the mangrove horseshoe crab Carcinoscorpius rotundicauda (Latreille, 1802) in Singapore. Mar Biol Res 17:513–522.

Linton DL, Taghon GL (2000) Feeding, growth, and fecundity of *Capitella* sp. I in relation to sediment organic concentration. Mar Ecol Prog Ser 205:229–240.

Liu C, Cui Y, Li X, Yao M (2021) Microeco: An R package for data mining in microbial community ecology. FEMS Microbiol Ecol 97:1–9.

Liu Z, Liu J (2013) Evaluating bacterial community structures in oil collected from the sea surface and sediment in the northern Gulf of Mexico after the Deepwater Horizon oil spill. Microbiologyopen 2:492–504.

Lix LM, Keselman JC, Keselman H. (1996) Consequences of Assumption Violations Revisited : A Quantitative Review of Alternatives to the One-Way Analysis of Variance " F " Test. Rev Educ Res 66:579–619.

Louca S, Parfrey LW, Doebeli M (2016) Decoupling function and taxonomy in the global ocean microbiome. Science (80-) 353:1272–1277.

Macavoy SE, Carney RS, Fisher CR, Macko SA (2002) Use of chemosynthetic biomass by large, mobile, benthic predators in the Gulf of Mexico. Mar Ecol Prog Ser 225:65–78.

MacAvoy SE, Carney RS, Morgan E, Macko SA (2008) Stable isotope variation among the

mussel *Bathymodiolus childressi* and associated heterotrophic fauna at four cold-seep communities in the Gulf of Mexico. J Shellfish Res 27:147–151.

MacDonald IR, Boland GS, Baker JS, Brooks JM, Kennicutt MCI, Bidigare RR (1989) Gulf of Mexico hydrocarbon seep communities. Mar Biol 101:235–247.

Manning LM, Lindquist N (2003) Helpful habitant or pernicious passenger: Interactions between an infaunal bivalve, an epifaunal hydroid and three potential predators. Oecologia 134:415–422.

Martin BD, Schwab E (2012) Symbiosis: 'Living together' in chaos. Stud Hist Biol 4:7–24.

Mason OU, Han J, Woyke T, Jansson JK (2014) Single-cell genomics reveals features of a *Colwellia* species that was dominant during the Deepwater Horizon oil spill. Front Microbiol 5:1–8.

McDiarmid H, Day R, Wilson R (2004) The ecology of polychaetes that infest abalone shells in Victoria, Australia. J Shellfish Res 23:1179–1188.

McEuen FS, Wu BL, Chia FS (1983) Reproduction and development of Sabella media, a sabellid polychaete with extratubular brooding. Mar Biol 76:301–309.

McGaw IJ (2005) Burying behaviour of two sympatric crab species: *Cancer magister* and *Cancer productus*. Sci Mar 69:375–381.

McGaw IJ (2006) Epibionts of sympatric species of Cancer crabs in barkley sound, British Columbia. J Crustac Biol 26:85–93.

McKnight DT, Huerlimann R, Bower DS, Schwarzkopf L, Alford RA, Zenger KR (2019) Methods for normalizing microbiome data: An ecological perspective. Methods Ecol Evol 10:389–400.

McLeod IM, Heller-Wagner G, Gillies C, Boström-Einarsson L, Dwyer PG (2020) Hitching a ride on Hercules: fatal epibiosis drives ecosystem change from mud banks to oyster reefs. Ecology 101:1–3.

McMurdie PJ, Holmes S (2013) Phyloseq: An R Package for Reproducible Interactive Analysis and Graphics of Microbiome Census Data. PLoS One 8.

Meyer KS, Li Y, Young CM (2018) Oceanographic and biological influences on recruitment of benthic invertebrates to hard substrata on the Oregon shelf. Estuar Coast Shelf Sci 208:1–8.

Minagawa M, Wada E (1984) Stepwise enrichment of 15N along food chains: Further evidence and the relation between δ15N and animal age. Geochim Cosmochim Acta 48:1135–1140.

Murray JM, Watson GJ, Giangrande A, Bentley MG, Farrell P (2011) Reproductive biology and

population ecology of the marine fan worm *Sabella pavonina* (savigny) (polychaeta: Sabellidae). Invertebr Reprod Dev 55:183–196.

Nájera-Hillman E, Bass JB, Buckham S (2012) Distribution patterns of the barnacle, *Chelonibia testudinaria*, on juvenile green turtles (*Chelonia mydas*) in Bahia Magdalena, Mexico. Rev Mex Biodivers 83:1171–1179.

Neave MJ, Apprill A, Ferrier-Pagès C, Voolstra CR (2016) Diversity and function of prevalent symbiotic marine bacteria in the genus Endozoicomonas. Appl Microbiol Biotechnol 100:8315–8324.

Negreiros-Fransozo ML, Costa TM, Fransozo A (1995) Epibiosis and molting in two species of *Callinectes* (Decapoda: Portunidae) from Brazil. Rev Biol Trop 43:257–264.

Newman WA, Jumars PA, Ross A (1976) Diversity trends in coral-inhabiting barnacles (Cirripedia, Pyrogomatinae). Micronesica 12:69–82.

Oakes FR, Fields RC (1996) Infestation of *Haliotis rufescens* shells by a sabellid polychaete. Aquaculture 140:139–143.

Okansen J, Simpson G, Blanchet F, Kindt R, Legendre P, Minchin P, O'Hara R, Solymos P, Stevens M, Szoecs E, Wagner H, Barbour M, Bedward M, Bolker B, Borcard D, Carvalho G, Chirico M, De Carceres M, Durand S, Evangelista H, FitzJohn R, Friendly M, Furneaux B, Hannigan G, Hill M, Lahti L, McGlinn D, Ouellette M, Ribeiro Cunha E, Smith T, Stier A, Ter Braak C, Weedon J (2022) Vegan: Community Ecology Package.

Olu K, Duperret A, Sibuet M, Foucher JP, Fiala-Médioni A (1996) Structure and distribution of cold seep communities along the Peruvian active margin: Relationship to geological and fluid patterns. Mar Ecol Prog Ser 132:109–125.

Orcutt BN, Joye SB, Kleindienst S, Knittel K, Ramette A, Reitz A, Samarkin V, Treude T, Boetius A (2010) Impact of natural oil and higher hydrocarbons on microbial diversity, distribution, and activity in Gulf of Mexico cold-seep sediments. Deep Res Part II Top Stud Oceanogr 57:2008–2021.

Orensanz J., Gallucci V. (1988) Comparative Study of Postlarval Life-History Schedules in Four Sympatric Species of *Cancer* (Decapoda: Brachyura: Cancridae). J Crustac Biol 8:187–220.

Osman RW (1977) The establishment and development of a marine epifaunal community. Ecol Monogr 47:37–63.

Ovsyannikova II (2010) Biodiversity of epibionts of the scallop *Mizuchopecten yessoensis* in the Peter the Great Bay, Sea of Japan. In: *Sciences-New York*.

Ovsyannikova II, Levin VS (1982) Growth dynamics of the barnacle *Solidobalanus hesperius* on valves of Yezo scallop in conditions of bottom cultivation. Sov J Mar Biol 8:44–51.

Pasternak Z, Abelson A, Achituv Y (2002) Orientation of *Chelonibia patula* (Crustacea: Cirripedia) on the carapace of its crab host is determined by the feeding mechanism of the adult barnacles. J Mar Biol Assoc United Kingdom 82:583–588.

Patti FP, Gambi MC, Giangrande A (2003) Preliminary study on the systematic relationships of Sabellinae (Polychaeta, Sabellidae), based on the C1 domain of the 28s rDNA, with discussion of reproductive features. Ital J Zool 70:269–278.

Paul BG, Ding H, Bagby SC, Kellermann MY, Redmond MC, Andersen GL, Valentine DL (2017) Methane-oxidizing bacteria shunt carbon to microbial mats at a marine hydrocarbon seep. Front Microbiol 8:1–13.

Paull CK, Jull AJT, Toolin LJ, Linick T (1985) Stable isotope evidence for chemosynthesis in an abyssal seep community. Nature 317:7–9.

Pianka ER (1970) On r- and K-selection. Am Nat 104:592–597.

Presnell JK, Schreibman MP (1997) Humason's Animal Tissue Techniques, 5th ed. The Johns Hopkins University Press.

Puccinelli E, McQuaid CD (2021) Commensalism, antagonism or mutualism? Effects of epibiosis on the trophic relationships of mussels and epibiotic barnacles. J Exp Mar Bio Ecol 540:151549.

Qian PY, Chia FS (1991) Fecundity and egg size are mediated by food quality in the polychaete worm *Capitella* sp. J Exp Mar Bio Ecol 148:11–25.

Quast C, Pruesse E, Yilmaz P, Gerken J, Schweer T, Yarza P, Peplies J, Glöckner FO (2013) The SILVA ribosomal RNA gene database project: Improved data processing and web-based tools. Nucleic Acids Res 41:590–596.

R Core Team (2023) R: A language and environment for statistical computing. https://www.r-project.org/.

Ramirez-Llodra EZ (2000) Reproductive patterns of deep-sea invertebrates related to phylogeny and energy availability. University of Southampton.

Rasmuson LK (2013) The biology, ecology, and fishery of the Dungeness Crab, *Cancer magister*. Adv Mar Biol 65:95–148.

Razaghian H, Esfandabad BS, Hesni MA, Shoushtari RV, Toranjzar H, Miller J (2019) Distribution patterns of epibiotic barnacles on the Hawksbill turtle, *Eretmochelys imbricata*, nesting in Iran. Reg Stud Mar Sci 27:100527.

Read GB, ten Hove HA, Sun Y, Kupriyanova EK (2017) *Hydroides* Gunnerus, 1768 (Annelida, Serpulidae) is feminine: A nomenclatural checklist of updated names. Zookeys 642:1–52.

Reeburgh WS (2007) Oceanic methane biogeochemistry. Chem Rev 107:486–513.

Riascos JM, Heilmayer O, Oliva ME, Laudien J, Arntz WE (2008) Infestation of the surf clam Mesodesma donacium by the spionid polychaete *Polydora bioccipitalis*. J Sea Res 59:217–227.

Robinson NJ, Lazo-Wasem EM, Butler BO, Lazo-Wasem EA, Zardus JD, Pinou T (2019) Spatial distribution of epibionts on olive ridley sea turtles at Playa Ostional, Costa Rica. PLoS One 14:e0218838.

Romero M V., Casadio SA, Bremec CS, Giberto DA (2022) Sclerobiosis: A term for colonization of marine hard substrates. Ameghiniana 59:265–273.

Rouse G, Fitzhugh K (1994) Broadcasting fables: Is external fertilization really primitive? Sex, size, and larvae in sabellid polychaetes. Zool Scr 23:271–312.

Rouse GW, Kupriyanova EK, Nishi E (2006) Sabellida. In: *Reproductive Biology and Phylogeny of Annelida*. Rouse GW, Pleijel F (eds) Science Publishers, Enfield, NH, p 521–563.

Ruff SE, Biddle JF, Tesked AP, Knittel K, Boetius A, Ramette A (2015) Global dispersion and local diversification of the methane seep microbiome. Proc Natl Acad Sci U S A 112:4015–4020.

Seed R (1985) Ecological pattern in the epifaunal communiteis of coastal macroalgae. In: *The Ecology of Rocky Coasts*. Moore PG, Seed R (eds) Hodder and Stoughton, London, p 22–35.

Shanks AL (2001) An identification guide to the larval marine invertebrates of the Pacific Northwest. Oregon State University Press, Corvallis.

Shapiro S, Wilk M (1965) An analysis of variance test for normality (complete samples). Biometrika 52:591–611.

Silina A V. (2002) The effect of muddy bottom sediment on the abundance and life span of the barnacle, *Hesperibalanus hesperius*, epizoic on scallop shells. Biofouling 18:263–268.

Silina A V., Zhukova N V. (2014) Association of the scallop *Patinopecten yessoensis* and epibiotic barnacle *Balanus rostratus*: Inter-specific interactions and trophic relationships determined by fatty acid analysis. Mar Ecol 37:257–268.

Simon CA, Kaiser H, Britz PJ (2005) The effect of age on the reproductive output of the abalone pest *Terebrasabella heterouncinata* (Polychaeta: Sabellidae: Sabellinae). African J Mar Sci 27:513–516.

Sinner M, Hong WL, Michel LN, Vadakkepuliyambatta S, Knies J, Sen A (2023) Lack of detectable chemosynthesis at a sponge dominated subarctic methane seep. Front Earth Sci

11:1–25.

Sogin EM, Leisch N, Dubilier N (2020) Chemosynthetic symbioses. Curr Biol 30:R1137–R1142.

Sokolova IM, Frederich M, Bagwe R, Lannig G, Sukhotin AA (2012) Energy homeostasis as an integrative tool for assessing limits of environmental stress tolerance in aquatic invertebrates. Mar Environ Res 79:1–15.

Thamrin, Tokeshi M, Nojima S (2001) Effect of coral-inhabiting barnacle (*Cantellius pallidus*) on planula production in a scleractinian coral *Alveopora japonica*. Ophelia 55:93–100.

Thiel V, Hügler M, Blümel M, Baumann HI, Gärtner A, Schmaljohann R, Strauss H, Garbe-Schönberg D, Petersen S, Cowart DA, Fisher CR, Imhoff JF (2012) Widespread occurrence of two carbon fixation pathways in tubeworm endosymbionts: Lessons from hydrothermal vent associated tubeworms from the mediterranean sea. Front Microbiol 3:1–20.

Thurber AR, Levin LA, Rowden AA, Sommer S, Linke P, Kröger K (2013) Microbes, macrofauna, and methane: A novel seep community fueled by aerobic methanotrophy. Limnol Oceanogr 58:1640–1656.

Tilic E, Sayyari E, Stiller J, Mirarab S, Rouse GW (2020) More is needed—Thousands of loci are required to elucidate the relationships of the 'flowers of the sea' (Sabellida, Annelida). Mol Phylogenet Evol 151:106892.

Toone TA, Washburn TW (2020) Phytodetritus, chemosynthesis, and the dark biosphere: Does depth influence trophic relationships at deep-sea Barbados seeps. Deep Res Part I 165.

Tovar-Hernández MA, Dean H (2014) A new gregarious sabellid worm from the Gulf of California reproducing by spontaneous fission (Polychaeta, Sabellidae). J Mar Biol Assoc United Kingdom 94:935–946.

Tovar-Hernández MA, ten Hove HA, Vinn O, Zatoń M, De León-González JA, García-Garza ME (2020) Fan worms (Annelida: Sabellidae) from Indonesia collected by the Snellius II Expedition (1984) with descriptions of three new species and tube microstructure. PeerJ 8:e9692.

Tovar-Hernández MA, Méndez N, Salgado-Barragán J (2009) *Branchiomma bairdi*: a Caribbean hermaphrodite fan worm in the south-eastern Gulf of California (Polychaeta: Sabellidae). Mar Biodivers Rec 2:1–8.

Tovar-hernández MANA, Yáñez-rivera B, Giangrande A, Gambi MC (2012) Notes on the species of *Perkinsiana* (Polychaeta: Sabellidae) from Antarctica with the description of *P. brigittae* sp. nov. Zootaxa 3485:56–68.

Uriz M-J, Rosell D, Maldonado M (1992) Parasitism, commensalism or mutualism? The case of

Scyphozoa (Coronatae) and horny sponges. Mar Ecol Prog Ser 81:247–255.

Vestheim H, Kaartvedt S (2016) A deep sea community at the Kebrit brine pool in the Red Sea. Mar Biodivers 46:59–65.

Visscher JP (1928) Reactions of the cyprid larvae of barnacles at the time of attachment. Biol Bull:327–335.

Wahl M (2009) Epibiosis: Ecology, effects, and defenses. In: *Marine Hard Bottom Communities*, Ecological. Wahl M, Caldwell MM, Heldmaier G, Jackson RB, Lange OL, Mooney HA, Schulze E-D, Sommer U (eds) Springer-Verlag Berlin Heidelberg, p 61–72.

Wahl M (1997) Living Attached: Aufwuchs, Fouling, Epibiosis. In: *Fouling Organisms of the Indian Ocean: Biology and Control Technology*. Nagabhushanam R, Thompson MF (eds) Oxford and IBH Publishing, New Delhi, p 31–83.

Wahl M (1989) Marine epibiosis. I. Fouling and antifouling: some basic aspects. Mar Ecol Prog Ser 82:275–282.

Wahl M, Mark O (1999) The predominantly facultative nature of epibiosis: experimental and observational evidence. Mar Ecol Prog Ser 187:59–66.

Wang Q, Garrity GM, Tiedje JM, Cole JR (2007) Naïve Bayesian classifier for rapid assignment of rRNA sequences into the new bacterial taxonomy. Appl Environ Microbiol 73:5261–5267.

Wargo RN, Ford SE (1993) The effect of shell infestation by *Polydora* sp. and infection by *Haplosporidium nelsoni* (MSX) on the tissue condition of oysters, *Crassostrea virginica*. Estuaries 16:229–234.

Wells HW (1966) Barnacles of the Northeastern Gulf of Mexico. Q J Florida Acad Sci 29:81–95.

Wells RJD, Rooker JR (2009) Feeding ecology of pelagic fish larvae and juveniles in slope waters of the Gulf of Mexico. J Fish Biol 75:1719–1732.

Xu Z, Burns CW (1991) Effects of the epizoic ciliate, *Epistylis daphniae*, on growth, reproduction and mortality of *Boeckella triarticulata* (Thomson) (Copepoda: Calanoida). Hydrobiologia 209:183–189.

Yan Y, Chan BKK, Williams GA (2006) Reproductive development of the barnacle *Chthamalus malayensis* in Hong Kong: implications for the life-history patterns of barnacles on seasonal, tropical shores. Mar Biol 148:875–887.

Yoshioka RM, Brown S, Treneman NC, Schram JB, Galloway AWE (2023) A Rhizocephalan parasite induces pervasive effects on its shrimp host. Biol Bull 244:201–216.

Young CM (1986) Defenses and refuges: alternative mechanisms of coexistence between a

predatory gastropod and its ascidian prey. Mar Biol 91:513–522.

Yun SG, Kikuchi T (1991) Reproduction of *Chone duneri* Malmgren (Polychaeta: Sabellidae). Publ from Amakusa Mar Biol Lab Kyushu Univ 11:19–30.

Zapalski MK (2011) Is absence of proof a proof of absence? Comments on commensalism. Palaeogeogr Palaeoclimatol Palaeoecol 302:484–488.

Zhang C, Fang YX, Yin X, Lai H, Kuang Z, Zhang T, Xu XP, Wegener G, Wang JH, Dong X (2023) The majority of microorganisms in gas hydrate-bearing subseafloor sediments ferment macromolecules. Microbiome 11:1–17.

Zhao Y, Xu T, Law YS, Feng D, Li N, Xin R, Wang H, Ji F, Zhou H, Qiu JW (2020) Ecological characterization of cold-seep epifauna in the South China Sea. Deep Res Part I Oceanogr Res Pap 163:103361.

Zhukova N V. (2000) Fatty acid components of two species of barnacles, *Hesperibalanus hesperius* and *Balanus rostratus* (Cirripedia), as indicators of food sources. Crustaceana 73:513–518.

Zullo VA, Marincovich LJ (1990) Balanoid barnacles from the Miocene of the Alaska Peninsula, and their relevance to the extant boreal barnacle fauna. J Paleontol 64:128–135.

SUPPLEMENTAL FILES

Table S4.1. P–values from the pairwise post-hoc Tukey's HSD tests examining the effects of season and sample site on $\delta^{13}C$ (above the grey diagonal) and $\delta^{15}N$ (below the grey diagonal). Significant p-values are bolded. BP = Brine Pool NR1; GC = Green Canyon 234; BH = Bush Hill; Oct = October; Jun = June; Feb = February.

	BP Feb	**BH Feb**	**GC Feb**	**BP Jun**	**BH Jun**	**GC Jun**	**BP Oct**	**BH Oct**	**GC Oct**
BP Feb		**0.0000**	**0.0000**	0.9963	**0.0000**	**0.0000**	**0.0000**	**0.0000**	**0.0000**
BH Feb	**0.0000**		**0.0226**	**0.0000**	0.0563	**0.0001**	**0.0000**	0.9997	**0.0239**
GC Feb	0.9995	**0.0052**		**0.0005**	0.8417	0.9999	**0.0000**	**0.0423**	0.9296
BP Jun	0.0921	0.0632	0.8232		**0.0000**	**0.0000**	**0.0000**	**0.0000**	**0.0000**
BH Jun	0.2235	**0.0000**	0.2965	**0.0000**		0.5616	**0.0000**	0.1009	0.9999
GC Jun	0.6422	**0.0000**	0.5922	**0.0001**	0.9983		**0.0000**	**0.0001**	0.8082
BP Oct	0.9962	**0.0000**	0.9534	**0.0020**	0.4723	0.9314		**0.0000**	**0.0000**
BH Oct	**0.0048**	**0.0475**	0.5408	**0.9999**	**0.0000**	**0.0000**	**0.0000**		**0.0413**
GC Oct	0.9451	**0.0000**	0.8525	**0.0006**	0.8633	0.9984	0.9998	**0.0000**	

Table S4.2. P-values from the pairwise post-hoc Tukey's HSD test examining the effects of season and sample site on $\delta^{34}S$. Significant p-values are bolded. BP = Brine Pool NR1; GC = Green Canyon 234; BH = Bush Hill; Oct = October; Jun = June.

	BP Jun	**BH Jun**	**GC Jun**	**BP Oct**	**BH Oct**	**GC Oct**
BP Jun						
BH Jun	**0.0005**					
GC Jun	0.9459	**0.0289**				
BP Oct	0.9996	**0.0000**	0.7629			
BH Oct	0.9999	**0.0000**	0.7817	0.9999		
GC Oct	0.0896	0.0518	0.7693	**0.0006**	**0.0003**	

Table S3. P-values from the pairwise post-hoc Tukey's HSD tests examining the effects of collection and microhabitat on $\delta^{13}C$ (above the grey diagonal) and $\delta^{15}N$ (below the grey diagonal). Significant p-values are bolded. BP = Brine Pool NR1; GC = Green Canyon 234; BH = Bush Hill; Oct = October; Jun = June; Feb = February; Epi = Epibiotic; FL = Free-living.

	BP Feb Epi	**BP Feb FL**	**BP Oct Epi**	**BP Oct FL**	**BH Jun Epi**	**BH Jun FL**	**GC Jun Epi**	**GC Jun FL**
BP Feb Epi		0.9864	**0.0480**	**0.0001**	**0.0000**	**0.0001**	**0.0000**	**0.0001**
BP Feb FL	**0.0000**		**0.0011**	**0.0000**	**0.0000**	**0.0018**	**0.0004**	**0.0011**
BP Oct Epi	0.2952	**0.0007**		0.2901	**0.0000**	**0.0000**	**0.0000**	**0.0000**
BP Oct FL	**0.0224**	**0.0152**	0.8990		**0.0000**	**0.0000**	**0.0000**	**0.0000**
BH Jun Epi	0.4016	**0.0000**	**0.0000**	**0.0000**		0.1484	0.3050	0.3044
BH Jun FL	**0.0001**	0.7974	**0.0284**	0.3444	**0.0000**		0.9999	0.9999
GC Jun Epi	0.9592	**0.0000**	0.8205	0.1183	**0.0064**	**0.0004**		**1.0000**
GC Jun FL	0.1542	**0.0060**	0.9996	0.9973	**0.0000**	0.1522	0.5642	

Table S4. P-values from the pairwise post-hoc Tukey's HSD test examining the effects of collection and microhabitat on $\delta^{34}S$. Significant p-values are bolded. BP = Brine Pool NR1; BH = Bush Hill; Oct = October; Jun = June; Epi = Epibiotic; FL = Free-living.

	BH Jun Epi	**BH Jun FL**	**BP Oct Epi**	**BP Oct FL**
BH Jun Epi				
BH Jun FL	0.0938			
BP Oct Epi	**0.0001**	**0.0350**		
BP Oct FL	**0.0013**	0.1915	0.8662	

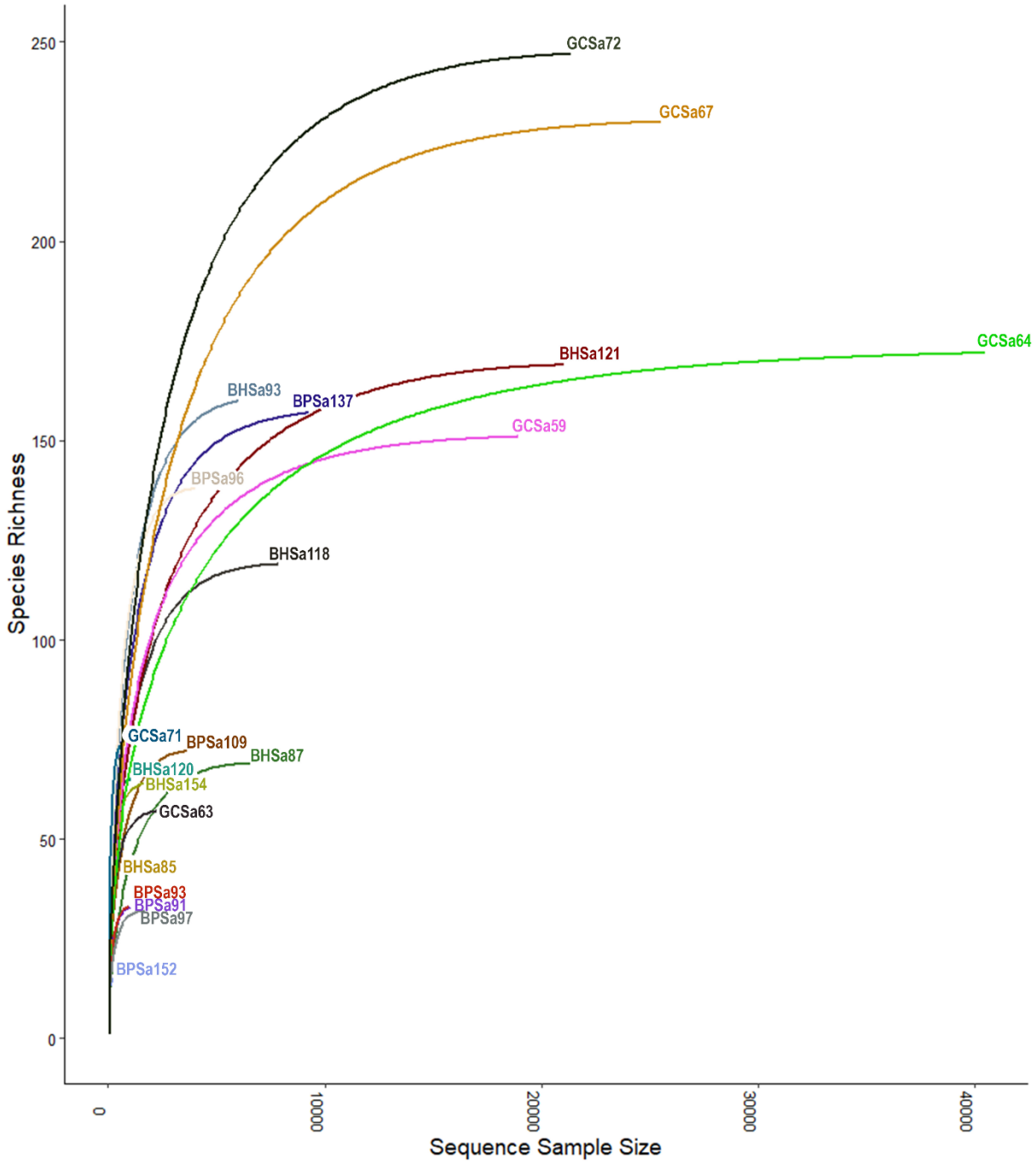

Figure S4.1. ASV rarefaction curves for each sample examined in this study.

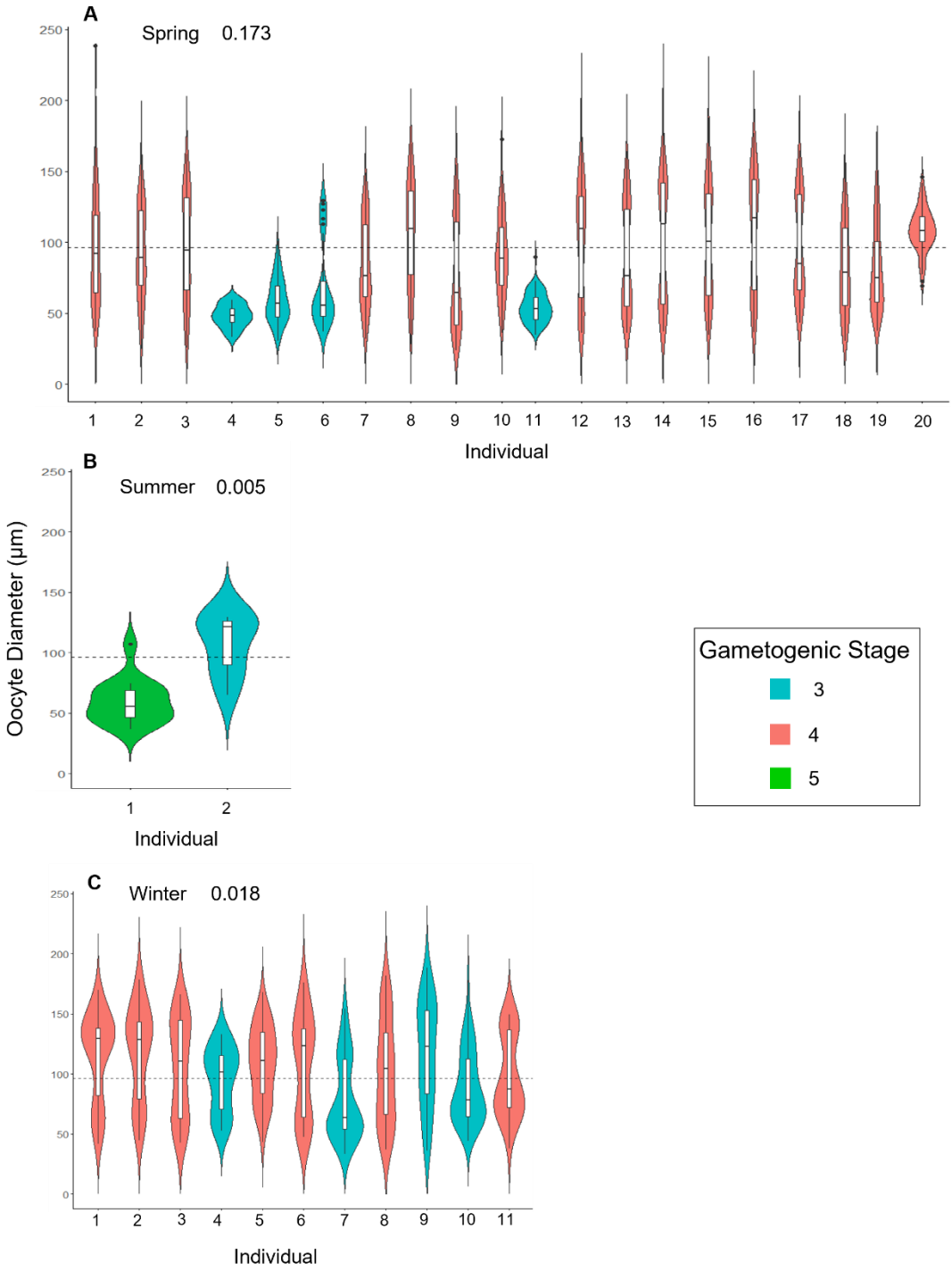

Figure S5.1. Violin plots of individual oocyte-size frequency distributions for *Seepicola viridiplumi* collected from Brine Pool NR1 in A) spring 2020, B) summer 2021, and C) fall 2022. Horizontal dash lines represent the average oocyte size for that collection. The numbers next to the season are the η^2[H] effect sizes calculated from a Kruskal-Wallis testing for synchronicity among females within each collection.

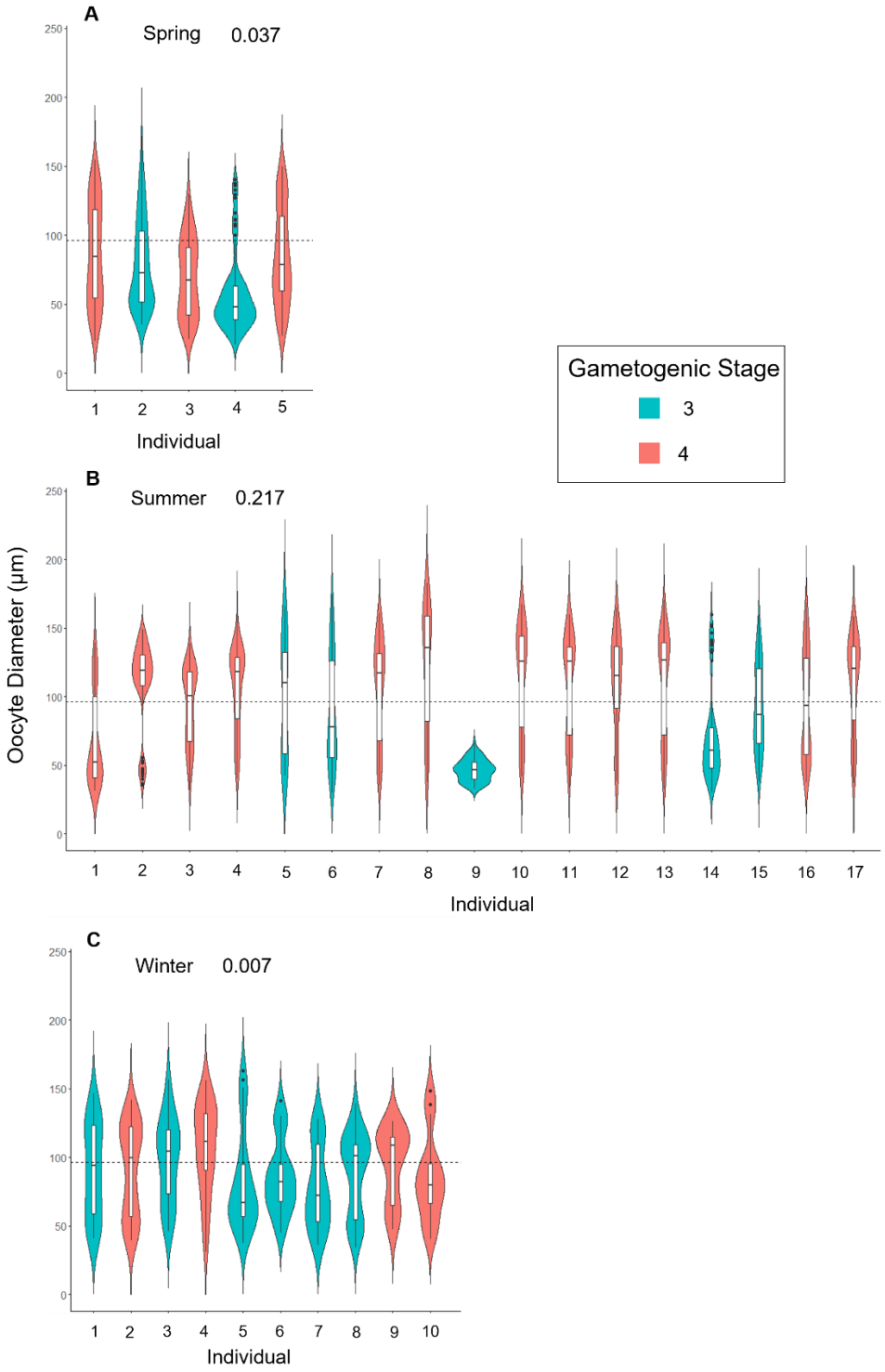

Figure S5.2. Violin plots of individual oocyte-size frequency distributions for *Seepicola viridiplumi* collected from Bush Hill in A) spring 2020, B) summer 2021, and C) fall 2022. Horizontal dash lines represent the average oocyte size for that collection. The numbers next to the season are the η^2[H] effect sizes calculated from a Kruskal-Wallis testing for synchronicity among females within each collection.

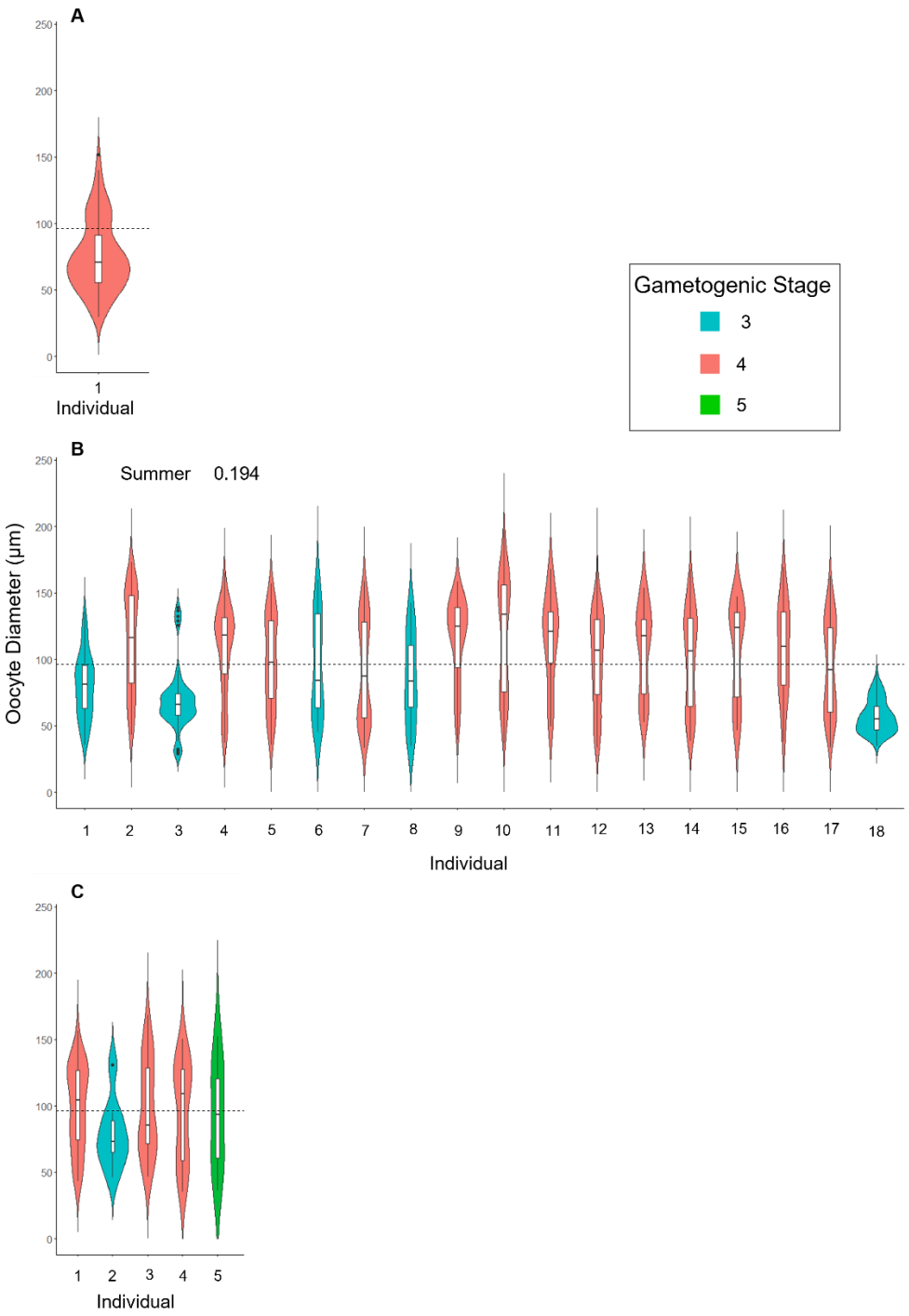

Figure S5.3. Violin plots of individual oocyte-size frequency distributions for *Seepicola viridiplumi* collected from Bush Hill in A) spring 2020, B) summer 2021, and C) fall 2022. Horizontal dash lines represent the average oocyte size for that collection. The numbers next to the season are the η^2[H] effect sizes calculated from a Kruskal-Wallis testing for synchronicity among females within each collection.